UNIVERSITÀ DEGLI STUDI DI CATANIA

International PhD Programme
"Nuclear and Particle Astrophysics"
XXIV Ciclo

Danilo Jaccarino

A complete calculation of shear viscosity in strongly interacting matter

Doctoral thesis

Supervisor: Prof. Umberto Lombardo
Tutor: Dr. Vincenzo Greco

Danilo Jaccarino
✉ jaccarino@lns.infn.it

Room #227

INFN - Laboratori Nazionali del Sud
via S.Sofia 62, 95125 Catania, ITALY
☎ +39.095.542.291

Room #N22

Scuola Superiore di Catania
via Valdisavoia 9
95123 Catania, ITALY
✆ +39.329.6538719

✡ Written in Catania, November-December 2011.
✡ **Format:** LaTeX generated .dvi, distilled to Pdf/A-1b standards.
✡ **Printed in:** *see printed edition*
✡ **Cover picture:** *see printed edition*

Ai miei genitori.

Table of Contents

Abstract

A complete calculation of shear viscosity in strongly interacting matter

The last observations from the Heavy Ion Collider facilities keep marking new territories in the unexplored field of the high temperature $T \gg \mu$ Quark-Gluon Plasma, with new discoveries that seem to enforce the hypothesis that such an exotic state of Strongly Interacting matter can indeed exist, making it an established fact. Things in the finite μ opposite regime are much harder as QCD, and its Lattice formulation, cannot yield any quantitative prediction to date, due to the strong-colour confinement effects in matter at high densities. Nevertheless its behaviour can be inferred from the empirical observations of Neutron Stars, that are sensitive to the composition, and thermodynamical properties of the Nuclear Matter Equation of State.
This thesis is focused on the construction of a Hybrid Equation of State, imposing a First-Order colour deconfinement transition of the Second Kind - as pointed out by Lattice QCD studies - between the two phases. Nuclear Matter is described by means of the microscopic Brueckner-Hartree Fock Many Body theory, that builds the *in medio* properties of interacting nucleons starting from the consistent treatment of realistic Bonn B 2-body *vacuum* interactions plus effective 3-body forces; Quark Matter is instead treated as a free gas of massless u, d, s quarks with the MIT Bag Model. Shear Viscosity of the strongly interacting Fermi liquid is then calculated in a low-temperature Boltzmann-Landau transport approach, yielding a slight deviation from the T^{-2} standard result at quark degrees of freedom dominated densities. The calculations are finally applied to the Astrophysics of Compact Objects: Neutron Stars static configurations are evaluated by means of the relativistic "Tolman-Oppenheimer-Volkoff" structure equations, finding a upper mass limit of 1.81 $M_\odot$ for the Hybrid Equation of State; furthermore, the estimate of the damping timescales of rotational r-mode Oscillations in Neutron Stars, sensitive to both the Equation of State and to Shear Viscosity of Hybrid Matter, are performed and confronted with the typical Gravitational Radiation instability timescales: the latter dominate in young, cooling Neutron Stars and this could be a promising signal for the LIGO facility, while in old Neutron Stars, at $T \sim 10^{-5}$ MeV, the $l = m = 2$ rotational-mode is alone able to suppress the GW emission. Despite the title, the calculation is far from being "complete", but it describes many features in a consistent way supported from the solidity of microscopic calculations of the Strongly Interacting matter properties.

Part I

Review of Quark-Gluon Plasma properties

There are two forms of judgement, one legitimate, the other bastard. And all these are of the bastard kind: sight, hearing, smell, taste, touch. The other is legitimate and its objects are hidden.

Democritus, III Century B.C.

0 Introduction

It has been well known over the last century that a fourth state of matter exists in addiction to the well known gas, liquid and solid: "plasma". The name was coined in 1928 by the Nobel Prize I. Langmuir [1] from the greek word πλάσμα, used to address 'anything formed', in analogy with the blood plasma. But the first experimental evidences are to be dated back to 1879, in the work of Sir William Crookes [2] with cathode rays. The aim of this Part is to present what is today addressed as "Quark-Gluon Plasma" (QGP), a system made out of deconfined quarks and gluons, believed to have dominated the first phases of existence of the Universe, and today reproducible in heavy-ion collision experiments and in the interior of Neutron Stars. The starting point is a brief discussion on its plasma properties, together with some basic phenomenology; this will be followed by a survey of the established ontological evidences of such a system and of its theoretical-inferred properties, among which the most striking is the existence of a phase transition to confined hadronic matter – also the most interesting from the perspective of this work. Instead of presenting a to-date picture of what QGP should be by describing it theoretically from sketch, a list of supporting arguments and inferred characteristics is here presented, without any spurious claim of completeness. All the general arguments are taken from some recent QGP textbooks like Kogut and Stephanov [3], Letessier and Rafelski [4] and Yagi, Hatsuda and Miyake [5].

0.1 The fourth state of matter

Our most common everyday experiences can be explained in terms of two of the four fundamental forces: Gravity and Electromagnetism. Even if the quantitative and deterministically complete description of "basic" phenomena - like, for example, an apple falling on the ground or the exact motion of a

Observable	Terrestrial plasmas	Astrophysical plasmas
Size	10^{-6} m (laboratories)	10^{-2} m (spacecr.sheath)
in meters	10^{-2} m (lightning)	10^{25} m (intergal. nebulae)
Lifetime	10^{-12} s (laser pl.)	10^{1} s (solar flares)
in seconds	10^{7} s (fluo lights)	10^{17} s (intergal. pl.)
Density	10^{7} m^3	1 m^3 (intergal. *medium*)
in particles/m^3	10^{32} m^3	10^{30} m^3 (stellar cores)
Temperature	1 K (cristalline pl.)	10^{2} K (aurora)
in kelvins	10^{8} K (magnetic fusion)	10^{7} K (solar core)
Magnetic Fields	10^{-4} T (laboratories)	10^{-12} T (intergal. *medium*)
in teslas	10^{3} T (pulsed power pl.)	10^{11} T (pulsar surface)

Table 1: Range of plasma parameters

bowling ball - is often a task well beyond calculating possibilities, a physicist can very well understand the underlying dynamics in terms of mathematical concepts and furthermore, in a broad spectrum of cases, find a reasonable solution, through simplifying assumptions and consequent algebraic approximations.

Among the possible systems, matter is the one that "matters" here: we know that its scientifically established states - Gaseous, Solid, Liquid, and our fourth: Plasma - are different realisations of the Electromagnetic interactions among its basic constituents, atoms and molecules. But already centuries before quantum mechanics, even centuries before science itself, matter was classified by Presocratic philosophers of ancient Greece to happen in four distinct "essences": Air, Earth, Water and Fire - plus a fifth: Aether - from their properties, i.e. their properties of being hot, wet, cold and dry, and today they can be seen as primordial representations of the aforementioned contemporary analogues.

Plasma can be regarded on phenomenological grounds as an ionised system of charged constituents (usually electrons and ions), as it's obtained after a phase transition from a gas; it has no definite shape nor volume, like its progenitor state, but differently from the latter, the high concentration of charge carriers gives it paraelectric and paramagnetic properties, well known in the observations of "filaments", striations or string-like structures. Its realisations can be easily found in Nature [→ tab. 1] : from terrestrial phe-

nomena like lightnings, flames and *aurorae*, to artificial plasmas like neon signs, cathode tubes and the last-generation televisions, up to astrophysical systems: about 99% of the entire visible Universe is in the plasma phase, making it by far the most abundant; stars, for example, are formed in nebulas of ionised gas; more generically, the interstellar and intergalactic *medium* are very sparse plasmas. The measured values of physical observables for these systems can vary over many orders of magnitude, giving a very complex and various phenomenological picture.

§ **0.1.1. Definition of plasma.**— The experimentally-inspired definition given above lacks of generality and fails in pinning the most important features of the so-called "fourth state of matter". A more complete and logically valid definition can be given specifying three fundamental microscopic properties, which in turn can then be related to actual empirical observables. A plasma is a many-body system of charged constituents that shows:

- **Collective dynamics:** the motion of a single particle in the *medium* is mainly affected by the charged-interaction particles that surround it, rather than from other individual particles it may encounter. This happens after a redistribution of the charge carriers that - if sufficiently dense - can effectively damp any local charge excess, a phenomenon known as "Debye Screening" [6] (estensively treated in textbooks, such as [7]). Quantitatively speaking, this phenomenon introduces a parameter inside the plasma, the so-called "Debye screening length" λ_D, at which a charge is statistically screened. The corresponding condition requires that the density of charge carriers inside a Debye sphere be much bigger than unity.

- **Quasineutrality:** the system must be globally neutral, and the Debye screening length must be much smaller that the physical size of the plasma. This makes bulk interaction more important than the boundary effects, so that on large scales any portion of the system is approximatively neutral.

- **Supremacy of charged-interactions:** the dynamics inside the system are dominated by the interactions between charged particles, so that the effects from gas-like collisions between charged particles and neutral constituents are negligible.

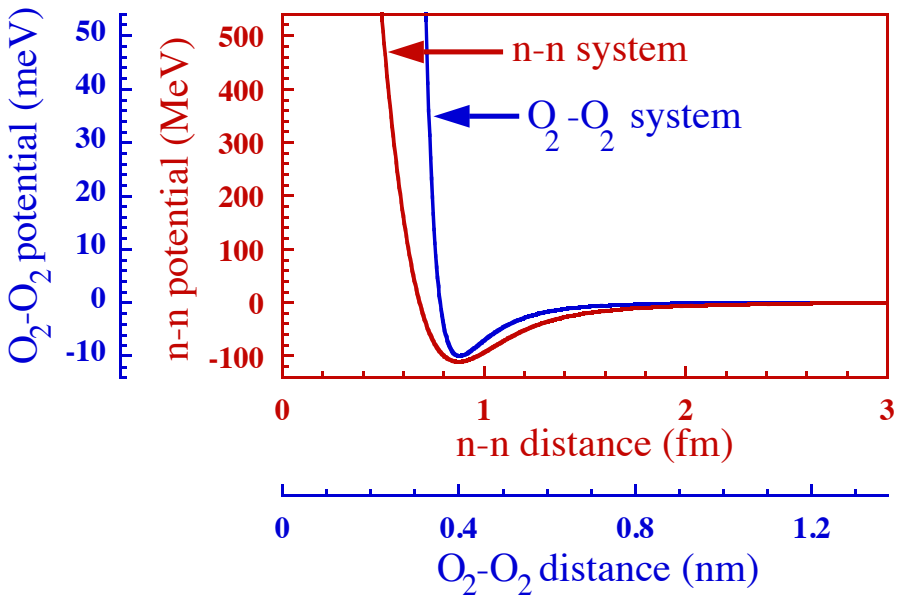

Figure 1: a comparison of the n-n Argonne v_{18} potential in the $^1S_0$ channel, with the Lennard-Jones potential between two O_2 molecules; taken from [8].

A fourth consideration can be further exploited: being a phase of matter, plasma can be obtained from a gas and back by a phase transition, by means of ionisation and recombination processes.

§ **0.1.2. Electromagnetic systems: some numbers.**— The vast majority of the systems studied during the last century - some of which were listed in the beginning of the chapter - are essentially composed by atomic or molecular ions, whose dynamics are ruled by the electromagnetic interaction. At Normal Conditions ($T_N = 20°C$ and $P_N = 1$ atm) and thermodynamical equilibrium the thermal energy per degree of freedom is approximatively $k_B T_N \approx 1/40$ eV, that compared with the molecular first ionisation energy scales (≈ 1 eV) clearly favours the gas phase. But already at temperatures of $10^3 \div 10^4$ K a consistent fraction of the molecules can (depending on the chemical specie) be ionised, giving rise to a plasma. Furthermore, at $T_H = 12000$ K a Hydrogen gas can easily be considered completely ionised, as $k_B T_H \approx 1$ eV; the same applies to atoms inside a star: our Sun, in the centre, has a modelled temperature of $T_\odot = 15.7 \times 10^6$ K; in equilibrium conditions each degree of freedom has a thermal energy of $k_B T_\odot \approx 1.35$ keV, two orders of magnitude more than the Hydrogen ionising potential, 13.7 eV. The atoms themselves cannot survive anymore bound.

§ **0.1.3. Strongly interacting matter.**— But atoms, despite the etymon of the word, which comes from the greek ἄτομος and means "indivisible", are not elementary particles; at their centre lie *nuclei*, neutrons and protons bound together by the strong interaction. They in turn are composed by quarks and gluons, carriers of the colour charge and - to date believed to be - the true fundamental bricks of the universe. This moves the question to a deeper level: is it possible to have strongly interacting matter? What can be its properties?

The answer is yes, provided that one understands the differences between the underlying interactions; such a system is referred to in literature as "nuclear matter". The first, striking similarity with common electromagnetic matter is shown in fig. 1: nucleons and molecules have similarly shaped potentials on different energy ranges [8]; this is due to the fact that both systems experience what is called a "residual interaction", mediated by meson exchange on one side, by Van Der Waals forces on the other. In this way nucleons can be bound together; without deeper investigation – this being the topic of the next chapters – a number of theoretical and experimental evidences of phases of nuclear matter can be given: as a first example, C. F. von Weizsäcker (1935) and H. Bethe (1936) formulated the "liquid drop model" to describe nuclear properties in analogy with a drop of liquid, and more generally a milestone work that led to the evidence that at Normal Conditions *nuclei* are in a liquid phase; J. Negele and D. Vautherin in 1973 studied the possibility to have lattices of neutron-rich *nuclei* just below the drip-line in Neutron Stars, that can be thought as a a realization of solid-state "nuclear matter" [9]; many experiments in high energy heavy-ion collisions have shown evidences of a possible liquid-gas phase transition, so that already in 1995 a German-Italian collaboration (among which there was our beloved and prematurely deceased prof. G. Raciti) could measure the caloric curve of the transition [10]; it is reported in fig. 2. The critical temperature is $T_c^{lg} \approx 10$ MeV; the convention to use the energy $k_B T$ instead of the temperature T in Kelvins itself was introduced in order to ease the comparison with the excitation energies of *nuclei*, that typically lie in the range of a few MeV. In quantum-theoretical approaches it is common to use the so-called "natural units", redefining quantities in order to avoid the explicit show-up of the most common constants (like $\hbar$, the reduced Planck constant, c, the speed of light in *vacuum* and in statistical applications, also k_B, the Boltzmann constant). This procedure is addressed stating that $\hbar = c = 1$ [→ App. A].

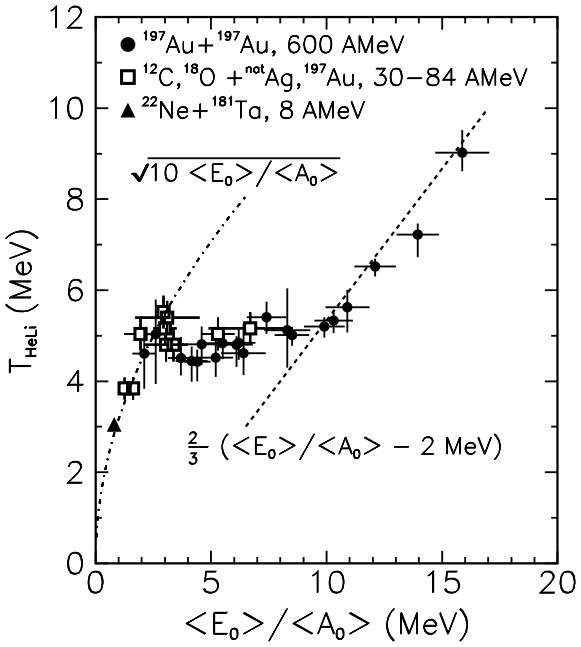

Figure 2: Caloric curve of *nuclei* determined by the dependence of the isotope temperature T_{HeLi} on the excitation energy per nucleon. Taken from [10].

§ **0.1.4. Strongly interacting plasma.**— This can be applied to plasma as well: the subject of this chapter, the Quark-Gluon Plasma, can be regarded as a fourth state of interacting matter in the same sense as one can speak - given the examples listed above - of phases of nuclear matter, i.e. provided an analogy with the analogous electromagnetic interaction dominated systems. There is anyway an ontological difficulty concerning the definition of the properties of such a system, and this requires the opening of a short parenthesis about the investigating method. It is instructive to refer to an historical example, in order to exploit it: at the early stages of science the differences among the states of matter were merely phenomenic and generally based on their macroscopic properties. It is only with the discovery of Quantum Mechanics in 20th century and later applications to the study of the structure of matter that the microscopic properties of the states of matter could be finally grasped. So plasma phase could be recognised and separated from the gas one; the huge quantity of subsequent theoretical and experimental investigation led to an amount of knowledge sufficient to provide good definitions and explanation of the properties of this exotic state. When switching to strong interacting matter, science faces the same difficul-

ties, but on a scale much less easy to investigate, due to the exotic character of the systems involved; the differences between interactions introduce lots of difficulties: solid state nuclear matter for example is usually unbound due to the medium range saturation of the strong force and Coulomb repulsion, and gets bound only by gravity. QGP has been extensively studied during the last 40 years, but it is early to conclude unanimously for its properties and characteristics, maybe even for its existence. So the subsequent discussion is to be considered on the same grounds of frontier topics.
What is then QGP? It is a state of strongly-interacting matter widely believed to have been produced at CERN SPS during the 90s, and theoretically inferred to be present inside astrophysical compact objects; in addiction it is one of the states straddled by our universe during its first seconds of existence. The analogous of electromagnetic ionisation, that drives the phase transition, is here colour deconfinement, or the way in which the strong bond among quarks is dynamically overcome.

§ **0.1.5. A bit of History.**— If the concept of "quark" made its appearance during the 60s, in the works of Murray Gell-Mann and Zweig and under the name of "parton" - a term coined by Feynman to address point-like structures found inside the hadrons seen in the experiments at SLAC in Stanford - it is during the 70s that a large part of the scientific community begun believing in their existence, finally giving credit to what to date was seen as a mere mathematical trick to solve, in an elegant group-theoretical fashion, the puzzle of the "particle zoo". The most symbolic year in this sense was 1974, when two independent groups, one at SLAC, the other at Brookhaven, discovered independently a meson to be recognised as a charm-anticharm state, later to be called J/ψ, from the names that each of the groups gave it. That particular event proven many theoretical investigations and finally convinced the biggest majority of the audience about the existence of quarks. Gluons unmistakable observations came only in 1979, in three-jet events at DESY, Hamburg (PETRA and DORIS experiments). In the meanwhile Quantum Chromo-Dynamics (QCD) was being developed as a non abelian gauge theory built on the $SU(3)$ colour group, gaining credibility as the definitive theory of Strong Interaction.
It is in such scheme that the first known ideas about QGP arose. In particular, among the first, two works are to be noticed. The first, by N. Cabibbo

and G. Parisi, proposed a solution to the problem of the Hagedorn limiting temperature for the existence of hadronic states [11]. In their words:

> *We suggest that the "observed" exponential spectrum is connected to the existence of a different phase of the* vacuum *in which quarks are not confined.*

They concluded stating the general form of the phase transition and drawing a tentative $T - \rho_B$ phase-diagram, oddly enough, with axes reverted with respect to the ones spread today.
A second, by J. Collins and M. Perry, deals with matter inside Neutron Stars. Here the authors point out that according to an asymptotically-free theory, the interior of such exotic compact stars should be composed by quarks rather than hadrons [12]. They reported:

> *Our basic picture then is that matter at densities higher than nuclear consists of a quark soup. The quarks become free at sufficiently high density. A specific realisation is an asymptotically free field theory. For such a theory of strong interactions, high-density matter is the second situation where one expects to be able to make reliable calculations — the first is Bjorken scaling.*

The early works spoke of a "quark soup"; the name "Quark-Gluon Plasma" was coined by E. Shuriak in 1978 [13] and came with a short statement of why such a system could be regarded as a plasma state of strongly interacting matter. At that time it was common to think it as a gas of free quarks and gluons, in which the strong binding was broken. But it soon was evident that this was not the case, due to remnant effects of confinement [14]. Theoretical investigation continued to fruitfully understand aspects of the transition and to give phenomenological predictions of QGP properties.
In the meanwhile, many experiments were beginning to explore the field, mainly at CERN (Geneva) and BNL (Brookhaven); aside from this efforts, theorists were trying to understand observable mechanisms that could constraint the QGP by showing behaviours different from the well-known hadronic scenarios. One of the most famous works in this direction was prepared in 1986 by T. Matsui and H. Satz, and proposed that J/ψ meson suppression in QGP would be one of such "signatures" [15]:

> *[...] there appears to be no mechanism for J/ψ suppression in nuclear collisions except the formation of a deconfining plasma,*

> *and if such a plasma is produced, there seems to be no way to avoid J/ψ suppression. Furthermore, our estimates indicate that the measurement of the dilepton spectrum from nuclear collisions should allow a clear test of this phenomenon.*

During the 80s and 90s the NA and WA installations at CERN SPS collected enough data to test the properties of hot and compressed heavy *nuclei* at temperatures between $100 \div 170$ MeV, a region marked as "promising" from phenomenology. The teams working in those collaborations could list a series of signatures of the existence of a QGP, among which the most clear was J/ψ suppression. This led to the announcement that a new state of matter was produced; thus spoke prof. L. Maiani on the 10th February 2000:

> *The combined data coming from the seven experiments on CERN's Heavy Ion programme have given a clear picture of a new state of matter. This result verifies an important prediction of the present theory of fundamental forces between quarks. It is also an important step forward in the understanding of the early evolution of the universe. We now have evidence of a new state of matter where quarks and gluons are not confined.*

Soon after the construction of the Large Hadron Collider begun at CERN; the challenge was so taken on by the Relativistic Heavy Ion Collider at BNL. In 2005 a press event confirmed tentatively the scenario of five years earlier, adding evidence that the QGP should be a strongly coupled liquid rather than a gas of free particles. The definitive startup of the LHC during 2009, and the first Pb-Pb collisions, observed in Fall 2010, seem to confirm the scenario at RHIC, yet adding some new features, such as the possibility of strong CP-violating evidences. At the end of 2011, during the writing of this thesis, the heavy ion program started back at LHC, while an independent proof of the existence of QGP is still to be given; yet a wide part of the scientific community believes in its existence. A brief review of the most recent experimental discoveries is reported in Chapt. 1.

§ 0.1.6. In Nature.— As far as it is known there are essentially two different thermodynamical regimes of QGP, realised in three different natural phenomena. Before actually looking at the phase transition in detail, it is interesting to fix ideas on the picture to-date. Some numbers are reported in Tab. 2, in a fashion similar to § 0.1.2. In detail:

Observable	QGP fireball	Quark core in NS
Volume	$10 \div 100$ fm^3	1 km^3
in cube meters	$\sim 10^{-44}$ m^3	10^9 m^3
Lifetime	$2 \div 10$ fm/c	stable
in seconds	$\sim 10^{-23}$ s	/
Density	vanishing	$2 \div 5\,\rho_0$ (nucl. sat.)
in g/cm^3	/	$\sim 10^{15}$ g/cm^3
Temperature	$150 \div 200$ MeV	$10^{-6} \div 10$ MeV
in kelvins	$\sim 10^{11}$ K	$\sim 10^4 \div 10^{10}$ K

Table 2: Range of QGP parameters

- **High ρ_B regime:** Imagine to compress adiabatically an infinite lattice of nucleons, keeping the temperature T low enough to statistically forbid excitations of the nucleons and relativistic effects. Such a system would have prominent bulk properties, and a good quantity to look at would be ρ_B, baryon density, as the number of antibaryons would be negligible. At very high densities, such as 1 baryon/fm^3, several nucleonic wavefunctions would superimpose at every point, with partonic degrees of freedom becoming preponderant, thus making hard to distinguish the original particles. Such a system would be ionised in a fashion totally different from the standard EM plasmas, but would show similar properties - provided one takes into account substantial differences in the mass of the constituents and consequent mobilities of the species.

- **High T regime:** On the other side, one can imagine to heat a portion of strongly interacting *vacuum*: thanks to the thermal energy, many hadronic degrees of freedom are polarised - lowest lying states meson and anyway "white"-coloured particles due to colour charge confinement. Above a critical density these hadrons would overlap and melt in a dynamical medium, in which colour charge is screened. Such a system is ionised in a way that resembles a lot the EM plasmas, but would have vanishing baryonic density and so properties very different from such a system.

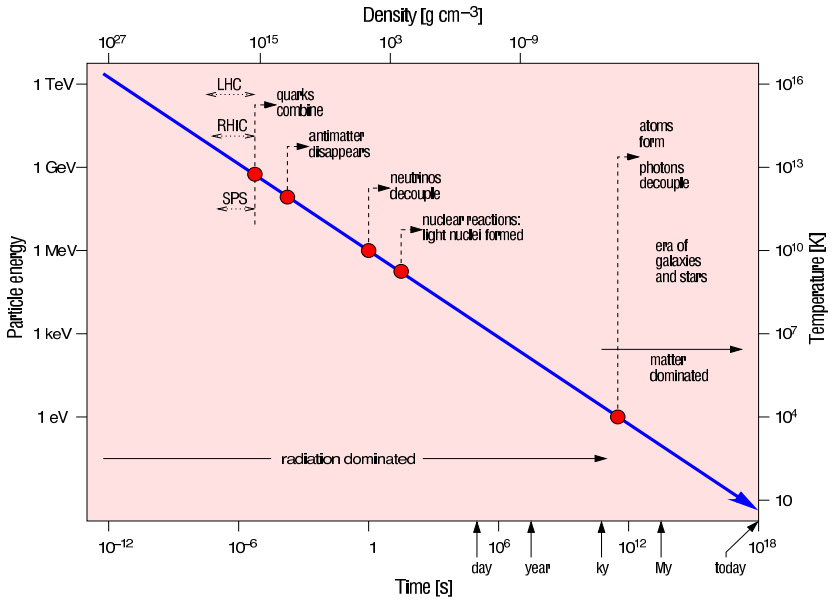

Figure 3: Schematic timeline of Big-Bang evolution of our Universe in Energy/Temperature scale. Around 10^{-6} after the explosion, the hot fireball underwent to a QCD phase-transition, with the onset of colour confinement. The picture also reports the zone experimentally investigated during the last 30 years. Taken from ref. [4].

What kind of conditions could lead to the formation of the two kinds of QGP? The first seems likely to happen inside the cores of Neutron Stars, where the density, due to the gravity of the superimposing neutron layers, can reasonably go several times beyond the nuclear saturation density $\rho_0 = 0.17\ \text{fm}^{-3} = 2.7 \times 10^{14}\ \text{g/cm}^3$.
The second is believed to have been one of the states touched by our Universe during its first Big-Bang expansion [→ fig. 3]: soon after the Electroweak decoupling the hot fireball was composed by a QGP of chiral constituents (i.e. that satisfy the so-called "chiral symmetry", valid only in the massless limit, later to be treated in more detail) that, following the expansion with consequent lowering of the temperature, crossed the critical temperature around $T \sim 150 \div 200$ MeV, finally forming white hadrons and breaking chiral symmetry, thus gaining a mass. This kind of situation is reproduced in heavy ion collisions, where the two *nuclei* colliding form a hot and energy-dense fireball in which, at sufficient center-of-mass energies, it is possible to cross the barrier of QGP.

We now have evidence of a new state of matter where quarks and gluons are not confined.

L. Maiani - Cern (2000)

1 Quark Gluon Plasma

After the long discussion of sec. 0.1, that was meant to explain the general idea behind the concept of strong interacting plasma, it is now the moment to switch to a more quantitative description of QGP and its properties. The starting point is a review of Quantum Chromo-Dynamics (QCD) and of its features more interesting from this point of view. References include standard textbooks of Quantum Field Theory, like Peskin and Schröeder [16]. It is implicitly assumed that $\hbar = c = 1$ [→ App. A].

1.1 Quantum Chromo-Dynamics

The fundamental degrees of freedoms of QCD are quarks and gluons. Quarks are spin-$\frac{1}{2}$ fermions that carry a standard set of particle quantum numbers, plus "flavour" - there are six in total, with different masses - and "colour" - that sets their strong-charge state; their properties are briefly reported in the first four columns of tab. 1.1; they are arranged in three doublets of alternate charge $+\frac{2}{3}e$ and $-\frac{1}{3}e$, with e being the electron charge. They are elementary particles and this makes them the fundamental bricks of matter, as nucleons and more generally hadrons can be interpreted as their bound states. Gluons are massless vector bosons of spin 1, known to carry colour charge and to be responsible for the mediation of the strong interaction. A short story of their discovery was presented in § 0.1.3.

The concept of colour was introduced by Greenberg [17], Han and Nambu [18] and definitively proposed by Bardeen, Fritzch and Murray Gell-Mann [19] to solve the puzzle of the $S = \frac{3}{2}$, Δ^{++} baryon, that according to the decuplet of the "Eightfold way" by Gell-Mann and Zweig should have been composed by three u quarks with exactly the same set of quantum numbers, thus forbidding the Pauli principle. It was realised that if the three quarks could have different colour states, then they would be able to build a com-

Name	Flavour f	EM charge	Running mass	Energy scale k
Up	u	$+\frac{2}{3}e$	$1.5 \div 4.5$ MeV	2 GeV
Down	d	$-\frac{1}{3}e$	$5 \div 8.5$ MeV	2 GeV
Strange	s	$+\frac{2}{3}e$	$80 \div 155$ MeV	2 GeV
Charm	c	$-\frac{1}{3}e$	$1 \div 1.4$ GeV	m_c
Top	t	$+\frac{2}{3}e$	~ 175 GeV	m_t
Bottom	b	$-\frac{1}{3}e$	$4 \div 4.5$ GeV	m_b

Table 1.1: Quark Families and masses in the $\overline{MS}$ scheme.

pletely antisymmetric wavefunction, finally reconciling with the validity of the spin-statistics theorem. The number of different possible colours is set to $N_c = 3$; this can be proven experimentally and inferred theoretically. Technically speaking, Quantum Chromo-Dynamics (QCD) is a renormalisable non-abelian gauge theory based on the $SU(3)$ colour group. It is a part of the Standard Model of fundamental interactions.

§ **1.1.1. Short review of SU(3) properties.**— In order to build a Quantum-Field Theory for strong interactions it is necessary to allow for the following guidelines:

- **SU(3) is the colour symmetry group:** it is a compact semi-simple Lie group whose algebra is generated by a set of $N_c^2 - 1 = 8$ traceless and Hermitian 3×3 matrices $t_a = \lambda_a/2$, with λ_a known in literature as "Gell-Mann" matrices and $a = \{1, 2, ..., 8\}$ the octet colour index. The 8 generators satisfy the following commutation rules:

$$[t_a, t_b] = i \sum_{c=1}^{8} f_{abc} t_c \tag{1.1}$$

  where the f_{abc} (whose raising and lowering of indices is trivial) are real numbers known as "structure constants" of the $SU(3)$ group.

- **SU(3) gauge invariance:** It is a property of invariance pertaining to a certain class of Dirac algebraic structures from a three-dimensional representation of $SU(3)$ transformations in colour space. The representation is obtained assigning a set of 8 functions $\hat{\theta}_a(x) = \sum_{a=1}^{8} \frac{1}{2} \lambda_a \theta^a(x)$ of the space-time point x^μ that build the operator:

$$U(x) = \exp\left[ig\,\hat{\theta}_a(x)\right] \tag{1.2}$$

where g is the coupling strength of strong interactions - analogue of the EM charge e.

- **Quarks (antiquarks) are the fermionic degrees of freedom:** They are indeed an $SU(3)$ triplet in colour space i.e., they belong to the fundamental representation **3** of $SU(3)$; their quantum-relativistic dynamical evolution is expressed by the Dirac spinor of fields $q_i(x)$ of flavour $i = \{u, d, s, c, b, t\}$ and triplet colour index $\alpha = \{R, G, B\}$ specified in every point x:

$$q_i^\alpha(x) = \begin{pmatrix} q_i^R(x) \\ q_i^G(x) \\ q_i^B(x) \end{pmatrix} \tag{1.3}$$

with corresponding $\bar{q}$ for antiquarks. Flavour indices i will be suppressed from now on, for simplicity of notation; they take no dynamical role in the evolution of quark fields, as all the dynamical observables are diagonal in flavour space, and exist due to the experimentally observable mass hierarchy among quarks. They gauge transform as:

$$Q^\alpha(x) = \mathrm{e}^{ig\,\hat{\theta}_a(x)}\, q^\alpha(x) \tag{1.4}$$

with the operator $U(x)$ leaving unchanged the physical properties of the quark fields.

- **Gluons are the bosonic degrees of freedom:** Gluons arise as the Yang-Mills bosons as soon as a local gauge symmetry is imposed at Lagrangian level, and are minimally coupled to the quark fields in the covariant derivative. Their properties and number again come from $SU(3)$ group theoretical properties: there are 8 of them; indeed, being the force carriers and changing both colour (with q) and anti-colour (with $\bar{q}$), they belong to the product of the fundamental representation **3** and its conjugate $\overline{\mathbf{3}}$:

$$\mathbf{3} \otimes \overline{\mathbf{3}} = \mathbf{1} \oplus \mathbf{8} \tag{1.5}$$

where **1** is a colour singlet to which would correspond a hypothetical white gluon, not observed in nature, and **8** is the 8-dimensional $SU(3)$ adjoint representation, made of 3×3 matrices (under certain assumptions the Gell-Mann matrices can be taken to represent gluons).

§ **1.1.2. Classical Lagrangian.**— Once the basic ingredients of the theory are stated, the starting point of every Quantum Field Theory is the construction of a Lagrangian density that respects the chosen gauge symmetry in a Lorentz-covariant scheme. The QCD Lagrangian density is:

$$\mathcal{L}^{cl}_{\rm QCD} = \bar{q}(i\,\not{D}_\mu - m)q - \frac{1}{4}G^a_{\mu\nu}G^{\mu\nu}_a; \tag{1.6}$$

in the first term $m = m_i = \mathrm{diag}\,(m_u, m_d, ..., m_b)$ is the quark mass matrix, trivially diagonal in flavour space, while $\not{D}_\mu$ is the gauge covariant derivative acting on the colour triplet quark field, responsible for the coupling of the vector field $\hat{A}_\mu = \sum_{a=1}^{8} \frac{1}{2}\lambda_a A^a_\mu(x)$ with the quark fields:

$$\not{D}_\mu = \gamma^\mu D_\mu = \gamma^\mu\big(\partial_\mu - ig\hat{A}_\mu), \tag{1.7}$$

in which γ_μ are the Dirac matrices for $\mu = \{1, 2, 3, 4\}$. The second term of eq. (1.6) is the trace of the gluon field strength tensor $G^a_{\mu\nu}$:

$$G^a_{\mu\nu} = \partial_\mu A^a_\nu - \partial_\nu A^a_\mu + g\, f^{abc} A^b_\mu A^c_\nu, \tag{1.8}$$

which contains a gluon self-coupling term $A^b_\mu A^c_\nu$ mediated by the $SU(3)$ antisymmetric structure constants f^{abc}, features of the non-abelianity of the gauge group. No gauge-breaking interaction terms as $A^a_\mu A^\mu_a$ can be included: gluons are costrainted to be massless.
The built Lagrangian density of eq. (1.6) shows $SU(3)$ gauge symmetry as $G^a_{\mu\nu}$ and D_μ are built to transform covariantly under action of the operator $U(x)$ [→ eq. (1.2)]:

$$G^a_{\mu\nu}(x) \to U(x) G^a_{\mu\nu} U^\dagger(x) \tag{1.9}$$

$$D_\mu(x) \to U(x) D_\mu U^\dagger(x); \tag{1.10}$$

the same applies to the fields $q^\alpha(x)$ and $\hat{A}_\mu$, that transform respectively as the fundamental [→ eq. (1.4)] and adjoint representations of $SU(3)$:

$$\begin{aligned} Q^\alpha(x) &= \mathrm{e}^{ig\,\hat{\theta}_a(x)}\, q^\alpha(x) \\ \hat{A}'_\mu &= \mathrm{e}^{ig\,\hat{\theta}_a(x)} \left(\hat{A}_\mu - \frac{i}{g}\partial_\mu\right) \mathrm{e}^{-ig\,\hat{\theta}_a(x)}. \end{aligned} \tag{1.11}$$

But in order to gain full predictive power the theory must undergo two fundamental procedures: the first is quantization, or the promotion of classical

fields to field operators that act on quantum state vectors of a pertaining vector space, generally ending up with a perturbative formulation put in a diagrammatic fashion thanks to the development of a set of so-called "feynman rules"; the second is renormalization, or the careful reanalysis of a theory in order to avoid the showing up of infinitives when calculating physical amplitudes at all orders of perturbation theory, usually ending up with a redefinition of the experimentally measured parameters. The first procedure is particularly interesting, but not being directly relevant to the matter of this thesis; thus, only a particular feature will be discussed in what follows: the running of the QCD coupling constant.

§ **1.1.3. The set of symmetries.**— The QCD Lagrangian (1.6) is constructed to be invariant under the action of the standard symmetry group:

$$\mathscr{G}_l = SU_c(3) \otimes SO^+(1,3) \otimes \mathscr{F} \tag{1.12}$$

i.e. the local colour gauge group and the usual proper, orthochronous Lorentz group with metric signature $(+,-,-,-)$ [Bjorken and Drell textbook scheme: $\rightarrow$ [16], preamble section "Units and Conventions"]; $\mathscr{F} = \{\hat{P}, \hat{C}, \hat{T}\}$ is the set of discrete symmetries.
In addiction to $\mathscr{G}_l$ there is a group of global symmetries which are approximately realised or valid under certain assumptions. If the flavours would not show any mass hierarchy, i.e. $m = m_q \mathbb{I}$, then eq. (1.6) would contain a further $SU_f(6)$ flavour symmetry. This is not true in nature, but an approximate $SU_f(3)$ and the product representation:

$$\mathbf{3} \otimes \mathbf{3} \otimes \mathbf{3} = \mathbf{1} \oplus \mathbf{8} \oplus \mathbf{8} \oplus \mathbf{10}, \tag{1.13}$$

are the basis of the "Eightfold Way", including the famous baryon octet and decuplet representations that led to the explanation of hadrons as bound states of quarks (one can do a similar decomposition for mesons), and to the prediction, with subsequent discovery, of the Ω^- particle. Its $N_f = 2$ realisation for the light quarks, is approximatively realised in nature due to the small difference in mass ($m_u \approx m_d$) and generally knows as "isospin" symmetry in nuclear physics. In many theoretical applications it is also taken as exact.
Much more interesting is the $m_i \rightarrow 0$ limit. Under this circumstance in fact, one can operate a decomposition of the q fields - and of the Lagrangian - by means of the following projectors:

$$q_L = (1 - \gamma_5)q \qquad q_R = (1 + \gamma_5)q, \tag{1.14}$$

based on the application of the fifth Dirac matrix $\gamma_5 = i\gamma_0\gamma_1\gamma_2\gamma_3$ (with eigenvalues ± 1), that lets the separation of (L)eft and (R)ight handed components, with a meaning equivalent to the helicity of massless particles. The Lagrangian is then equivalent under a new class of transformations, with elements that belong to the group $SU_L(N_f) \times SU_R(N_f)$:

$$q_L \to e^{-i\tau_f^j \theta_L^j} q_L \tag{1.15}$$

$$q_R \to e^{-i\tau_f^j \theta_R^j} q_R; \tag{1.16}$$

the τ_f^j matrices are their group generators, and θ a set of global parameters. Such a symmetry was called "chiral" referring to the handedness of the states, from the greek χείρ, meaning "hand". In eq. (1.6) in nature it is explicitly broken by the presence of the mass term, but it is thought to be exactly realised in the QCD-dominated phase of our expanding Universe during the Big-Bang, and dynamically broken in the QCD phase transition.

§ **1.1.4. Running coupling and asymptotic freedom.**— The strength of an interaction in Quantum Field-Theories is expressed by the value of the coupling constant g. The name comes from the fine-structure constant of the ElectroMagnetic interaction:

$$\alpha = \frac{e^2}{4\pi} = \frac{1}{137} \ll 1, \tag{1.17}$$

whose small value justified the success of Quantum ElectroDynamics (QED) and its perturbative approach, allowing for a convergence of the relative series (even if it was found to be asymptotic!). It was soon discovered though, that the coupling is not constant at all, and that QED was apparently a particular case because the vast majority of its processes take place at a low energy scale. At the Z^0 boson scale (~ 90 GeV), for example, the coupling is 1/127.

The study of how a coupling g changes with the energy scale k is a central topic of the Renormalization Group theory; but it is a problem even deeper: QFTs give infinitive predictions at one-loop level due to intermediate high momentum states. The procedure of renormalization deals with these infinities combining them with the bare parameters of the Lagrangian and absorbing them in the renormalised parameters. The divergences are typically renormalised at some energy scale k; the observables cannot be k dependent, but quark masses turn out to be [→ tab. 1.1, last column]. The

aim of the Renormalization Group theory is then to solve the so-called "flow equation":

$$k\frac{\partial g}{\partial k} = \beta(g); \tag{1.18}$$

the right hand side is called β function and its evaluation, partially possible with perturbation theory in a narrow range of small g values (and also experimentally, in a discrete set of values), is crucial for the predictive power of the overlying QFT. In particular, the sign of β is very important: in QED it is positive, thus the resulting coupling is monotonically growing and leading to the Landau pole at infinite energy - a sign of the fact that perturbation theory loses its sense at some energy scale; in QCD it is negative, reaching some fixed point k^* in which $\beta(k^*) = 0$ at high energy. Keeping at next-to leading perturbative order (NLO) and following the most used procedure, known as "Minimal Subtraction scheme" ($\overline{MS}$), β depends only on g and can be expanded as:

$$\beta(g) = -\beta_0 g^3 - \beta_1 g^5 + \mathrm{O}(g^7); \tag{1.19}$$

the two coefficients of g, that in turn depend on N_f and are positive when $N_f \leq 8$, leading to a negative β are:

$$\beta_0 = \frac{1}{(4\pi)^2}\left(11 - \frac{2}{3}N_f\right) \tag{1.20}$$

$$\beta_1 = \frac{1}{(4\pi)^4}\left(102 - \frac{38}{3}N_f\right). \tag{1.21}$$

Generally the QCD coupling constant is given, to leading order (LO), as a function of the coupling strength g:

$$\alpha_s(k) = \frac{1}{4\pi\beta_0 \ln(k^2/\Lambda^2_{\mathrm{QCD}})} \tag{1.22}$$

as a logarithmically decreasing function of k, taken over a scale set by the parameter Λ_{QCD}. This is k-independent and to be fixed in experiments, in order for α_s to be determined. Its value must be given specifying the N_f and the subtraction scheme, i.e. the procedure used to obtain β_0 and β_1, due to their dependence in determining α_s. Quark masses calculated in the $\overline{MS}$ scheme are given in the last column if table 1.1; the scale parameter used is $\Lambda_{\overline{MS}} = 217 \pm 24$ MeV, under the bottom quark mass, for $N_f = 5$ "active" flavours.

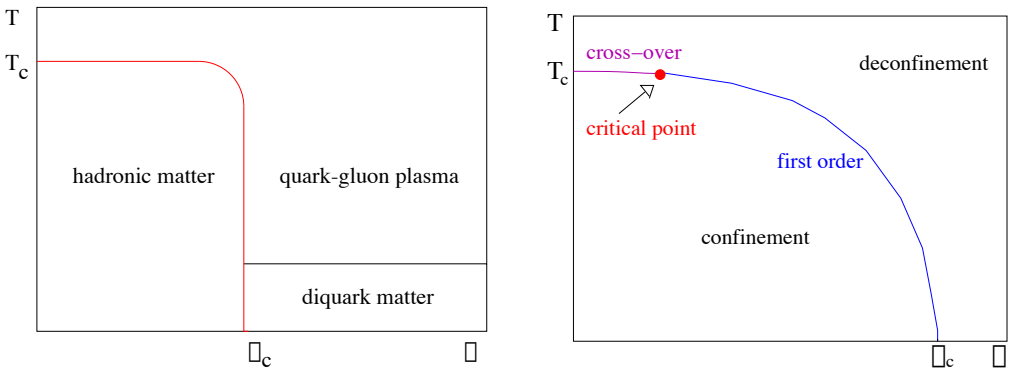

Figure 1.1: QCD (T, μ) Phase diagrams. *Left*: qualitative, as stated in § 0.1.6. *Right*: complete synthesis of the transition properties. Taken from ref. [22]

The negative β behaviour, discovered by the Nobel Prizes winners F. Wilczek, D. Gross [20] and D. Politzer [21], is known as "asymptotic freedom", and is a striking feature of Yang-Mills theories: the strength coupling decreases with increasing energy scale, explaining the partonic results of deep inelastic scattering experiments of the end of the 60s, in which highly energetic partons in hadrons seemed to initially react as free particles during collisions with suitable probes. The QCD *vacuum* thus shows an effect called "anti-screening": virtually polarised gluons enhance colour charge in the *vacuum* and change its colour.
The running coupling of eq. (1.22) goes to infinity in the range $[0, \Lambda_{\mathrm{QCD}}]$: this suggests that no perturbative approach has any sense therein and generally around the upper limit of ~ 200 MeV. The low energy limit of QCD is not perturbatively solvable and pertains to the experimentally observed feature of "colour confinement", i.e. the impossibility to isolate a colour charge. QCD is the definitive theory of strong interactions, but its relatively simple perturbative approaches - that had many success when dealing with other QFTs - fail in explaining the most common situation in our present Universe: the existence of white baryons and mesons, atomic *nuclei* and all the periodic table of elements.

1.2 Phase transition

Due to the two different realisations of QGP believed to exist in nature, as described in § 0.1.6, it is natural to observe and represent the states of strongly interacting matter in terms of its temperature T and baryonic density ρ_B - or alternatively the correspondent chemical potential μ_B. It is easy

to imagine that two phases of matter must be linked by some phase transition or critical phenomenon, just like a bridge connecting two banks of a river or a continuous function that changes its sign crossing the *abscissae* axis. The situation is depicted in the left panel of fig. 1.1: the hadronic and QGP phases are separated by a continuous line of transition points. Any system in the low (T, μ) hadronic region, i.e. in which both $T, \mu \ll \Lambda_{\mathrm{QCD}} \sim 200$ MeV, can be heated and/or compressed until it deconfines to a QGP, crossing the boundary at some $(T, \mu)_c$. In addition, at $T \to 0$ and $\mu > \Lambda_{\mathrm{QCD}}$, the QGP is realised in a state called "colour superconductor", with the analogue of Cooper pairs condensing at low temperature. The correlated states will melt just by heating.
The aim of this section is to elucidate the nature of the phase transition, whose properties are sketched in the realistic diagram of the right panel of fig. 1.1. The matter is not supposed to be highly technical - such a treatment is beyond the aim of this thesis; it is much more interesting to have a decent share of phenomenological insight on the problem. Together with the textbooks already cited, the following is based on a series of lectures given during 2009 by prof. H. Satz in Catania. An excellent transcription can be found in ref.[22].

§ **1.2.1. A crude model for the transition.**— A very easy model of the transition can be given introducing a drastic set of assumptions and starting from two ideal systems: a gas of massless pions and a QGP gas made of free and degenerate massless constituents. The pressure as a function of temperature for the first system can be expressed by a Stefan-Boltzmann law in a fashion similar to the treatment of blackbody radiation:

$$P_\pi = d_\pi \frac{\pi^2}{90} T^4, \tag{1.23}$$

where the degeneracy factor $d_\pi = 3$ accounts for the three charge states of the pion, which is a spin 0 boson internally composed by different superpositions of $u\bar{u}$ and $d\bar{d}$ states (photons would require $d_\gamma = 2$ for their polarization states). Once they melt they form a system of $N_f = 2$ and $N_c = 3$, whose degeneracy factor is:

$$d_{\mathrm{QGP}} = (2 \times 8)_g + \frac{7}{8} (3 \times 2 \times 2 \times 2)_q = 37, \tag{1.24}$$

that accounts for 2 spin and 8 colour degrees of freedom for the gluons plus 3 colours, 2 flavours, 2 spin configurations and 2 particle/antiparticle states for

the quarks, plus a 7/8 factor that accounts for a difference in the statistics (the Bose distribution at $\mu = 0$ is slightly broader than the corresponding Dirac for fixed single particle energy E). The corresponding pressure is given by:

$$P_{\mathrm{QCD}} = 37\frac{\pi^2}{90}T^4 - B; \tag{1.25}$$

the B parameter - called Bag constant - is a contribution that takes into account the difference between the physical *vacuum* and the ground state for quarks and gluons in a medium, and it is fixed to tune model predictions on physical values. In literature this way to sketch the QGP thermodynamics is called "MIT Bag model" [→ § 3.3.1] because it is the simplest and crudest way to "confine" quarks - hence the name for B.
From general thermodynamic arguments a system chooses the state of lowest free energy and consequently of highest pressure: the pressure of the two gases (1.23,1.24) are reported in the left panel of fig. 1.2, where it is possible to check that the hadronic gas is favoured up to a critical temperature:

$$T_c = \left(\frac{45}{17\pi^2}\right)^{\frac{1}{4}} \mathrm{B}^{\frac{1}{4}} \simeq 0.72\,\mathrm{B}^{\frac{1}{4}}; \tag{1.26}$$

this result, combined with $\mathrm{B}^{\frac{1}{4}} \simeq 0.2$ GeV, an estimate from hadronic spectroscopy, yields:

$$T_c \simeq 150\,\mathrm{MeV} \tag{1.27}$$

as deconfinement temperature. A similar calculation for the energy density ϵ is reported in the right panel of fig. 1.2: the discontinuity at T_c is the latent heat of deconfinement. The transition is - by construction - of the first order.
As seen in § 1.1.4, QCD is perturbatively solvable only in the asymptotically free regime, which clearly is opposite to the deconfinement phase transition of interest here. Nevertheless, QCD was discretised and numerically solved on a lattice with - at least initially - huge difficulties and demand for high computational power. Current calculations give as a value for the critical temperature around $T_c \simeq 175$ MeV, not so far from the crude estimate given here.
The transition, according to the right panel of fig. 1.1, is exactly first order at $T = 0$, and continues up to T_c as a line of first order transitions; the critical point is exactly second order, and beyond this there is no transition anymore, just a rapid crossover with exchange of the degrees of freedom.

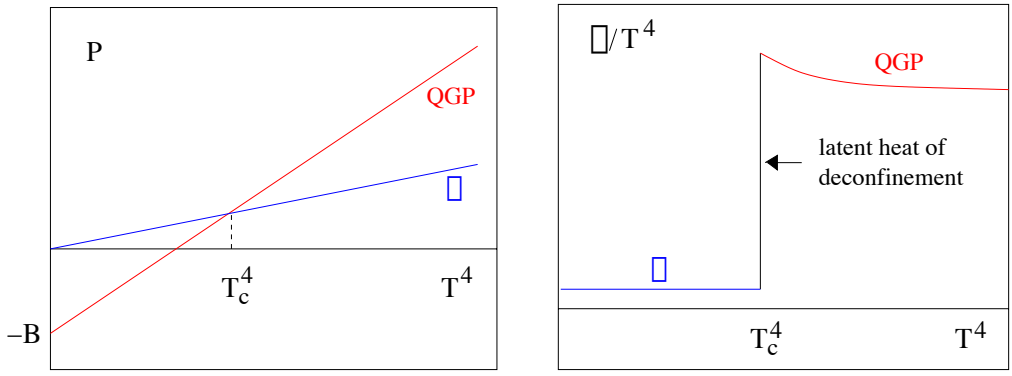

Figure 1.2: Pressure and energy density of pion and quark-gluon gas model of § 1.2.1. Taken from ref. [22]

§ **1.2.2. Lattice QCD.**— To go beyond the perturbative level and probe the theory in its "colour confining" limit, QCD is formulated in a finite temperature quantum field scheme, in which the lagrangian (1.6) is used as an input of the partition function Z of statistical mechanics, suitably expressed in a path integral functional:

$$Z(T,V) = \int \mathrm{d}A\,\mathrm{d}q\,\mathrm{d}\bar{q}\ \exp\left[-\int_V \mathrm{d}^3x \int_0^{\frac{1}{T}} \mathrm{d}\tau \mathcal{L}_{\mathrm{QCD}}(A,q,\bar{q})\right]; \qquad (1.28)$$

in the thermodynamic limit $V \to \infty$. Much more remarkable is the way in which the temperature enters the scheme: T is related to the thickness of the integration over τ (whose upper limit is $\beta = 1/T$), obtained by means of an imaginary rotation for the temporal component $\tau = ix_0$ in the path integral of eq. (1.28), thus turning the 4d-Minkowski space in which the fields are defined into an Euclidean manyfold. With this trick Temperature takes the role of imaginary time integration. The partition function can be evaluated non perturbatively, but numerically, by means of a particular regularisation scheme with subsequent discretisation; once it is known, one can calculate every thermodynamical quantity by means of its derivatives - according to the prescriptions of statistical mechanics [→ cap. 2].

§ **1.2.3. Proof of phase transition.**— In order to understand the picture coming from the first lattice simulations it is necessary to define two important variables connected with the transition. The first is the quark effective mass, or the temperature-dependent expectation value in the *vacuum* of the Lagrangian term $\langle\bar{q}q\rangle(T)$; the latter is the so-called "Polyakov Loop",

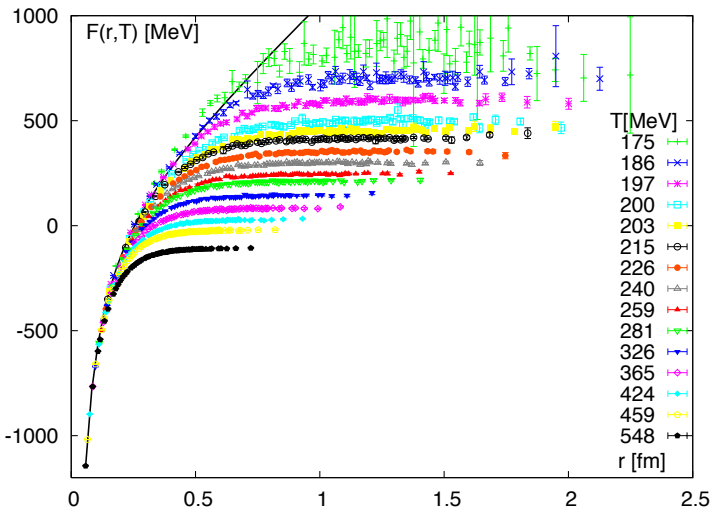

Figure 1.3: The color singlet quark-antiquark free energies $F1(r;T)$ at several temperatures close to the phase transition as function of distance in physical units - Results from lattice studies of 2-flavor QCD. Taken from ref. [23]

a name that identifies the quantity:

$$L(T) \sim \lim_{r\to\infty} \exp[-V(r)/T], \tag{1.29}$$

where V is the potential between a static heavy $q-\bar{q}$ pair at spatial distance r. Fig. 1.3 reports the free energy F of such a system for 2 flavour lattice simulations. This quantity can be used - under some assumptions - as a potential energy in charmonium studies and can be here taken as a good example. In a pure $SU(3)$ gauge theory - i.e. without light quarks - $V(r) \sim \sigma r$, with σ a positive constant called "string tension" (black line in fig. 1.3): under these circumstances $L(T) = 0$. By converse, in a deconfined medium, the high temperature - and consequently the onset of deconfinement - leads to colour charge screening, with $V(\infty)$ converging at some finite value (dots in fig. 1.3), and $L(T) > 0$. The peak in the Polyakov Loop susceptibility $\chi_L(T) \sim \langle L^2\rangle - \langle L\rangle^2$ can be interpreted as the critical temperature.
Any evaluation of QCD with bare masses $m_i \to 0$, i.e. in the chiral limit [→ § 1.1.3], the quarks gain an effective mass due to the dynamically spontaneous breaking of chiral symmetry, that leads to a non-vanishing value of $\langle\bar{q}q\rangle \sim 300$ MeV (typical value for a valence quark inside a proton). This symmetry is believed to be restored at sufficiently high temperature, in the deconfined phase. If the quark bare mass matrix is non vanishing, chiral symmetry is only approximated, so that the chiral limit is never reached.

Lattice QCD simulations in some particular limits can give enough supporting evidences for a phase transition:

- **Diverging bare quark mass $m_i \to \infty$:** quark dynamics become negligible and QCD reduces to a pure $SU(3)$ gauge theory. The transition is exactly analogous to a 3 spin Potts model [24] i.e. shares its same critical behaviour, with spontaneous Z_3 global symmetry breaking (Z_3 is the so-called discrete centre symmetry of $SU(3)$); the proof for QCD was given by Svetitsky and Yaffe [25] - the transition is second order for $N_c = 2$ and first order for $N_c = 3$.

- **Finite bare quark mass:** separating indefinitely a couple of quarks makes the potential V grow up to the point at which a $q - \bar{q}$ couple is polarised from the *vacuum*, corresponding to the creation of a hadron of mass M_H: hence V becomes arbitrary small but never vanishes, so that $L(T) \sim \exp[-V(M_H)/T]$. The situation is analogous to the ferromagnetic phase transition, in the case of a finite external field.

- **Vanishing bare quark mass $m_i \to 0$:** if one simulates QCD in the chiral limit [→ § 1.1.3], the quarks gain an effective mass due to the dynamically spontaneous breaking of chiral symmetry, that leads to a non-vanishing value of $\langle \bar{q}q \rangle \sim 300$ MeV (typical value for a valence quark inside a proton). This symmetry is believed to be restored at sufficiently high temperature, in the deconfined phase.

At vanishing μ_B then Lattice QCD predicts the onset of two transitions: one, to colour deconfinement, whose order parameter is the expectation value of the Polyakov Loop $L(T)$; the second, to chiral symmetry restoration, driven by the suppression of dynamical generated effective mass for quarks. Both chiral and Z_3 symmetries are only approximated in the physical case of interest of m_i finite; analizing the peaks in the second derivatives of the two order quantities - i.e. their susceptibilities - it is possible to see that the two transitions coincide in the considered limit - the proof is given in [26]. The critical temperature lies in the range $150 \div 200$ MeV.

§ **1.2.4. Nature of the transition at $\mu_B = 0$ and finite μ.**— Such a temperature lets any approach to stop at the $N_f = 3$ light quarks level; the physical situation discussed in the previous paragraph is synthesised in fig. 1.4. The nature of the transition at $\mu_B \to 0$ depends quite sensitively on the number of flavours N_f and the quark mass values:

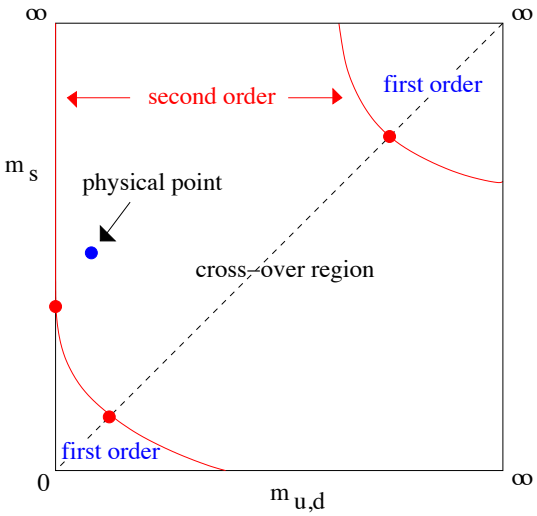

Figure 1.4: Three flavour diagram on the nature of the QCD phase transition at $\mu_B \to 0$. Taken from ref. [27]

- If $m_i \to \infty$, the case of pure $SU(3)$ gauge is recovered, and the phase transition for $N_c = 3$ is of the **first order**.
- If $m_i \to 0$, the Lagrangian is chirally symmetric. For three massless quarks the transition is again of the **first order**.
- If $0 < m_i < \infty$, none of the above is true; the area of first order discontinuity disappears on a line of second order transitions, above which there is a rapid **crossover**, with a rearrangement of the degrees of freedom: i.e. no phase transition in the sense of the description by means of a partition function; the physical situation, with small, approximatively equal m_u, m_d masses and bigger m_s lies certainly in this region.

In the case of finite μ_B there are lots of numerical difficulties, as the algorithms break down on states with negative norm. It seems that some of the difficulties were overcome, confirming the existence of a crossover region, that ends on a critical point - in which the transition is of the **second order**, followed by a continuous line of **first order** points that end at $T = 0$ [→ fig. 1.1, right panel].

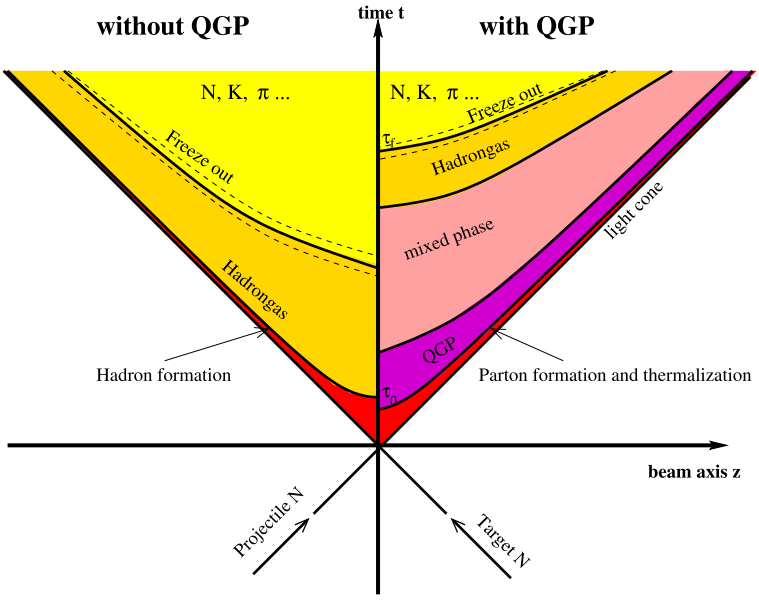

Figure 1.5: Dynamical evolution of the fireball in a case without (left) and with QGP (right). Taken from ref. [28]

1.3 Experimental evidences

This section is devoted to give a brief review of the experimental situation. After the CERN announcement of year 2000 about the "evidence for a new state of matter" [→ § 0.1.5] and the last ten years of surveys at RHIC (Brookhaven) - with preliminary data also coming from the CERN LHC (Geneva) - there seems to be enough evidence to finally proof the existence of QGP and to pin down a considerable amount of its features.
There are several difficulties in understanding the experimental picture, when coming from a theoretical background as the one briefly stated in the last sections; theory gives - under the strong assumption of thermodynamical equilibrium - results in terms of static observables: pressure and energy density of the plasma, to give an example. But the experimental picture is quite different: two *nuclei* with sufficiently high mass number A collide with a certain center of mass energy per nucleon pair $\sqrt{S_{NN}}$, at a given degree of centrality. The impact generates a core high energy density, called "fireball", that has two subsequent evolutions - depending on the event of QGP formation, as shown in fig. 1.5. Usually a large part of the energy is spent on a timescale of 1 fm/c in anelastic events (partonic excitations, QGP formation, etc.), with following hadronisation, leading to the observed particle distribution. Any observation is therefore indirect, and refers to non equi-

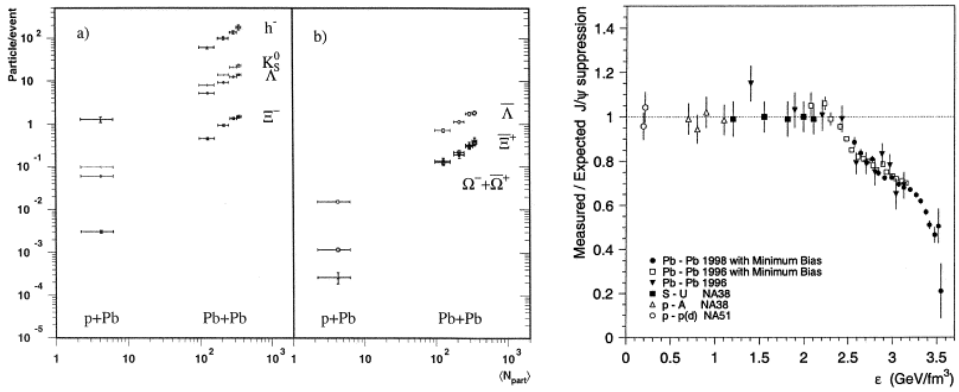

Figure 1.6: QGP signatures. *Left*: Strange particle enhancement versus strangeness content [29]. *Right*: Measured J/ψ production yields, normalised to the yields expected assuming that the only source of suppression is the ordinary absorption by the nuclear medium. The data is shown as a function of the energy density reached in the several collision systems [30].

librium observables, relying on a careful confrontation with purely hadronic scenarios. How is it possible to judge whether QGP was produced during an experiment? A first, rough estimate can be given using Bjorken formula for the energy density ϵ_0 of a fireball:

$$\epsilon_0 = \frac{1}{\pi R^2 \tau_0} \left(\frac{\mathrm{d}E_T}{\mathrm{d}y} \right)_{y \simeq 0}, \tag{1.30}$$

that is a function of the timescale of the collision τ_0, of the nuclear radius R and of the derivative of the total transverse energy E_T with respect to rapidity. A temperature of 170 MeV roughly corresponds to $\epsilon_0 \simeq 0.9$ GeV/fm^3.

§ **1.3.1. The signatures at CERN SPS.**— The Super Proton Synchrotron started its heavy ion programme in 1987, after being modified, with Sulfur and Oxygen beams with energies of 200 GeV per nucleon. In 1994 a Lead beam with energy 158 A GeV was made available for the experiments. At such energies, the lorentz-contracted nuclei have Ultra-Relativistic dynamics and can be thought as a collection of coherent free nucleons, not bound anymore. One might imagine a collision between two such systems as a large number of individual $n-n$ collisions, but the results proven the existence of some new collective effects, whose nature was interpreted to be a QGP.
The experimental results from the various collaborations showed indeed a series of possible "signatures" of a QGP formation, that all together led to the famous announcement. Using relation (1.30) and a measured $\mathrm{d}E/\mathrm{d}y$ of

450 GeV in Pb+Pb collisions, one obtains:

$$\epsilon_0 = \frac{1}{3.14 \times (8.3\,\mathrm{fm})^2 \times 1\,\mathrm{fm/c}} \times 450\,\mathrm{GeV} \approx 3\,\mathrm{GeV/fm^3}, \tag{1.31}$$

a value that exceeds the 0.9 GeV/fm^3 needed in order for the fireball to reach T_c, roughly pointing towards a QGP scenario. An excellent review is given in J. Stachel [31]. Briefly, a short compilation of the most interesting:

- **Strangeness enhancement:** the colliding nuclei have no strangeness content; the yields of strange K^0_s mesons, Λ, Ξ, Ω baryons and their anti-particles are studied in Pb+Pb collisions at the West Area 97 experiment [29] and confronted with the corresponding yields from p+Pb reactions, and plotted against the number of participants (fig. 1.6, left panel). A strong enhancement in strangeness production is observed (several orders of magnitude), and a further enhancement with growing strangeness content (particle specie). The high survival ratio seems to favour a QGP scenario over the standard hadronic one, in which a longer hadronization time should suppress more strange particles, due to their short lifetimes.

- J/ψ **suppression:** this was proposed as a clear signal for deconfinement already in 1986 [15] - an extensive citation from the authors is reported in sec. 0.1 [$\rightarrow$ § 0.1.5]. The North Area 38 and NA 50 experiments performed measurements of J/ψ and Drell-Yan cross-sections in Pb+Pb collisions and confronted them with the cross-sections obtained in several different setups: p+p, p+A, and A+A, reconstructing the $\bar{\mu}\mu$ Branching-Ratio, as a sum of various contributions (e.g. invariant mass spectrum of J/ψ and Drell-Yan processes) [32, 33]. They reported an evident suppression that goes up to the 70% of the trend-expected yield (fig. 1.6, right panel), stating that such a result could not be explained by the known hadronic suppression processes [30]. This particular effect, due to the cleanliness of results and to the high significance of the measure, has been cited as the most promising among the QGP signatures.

- **Enhancement of low mass dileptons:** similarly to the previous case, the invariant mass spectrum of e^+e^- was measured with more than 42 million events from the CERES spectrometer [34], reconstructing

the low mass vector mesons such as π^0, η, ρ, etc. in p+Be, p+Au and Pb+Au collisions; electrons produced in such decays have mean free paths much longer than the size of the fireball, so that they can carry information about the different stages of the collision. The observed spectrum shows a significant excess in the mass region below the ρ meson peak; the annihilation of thermal pions $\pi + \pi \rightarrow e^+e^-$ partly accounts for the excess, showing signs of a hot and dense medium, but fails in reproducing the whole dilepton excess.

- **Observation of direct photons:** under the assumption that QGP should be responsible for thermal photon emission, the total γ spectrum was reconstructed in p+A and Pb+Pb collisions by the West Area 98 experimental collaboration[35]; about the 97% of the observed spectrum, due to hadronic digamma decays such as $\pi^0 \rightarrow \gamma + \gamma$, was classified as bias; when confronting the multiplicities for the two cases, a sensible enhancement was find around $p_T = 2$ GeV/c in the Pb+Pb spectrum. An attempt was made on smaller systems: ^{32}S+Au collisions did not show a corresponding excess, which may point towards the initial hypothesis.

Even if no one could deny that new physics was found at CERN SPS, a considerable part of the scientific community did not believe in the QGP picture, stating that different evidences in dedicated experiments could not necessarily be added up to prove its existence. The need for new data, and new observations - possibly combined in the same experimental setup - shifted the interest of the community towards RHIC in year 2000.

§ **1.3.2. RHIC.**— The Relativistic Heavy Ion Collider situated at the Brookhaven National Laboratories in Upton, NY, is the first facility entirely dedicated to heavy ion collision experiments. It is operative since year 2000, and is capable of beams up to Au, with a maximum center of mass energy per nucleon pair $\sqrt{S_{NN}} = 200$ GeV. During year 2005 a BNL internal formal report was prepared and distributed on the Web [36]; it contained four review papers with preliminary results from the experimental activity. To date, the picture of RHIC discoveries is still very fragmentary; nevertheless while on one side some of the SPS evidences have been confirmed, other new features have been discovered:

- **Strongly coupled liquid:** what was once thought to be a gas of free

(weakly coupled) quarks and gluons, turns now out to have a perfect liquid behaviour (with very small viscosity; from estimates $\eta/s \sim 1/4\pi$, the lowest known for any liquid) whose particles interact strongly among themselves. This was possible thanks to careful reproduction of the early stages of the collision, like the measurement of the anisotropy in momentum space of the produced particle distributions in non-central collisions (the so-called "elliptic flow").

- **Jet quenching:** the observed yield of high p_T jets in A-A vs. p-p collisions shows a strong suppression with growing A, possibly related to anelastic interactions of the partons in the hot QGP medium.

- **Colour Glass Condensate:** it seems that the lorentz-contracted *nuclei* arrive at the transition with sort of "gluon walls", whose properties recall those of a glass (highly disordered state in which matter behaves on short timescales like a solid, while on longer timescales like a liquid) carrying the colour charge of its constituents gluons that are very dense, thus forming a condensate.

- **Parity violation:** very recent observations of the STAR Collaboration [37] seem to point towards Parity violations in strongly-interacting matter. The authors also indicate possible observables sensitive to such effects.

§ **1.3.3. Perspectives @ LHC.**— The much awaited upgrade of CERN colliders finally came in 2008, with the first runs of LHC. Lead ion experiments started on November 2010; the program lasted for 2 months, providing beams of *nuclei* with center of mass energy per nucleon pair $\sqrt{S_{NN}} = 2.76$ TeV, ten orders of magnitude more than RHIC. Preliminary results from the dedicated facility ALICE (A Large Ion Collider Experiment) [38] and ATLAS [39] so far confirm the trends of most of the SPS and RHIC discoveries, extending them smoothly to upper energy ranges (e.g. an increase of 30% of RHIC observed Elliptic Flow). Probably the most expected and interesting result is on J/ψ suppression, that seems to be decreased from RHIC results; for the first time it was observed the new phenomenon of Υ mesons suppression. It is of November 15th, 2011 the announcement of a new round of Lead beam experiments at LHC. The data collected will help to make the situation more clear and hopefully grasp the exotic and exciting QGP properties.

Part II

Theoretical framework

One of these movements [of quantum liquids] is normal, i.e. possesses the same properties as the movements of usual liquids; the other is superfluid.

L. D. Landau - Phys. Rev. **60**, 356(1941)

2

The system and its static properties

The states of Electromagnetic interacting matter - usual matter we have experience of everyday - can be described by some macroscopic theory (elasticity, mechanics, thermodynamics, fluid dynamics, etc.) whose input is a microscopic theory (solid state physics, kinetic theory of gases, etc.). This chapter is dedicated to the macroscopic equilibrium properties of strongly interacting matter, obtained by means of statistical mechanics and thermodynamics of liquids. A central role is played by the concept of "quasiparticle", a theoretical unit introduced in order to overcome the difficulty of treating interactions in many body systems: instead of calculating all the sums of two body potentials, one imagines the motion of a single particle in a *medium* composed by all the others, a sort of effective potential. This in turn leads to the renormalisation of its mass, so that, similarly to the case of an electron inside a metal, the sigle-particle motion is described as the motion of a free particle with different mass, whose difference accounts for the effect of the interaction. General arguments are taken from the textbooks of A. Fetter and J. Walecka [40], P. Nozieres [41], G. Baym and C. Pethick [42].

2.1 Strong-interacting constituents

The system - from the greek word Σύστημα, "whole compounded of several parts" - i.e. the subject of the investigation of this thesis - is an indefinitely large aggregate of strongly interacting protons and neutrons in β equilibrium. Its microscopic properties are determined by the small scale nature of the interaction, and are responsible for the macroscopic thermodynamical and hydrodynamical properties that itself shows in its physical realisations: from the bulk properties of *nuclei*, up to Neutron Stars.
As thoroughly discussed in Chapter 1, the natural observables of such a system are temperature T and baryonic density ρ_B - or correspondingly their

chemical potential μ_B; the system is expected to undergo a phase transition at a certain value of the pair (μ_c, T_c); at the present moment there is no theory that satisfactorily incorporates a mechanism for the transition, so that the two phases are studied separately and the transition is later on imposed, in order to study its effects.
This section is devoted to the sketching of "Nuclear Matter", technically meaning a Normal Fermi Liquid of Quasiparticles - in its broadest sense, i.e. allowing for the system to undergo a phase transition to a deconfined phase of QGP. As a liquid, it is essentially made by dense particles at a low temperature far from phase transition to gaseous/solid or superfluid phases, that interact within themselves by some sort of residual interaction.

§ **2.1.1. The idea of Nuclear Matter: Fermions.**— The basic constituents of the system are identical fermions: protons p, neutrons n and electrons e^- in one phase, up u, down d and strange s quarks in the other. When closely packed, and at such low temperature, the quantum correlations can not be ruled away: the particles try to occupy all the possible single particle states according to Fermi-Dirac statistics and thus experiencing the Pauli principle, that prevents identical particles from having the same set of quantum numbers.
The simplest strongly interacting system built on this simple ideas is the *nucleus*: the idea of "Nuclear Matter" comes directly from the systematics of nuclear properties. In particular, the binding energy B of a nuclide with Z protons and N neutrons and mass number $A = N + Z > 20$ - is given from the semi-empirical mass formula from Bethe and von Weiszäcker:

$$B = -a_1 A + a_2 A^{\frac{2}{3}} + a_3 Z^2 A^{-\frac{1}{3}} + a_4 (A - 2Z)^2 A^{-1} + \delta(A, Z), \qquad (2.1)$$

as a sum of terms that account respectively for its volume, surface, Coulombian, asymmetric and pairing properties. The corresponding parameters a_i, with $i = \{1, ..., 5\}$ are determined from a best-fit on experimental data.
The heaviest *nuclei* observed in nature have almost $A \simeq 300$; dropping the pairing term a_5, eq. (2.1), in the limit $A \to \infty$, describes a system in which only the a_1 and a_4 terms survive. This extrapolation is the central idea for the concept of Nuclear Matter: it can be imagined as a static homogeneous bulk of nucleons in arbitrarily large number, so that the Thermodynamic Limit is valid and the volume V is substituted by the two densities $\rho_n = N/V$ and $\rho_p = Z/V$ pertaining to the respective chemical species; the Electromagnetic interaction is "switched off" as it would give mathematical divergences

when dealing with thermodynamics, due to its relative local strength: this hypothesis is justified by the further assumptions of local charge neutrality and β-equilibrium, that introduces an non-vanishing electron density ρ_e in the system:

$$\rho_p = \rho_e \tag{2.2}$$

$$p + e^- \leftrightarrows n + \nu_e \tag{2.3}$$

where the ν_e (neutrinos) are *medium* transparent - thus escape; three fermionic degrees of freedom with two superimposed relations among them leave only one free quantity, that could be the density of one specie; but - of much more interest for the idea of a later phase transition - in practical matters the total baryon density is chosen:

$$\rho_B \equiv \frac{A}{V} = \rho_n + \rho_p, \tag{2.4}$$

together with ρ_e and $\rho_3 = \rho_n - \rho_p$, or the isospin (third-component) density, accounting for the stoichiometric asymmetry of nucleonic species. Isospin is an approximate $SU_f(2)$ light-flavour symmetry of the strong interaction, hence valid also at nuclear level; it was briefly discussed in § 1.1.3; the quantity $I = \rho_3/\rho_B = (N - Z)/A$ is called "asymmetry parameter", and appears in the homonym a_4 term of eq. (2.1). An extrapolation of nuclear characterstics finally leads to strongly interacting matter whose bulk properties are regulated by its particle-density.

§ 2.1.2. Why a Normal Liquid?.— Lev Landau wrote a lot of physics about quantum liquids, finally winning the Nobel Prize in 1962 for his phenomenological model of superfluid Helium II [43]; he used to distinguish the superfluid motion of the particles in a liquid from the "normal" motion, so that finally the name "normal liquid" was used to indicate a quantum liquid, i.e. a many-body system of weakly EM interacting atoms whose thermal de-broglie wavelength is comparable with the typical interatomic distance.
This definition can be extended for a liquid of strongly interacting fermions stating that is the temperature T the parameter to look at [→ § 0.1.3]: such a system, at a temperature low enough to make unavoidable the quantum effects, but to rule out any possibility of superfluidity. A nuclear temperature [→ App. A] of $k_B T = 1$ MeV corresponds to $T = 1.134 \times 10^{10}$ K: these extreme conditions for electromagnetic matter can be easily regarded as a

$T \to 0$ limit for Nuclear Matter, when confronted with the typical excitation energies of *nuclei*. For this reason, unless explicitly stated, the temperature will be ideally set at $T \to 0$ limit on the MeV scale, leaving ρ_B as the only scale to look at with respect to QGP and liquid properties. This assumption finds proper justification in the applications.

§ **2.1.3. Residual interaction and Quasiparticles.**— At liquid phase, matter is condensed, thus packed at a density comparable with ions in a solid, and much higher than particles in a gas. Such a state is maintained by the temperature, that plays an equally important role in phase transitions. A third characteristic of liquids, not yet discussed, is the form of the interactions: this microscopic input is responsible of much of its phenomenological properties, and must be understood in order to attack the problem from a theoretical point of view. The Many-Body problem for a liquid contains a huge number of two-body interactions that can be very complicated to treat: this justifies the introduction of Quasiparticles.
The original semi-phenomenological treatment of normal Fermi liquids devised by Landau and his coworkers is based on two striking microscopic ideas: (i) the adiabatic switch on of the interaction, that (ii) transforms the single particle states of the free particles in a Fermi gas into the energy levels of an interacting quantum liquid. Pauli Blocking prevents the low lying occupied states from any exchange or excitation, so that the only interacting particles lie around the Fermi surface. Here, the theory solves the problem with the concept of quasi-particles, the quantised collective excitations that arise in the *medium* and acquire a renormalised mass, due to the interaction - or "dressing" - of a "bare" particle with all the others as a whole.
The idea of treating Nuclear Matter in such a scheme has been extensively studied in literature; in particular, many positive efforts were carried out by A. B. Migdal and are reported in the book [44]. In practical matters the static properties - like the compressibility or the internal energy of the system - are calculated by means of statistical thermodynamics and the complicated Many-Body problem is solved within the Hartree-Fock scheme in a perturbative/diagrammatic fashion, obtaining a free gas-like single quasiparticle spectrum and thus virtually "cancelling" the interactions in an effective way. The full quantum liquid approach becomes necessary when one is interested in the dynamical non-equilibrium characteristics of the system, like

the calculation of the first and second viscosities, of collective excitations and the transport parameters. This point is extensively treated in a book of H. Hoffmann [45] and will indeed be reprised in Chapter 4.
In § 2.1.2 it was argued that a system of fermions at high density and low temperature should certainly behave as a quantum liquid. This is not strictly true, as it generally depends on the form of the interaction: in Electromagnetic liquids it is the residual molecular interaction, that includes an attractive well at medium range, accounting for particle aggregation by Van der Waals forces, plus a strong hard-core at short range, that avoids superpositions; the analogy of such a potential, sketched in fig. 1 at pag. 6, with the the nucleon-nucleon two-body potential in the *vacuum* has already been discussed. It can be proven that such potentials satisfy two fundamental requisites of Landau Theory, (i) letting a sufficiently slow change of the levels, whose lifetime must be long enough so that a new state can survive the process (ii) not allowing for the formation of bound states, of correlated states or excitations.

§ **2.1.4. Quark Matter.**— Very briefly - the same discussion can be straightforwardly done for a system of deconfined quarks and gluons. In particular, one does not explicitly deal with the bosonic degrees of freedom, as the properties of dense QGP systems are - in first approximation - given by the quarks; the interaction is then effectively treated and also in this case leads to a renormalisation - or dressing - of the quark bare mass. The system, composed thus by four species, must be $\beta-$stable and locally neutral, so that again $4_{\text{species}} - 3_{\text{eqtns}} = 1_{\text{free vars}}$, as the $\beta-$stability condition is here composed by two reactions. Thus, one free parameter can be used to describe the state of the system: $\rho_q = \rho_u + \rho_d + \rho_s$.

2.2 Equilibrium Thermodynamics

Before specifying the form of the interaction and its theoretical treatment, it is interesting to state a certain number of static properties of Nuclear Matter at equilibrium, i.e. a set of physical observables related to - at least in principle - measurable quantities whose expectation values are constant with time. The macroscopic theoretical framework is here statistical thermodynamics, and the knowledge to be sought, the Equation of State. General arguments are taken from textbooks of statistical mechanics like K. Huang

[46] (based on the Thermodynamics of E. Fermi) and a more technical review book by M. Baldo [47].

§ **2.2.1. The Equation of State.**— It is now clear that the states of Nuclear Matter can be studied as a function of the total baryon density ρ_B, expressed in nuclear natural units of baryons/fm^{-3} and of the temperature T, in MeV. Recalling the validity of the Thermodynamical Limit for the present case, it is possible to assume a very large volume V and divide every thermodynamical observable (Energy, Pressure, Enthropy, etc.) by it, working with the corresponding densities. Starting from the Helmoltz Free Energy density as thermodynamical potential,

$$f \equiv \epsilon - Ts = \sum_i \mu_i \rho_i - P, \tag{2.5}$$

where ϵ is the energy density, s is the entropy density μ_i the chemical potentials of the i species, (that can be n, p and e^- for the case of Nuclear Matter, and u, d, s quarks plus e^- for quark matter) and P the pressure density. From now on, the term "density" will be dropped and implicitly supposed valid. Furthermore, in the calculation of static properties, it will be assumed that $T = 0$: this is a drastic approximation, that makes the Energy of eq. (2.5) the relevant thermodynamical potential for the problem, but it is justified stating that the static properties of Nuclear Matter do not vary sensibly in the range $0 \div 1$ MeV. The knowledge of the thermodynamical potential lets a theorist to calculate any other thermodynamical observable, by means of the Maxwell relations:

$$P = \left(\frac{\partial f}{\partial V}\right)_T = -\left(\frac{\partial f}{\partial \rho_B}\frac{\partial \rho_B}{\partial V}\right)_T = \rho_B^2 \frac{\partial \epsilon}{\partial \rho_B}; \tag{2.6}$$

in this particular case there is a direct relationship between the Energy and the Pressure. Thus, the knowledge of the function $f(\epsilon, \rho_B)$ - or alternatively of $f(p, \rho_B)$ - allows the calculation of every static property of Nuclear Matter. The theory of such a tool, called "Equation of State" (approximate by the label EoS), is presented in the following sections; it will be calculated in Chapter 3, in which a particular microscopic approach to treat the interaction is presented, and consequently a scheme to build quasiparticles of the Fermi Liquid approach.

§ **2.2.2. Hadronic Equation of State.**— The internal energy density ϵ is usually substituted - in the case of Nuclear Matter - by the binding energy per nucleon, defined as:

$$\frac{E}{A} = \frac{V}{A} \cdot \epsilon = \frac{\epsilon}{\rho_B}, \tag{2.7}$$

following from the definition of ρ_B; being an Energy, and not an Energy density, it is measured in MeV. In principle E/A should depend on both ρ_B and ρ_3; under this assumption, it is commonly given as a parabolic expansion in function of the asymmetry parameter I, following ref. [48]:

$$\frac{E}{A}(\rho_B, I) = \frac{E}{A}(\rho_B, 0) + I^2 \frac{E_{\text{sym}}}{A}(\rho_B), \tag{2.8}$$

stopping at $O(I^2)$, as a sum of a term accounting for symmetric matter ($I = 0$) and a term depending only on ρ_B, called "Symmetry Energy". Its validity is proven up to $I \approx 0.6 \div 0.8$.
The Symmetry Energy has a very important physical meaning: it is the in-*medium* interaction in the iso-vector channel; it can be determined by subtraction from eq. (2.7), posing $I = 1$:

$$\frac{E_{\text{sym}}}{A}(\rho_B) = \frac{E}{A}(\rho_B, 1) - \frac{E}{A}(\rho_B, 0) \tag{2.9}$$

as the difference between the binding energy per nucleon of pure neutronic matter and of symmetric matter ($\rho_p = \rho_n$). Two more terms appear in the definitive form of the Equation of State:

$$\frac{E_{\text{tot}}}{A}(\rho_B, I) = \frac{E}{A}(\rho_B, I) + \frac{1 \pm I}{2} mc^2 + \frac{E_{e^-}}{A}, \tag{2.10}$$

the nucleon mass term - in perfect isospin symmetry - and a term accounting for the contribution of the electrons, here treated as a free gas, as there is no need to couple them with hadrons. Due to the β-equilibrium, expressed in the eq. (2.3), for the chemical potentials of the species holds:

$$\mu_e = \mu_n - \mu_p \equiv \mu_l; \tag{2.11}$$

the leptonic potential can be obtained by eq. (2.7) as a simple derivative:

$$\mu_l = 2 \left(\frac{\partial E/A}{\partial I} \right)_{\rho_B} = 4I \frac{E_{\text{sym}}}{A}(\rho_B) \tag{2.12}$$

from which, in turn, it is possible to obtain the corresponding electron density, as a simple Fermi gas of free particles, that enter the scheme with chemical potential μ_l:

$$\rho_e = \frac{1}{3\pi^2}\frac{1}{(\hbar c)^3}\mu_l^3 \tag{2.13}$$

remembering here the $\hbar c$ third power that makes the density ρ_e appear with its desired physical units. As discussed, the equations (2.2, 2.3) rule out the necessity of ρ_3; this makes the parameter I a function of ρ, or in other terms, fixes the asymmetry of Nuclear Matter at every value of the ρ_B. Defining a proton fraction as $x = \rho_p/\rho_B$, and substituting eqs. (2.2, 2.12) in eq. (2.7), one finds the algebraic equation:

$$3\pi^2(\hbar c)^3\rho_B x - \left[4(1-2x)\frac{E_{\rm sym}}{A}(\rho_B)\right]^3 = 0 \tag{2.14}$$

to be solved for every value of ρ_B, determining the chemical fractions of the species as a function of baryon density. This makes eq. (2.10) a function of only one variable, ρ_B.
In practical matters one must calculate the two terms in eq. (2.9) separately from some many-body approach, i.e. solving some complex quantum problem with the aim to calculate the energy of the ground state of a system of many interacting particles, usually introducing a set of plausible simplifications. Their linear combination yields the Symmetry Energy, that must be in turn substituted in eq. (2.14) to give the desired proton fraction x at every value of ρ_B. Finally, all the ingredients of the recipe can be put in eq. (2.10), together with the leptonic contribution, to complete the picture. Typical behaviours of the discussed quantities are represented in figs. 2.1-2.3.

§ **2.2.3. The state of art.**— As stated, the Equation of State is a static description of the thermodynamical states of Nuclear Matter; but in Nature, strictly speaking, the realisations of Nuclear Matter for high densities are not directly accessible, because locked in the interiors of Neutron Stars; the only way to reproduce any of its properties is in heavy-ion collisions, where it appears in small droplets and anyway in non-equilibrium conditions. Thus, at the present moment, the Equation of State is unconstrained and there are many approaches in its calculation. Nevertheless, there is a basic set of assumptions that every model must fulfil, coming from the systematic observations of atomic *nuclei* and a fruitful field of experimental trials to determine the Symmetry Energy.

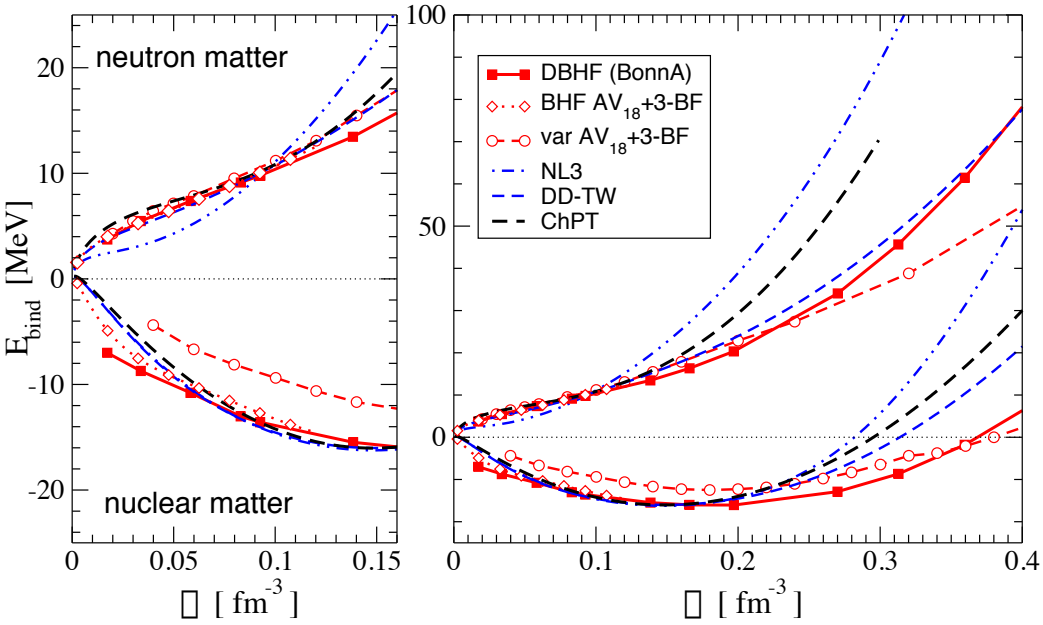

Figure 2.1: EOS in Nuclear Matter and Neutron Matter. BHF/DBHF and variational calculations are compared to some phenomenological models (NL3 and DD-TW and ChPT+corr). The left panel zooms the low-density range. Taken from ref. [49].

The various schemes are classified as semi-phenomenological or microscopic: the first are based on fits of the empirical properties of *nuclei*, employing a theoretical formalism that mimics a set of features of the full many-body problem - famous example are the Skyrme, Gogny and Migdal forces; the latter solve an *ab initio* many-body problem, whose input is the bare Nucleon-Nucleon force; two further sub-families can be individuated: the non-relativistic approaches, like the Brueckner-Hartree Fock (BHF) and the variational method (var) versus the relativistic ones, like the Dirac-Brueckner (DBHF) and the Relativistic Mean Field (RMF) theories.
An excellent review of the results in the various schemes is presented in ref. [49]; the authors discuss them also in relation to the known constraints coming from the heavy ion collisions, tentatively arguing for their overall predicting quality. A good sample is given fig. 2.2.

§ 2.2.4. Experimental constraints I: Nuclear Systematics.— A certain number of basic features come straight from the empirical properties of the atomic *nuclei*. Recalling the $A \to \infty$ limit in the semi-empirical mass formula of eq. (2.1), it is possible to give a list of basic features that every model of Equation of State must reproduce:

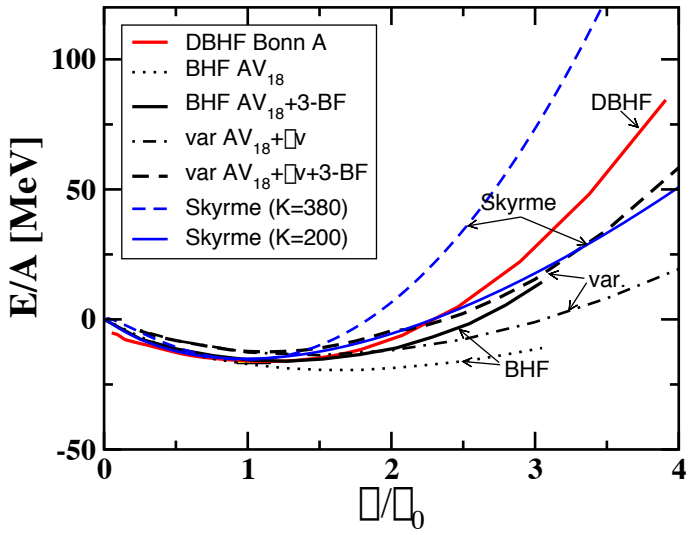

Figure 2.2: Predictions for the EOS of symmetric Nuclear Matter from microscopic ab initio calculations, i.e. relativistic DBHF, non-relativistic BHF and variational calculations. For comparison also soft and hard Skyrme forces are shown. Taken from ref. [49].

- **Nuclear saturation point:** the force that binds nucleons is attractive at short range ($\approx 1 \div 2$ fm); it is known that due to this effect, it "saturates", i.e. it is effective only on the closest primes. This is true already for $A > 4$; both volume and binding energies of *nuclei* are indeed proportional to the mass number A. the Free Energy per nucleon of symmetric Nuclear Matter must have a minimum at ρ_0:

$$\rho_0 = 0.17 \pm 0.01\,\mathrm{fm}^{-3}, \quad \frac{E}{A}(\rho_0, 1) = -16 \pm 1\,\mathrm{MeV}, \tag{2.15}$$

  as measured in EM probes scattering experiments and from eq. (2.1). The behaviour of the symmetric matter around saturation is displayed in fig. 2.2 for several approaches to the Many-Body problem.

- **Symmetry Energy at saturation:** from the asymmetric term a_4 of the semi-empirical mass formula it is possible to calculate what value must have the Symmetry Energy at the saturation point:

$$\frac{E_{\mathrm{sym}}}{A}(\rho_0) = 30 \pm 2\,\mathrm{MeV}. \tag{2.16}$$

  This constraint for different models in literature can be checked in the right panel of fig. 2.3: almost all the Equations agree at $\rho_B = \rho_0$.

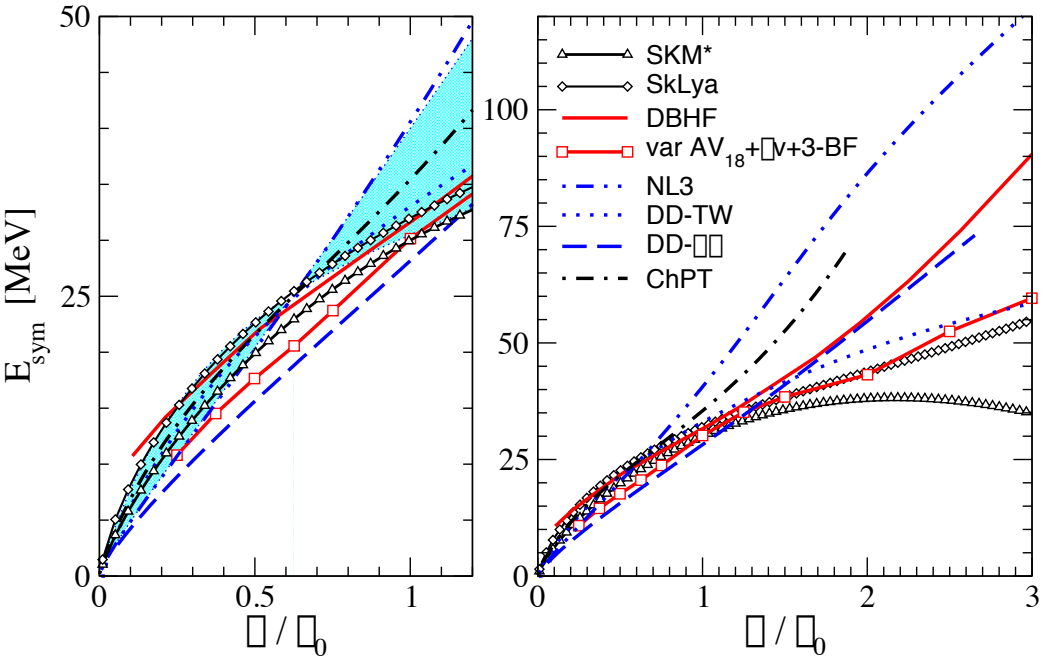

Figure 2.3: Symmetry energy as a function of density as predicted by different models. The left panel shows the low-density region, while the right panel displays the high-density range. Taken from ref. [49].

- **Compressibility at saturation:** it is possible to measure the compressibility of the nuclear fluid in experiments on the monopole resonances. The same parameter is a static property of Nuclear Matter, and can be evaluated both from the EoS or from a Landau normal liquid approach. Its value is:

$$K(\rho_0) = 220 \pm 30\,\mathrm{MeV}. \tag{2.17}$$

- **Causality condition:** the speed of sound in the *medium* must not exceed the speed of light. This leads to the condition:

$$\frac{c_s}{c} = \left(\frac{\partial p}{\partial \epsilon}\right)^{1/2} < 1. \tag{2.18}$$

§ **2.2.5. Experimental constraints II: Heavy Ion Collisions.**— At high density the picture is much more complicated, as there exists not any system that can easily be probed in equilibrium conditions. The high-density regime of the equations of state is then strictly model-dependent and deeply related with the E_{sym} term. Its different behaviours can be classified from their stiffness: a linearly growing term is called "asystiff"; a saturating or decreasing

term is by contrast called "asysoft"; quadratically diverging energies are said "superstiff" [→ fig. 2.3, right panel].
The symmetry term can be partially constrained at various densities by heavy ion collision experiments at various energies. Here a brief report, based on the report by V. Baran et al. [50]:

- **Sub saturation:** the situation, sketched in the left panel of fig. 2.3, can be constrained looking at fragments formation in low energy collisions; good systems are the giant monopole resonances in ^{90}Zr and ^{208}Pb, the giant dipole resonance and the neutron skin thickness in ^{208}Pb. Some results can be found in [51].

- **Around saturation:** here a nice tool is represented by an expansion of $E_{\rm sym}$ around the saturation density:

$$E_{\rm sym}(\rho_B) \simeq E_{\rm sym}(\rho_0) + \left(\frac{\partial E_{\rm sym}}{\partial \rho_B}\right)_{\rho_0}(\rho_B-\rho_0) + \frac{1}{2}\left(\frac{\partial^2 E_{\rm sym}}{\partial \rho_B^2}\right)_{\rho_0}(\rho_B-\rho_0)^2$$
$$= a_4 + \frac{L}{3}\left(\frac{\rho_B-\rho_0}{\rho_0}\right) + \frac{K_{\rm sym}}{18}\left(\frac{\rho_B-\rho_0}{\rho_0}\right)^2, \qquad (2.19)$$

  in which $L = (3/\rho_0)P_{\rm sym}(\rho_0)$ and $K_{\rm sym}$ are respectively its slope and curvature; the first is in turn related to the symmetry pressure at saturation by means of eq. (2.6).

- **High density:** the authors of ref. [50] compile a list of 11 observables that can give hints on the high-density regime of the Equation of State. The point lies in probing situations in which the asymmetry between the colliding ions drives some effect that can be somehow related to the static properties of Nuclear Matter. Typical phenomena include the liquid-gas phase transition, with isospin distillation and evaporation of neutrons; neck properties of the Intermediate Mass Fragments produced at intermediate energies, to study isospin migration; collective fluxes of n, p and particle production rates (especially the π^+/π^- yields), can be checked with transport theory predictions; finally also some deconfinement signature can be made eligible, studying the phenomenon of neutron trapping, the production of neutron rich fragments and the production of π, K mesons in high-density regions.

2.3 Building a phase transition

Strong theoretical evidences point towards a first order phase transition at a $2 \div 4$ times the nuclear saturation density ρ_0. At the present no theory can include a deconfinement mechanism in the finite μ_B limit for QCD matter; some effective models, like the Nambu-Jona Lasinio, can only account for half of the transition, the restoring of Chiral Symmetry [→ § 1.1.3]. When working with the static properties of strongly interacting matter it is then customary to **impose** a phase transition, starting from the Equations of State for the two phases.

§ 2.3.1. The Glendenning scheme.— According to the Lattice QCD simulations [→ § 1.2.4] and technically speaking, the transition here is of the first order and second kind: differently than H_2O then, Nuclear Matter is a complex system with two conserved quantities, electric charge e and baryon number N_B. N. K. Glendenning was the first to point out that for such a system the usual Maxwell scheme cannot be employed, defining the guidelines for a transition of the second kind [52, 53]; the keypoint is the relaxation of the local charge neutrality in the mixed phase - separately imposed on the two phases - in favour of the more "natural" global charge neutrality.
The Gibbs conditions say that in a two components system, (H)adrons and (Q)uarks are at equilibrium if their chemical potentials, temperatures and pressures are equal. Thus, the thermodynamical equilibrium bi-univocally implies chemical, thermal and mechanical *aequilibria*:

$$\mu_H = \mu_Q = \mu_{\rm eq} \tag{2.20}$$

$$T_H = T_Q = T_{\rm eq} \tag{2.21}$$

$$P_H(\mu_B, \mu_Q, T_{\rm eq}) = P_Q(\mu_B, \mu_Q, T_{\rm eq}) = P_{\rm eq}; \tag{2.22}$$

the last equation alone cannot be employed to calculate phase transitions properties: following the idea by Glendenning, it must be put together with an equation that imposes the global charge neutrality in the mixed phase, for a system with charge density $Z/V = q_H + q_Q$:

$$(1-\chi)\, q_H(\mu_B, \mu_Q, T_{\rm eq}) + \chi\, q_Q(\mu_B, \mu_Q, T_{\rm eq}) = \frac{Z}{V} \equiv \langle q \rangle, \tag{2.23}$$

in which $\chi = V_Q/V$ is the volume fraction of quarks. This equation states that the charges of both phases of the system at every value of the thermodynamical parameters must be equal to the average charge density. With

astrophysical applications in mind, $Z = 0$, as Neutron Stars are supposed to be neutral objects. The two equations (2.22),(2.23) must be solved at fixed T for $0 \leq \chi \leq 1$, yielding as solutions $\mu_H = \mu_H(T, \chi)$ and $\mu_Q = \mu_Q(T, \chi)$, the chemical potentials of the two coexisting phases. A relationship analogous to eq. (2.23) can be exploited for the total baryon density:

$$(1 - \chi)\, \rho_B(\mu_B, \mu_Q, T_{\rm eq}) + \chi\, \rho_q(\mu_B, \mu_Q, T_{\rm eq}) = \frac{B}{V} \equiv \langle \rho_B \rangle; \tag{2.24}$$

the energy density in the mixed phase is then:

$$\epsilon_{\rm mp} = (1 - \chi)\, \frac{E_{\rm tot}}{A} + \chi\, \epsilon_q, \tag{2.25}$$

providing that both Equations of State are known, and calculated in some Many-Body scheme.

The Many-Body problem has attracted attention ever since the philosophers of old speculated over the question of how many angels could dance on the head of a pin.

R. D. Mattuck - (1967)

3 The Many Body Problem

The determination of the static thermodynamical properties of Nuclear Matter - i.e. its Equation of State - relies on a proper Many Body scheme. In systems at the Thermodynamic Limit, the number of constituents is arbitrarily high, so that every particle experiences a solicitation superposition of many two-body forces. The task to explicitly write down a whole potential term of the Hamiltonian without recurring to formal abbreviations is often far from trivial itself. Any exact solution is impossible, so the problem is simplified with some assumptions and then solved perturbatively with some proper diagrammatic prescription to include all the relevant contributions to the energy eigenvalue at some given order of approximation. The aim of this chapter is to complete the picture of Chapt. 2 elucidating how to calculate $E/A(\rho_B)$: the starting point is the free gas system; the next step includes the sketching of the idea behind quasiparticle schemes: the semiphenomenological Landau theory for Normal Fermi liquids and the Hartree-Fock method, a way to transform two-body potentials into effective one-body operators that describe the interacting system as a mean field. Finally the theories employed in actual Nuclear and Quark Matter calculations are presented. General references are taken from the textbooks from Fetter and Walecka [40] and Baldo et al. [47].

3.1 Formulation

This section is dedicated to a brief statement of the problem, with a qualitative discussion on how it is solved in this thesis work. Many Body problems can be solved exactly for a few class of very simple systems; in general it is necessary to employ some approximation scheme. The one chosen here is the Quasiparticle method; for a system at liquid phase, it is natural to apply Landau semi-phenomenological theory; this is a very complicated task

due to the nature of the interaction, and it is the basis for transport theory and dynamical properties of Nuclear Matter, treated in Chapt. 4. Static properties are calculated in a microscopic approach, with the Hartree-Fock method, that leads to a free gas-like energy spectrum.
Every quantum problem is posed specifying a proper Hamiltonian, containing all the relevant degrees of freedom and stating the interactions among them. In the present case it is Nuclear Matter, a system of A nucleons with mass m - supposing isospin symmetry and no Coulomb interactions - for which:

$$\hat{H}^{\mathrm{NM}} = \sum_{i=1}^{A} \hat{T}_i^c + \sum_{i<j}^{A} \hat{u}_{ij} = \hat{H}_0 + \hat{H}_1; \tag{3.1}$$

with the indexes $i, j = \{1, 2, ..., A\}$ running over the different degrees of freedom (the $i < j$ is written to exclude double counting); the Hamiltonian $\hat{H}$, the one-body kinetic energy $\hat{T}_i^c$ and the two body interaction $\hat{u}_{ij}$ are Hermitian operators, whose representations are matrices defined on suitable finite dimensional Hilbert spaces by the choice of a particular base. In the following this notation will be dropped, for simplicity of notation; for the same reason, the nucleon spin degrees or freedom will be ignored throughout all this section, as the arguments here are very general and meant just to give a general idea of the methods.
The u two body potential is the Nucleon-Nucleon potential in the *vacuum*; it is an input and its analytic form comes from fits of experimental data, due to the complicate nature of strong interactions and of the non-analytic solvability of QCD in the confined region; it is determined with relativistic effective theories: the different interaction channels are represented by the exchange of a lowest-lying octet meson, following Yukawa's idea; such theories are non renormalizable and the arising parameters are fitted to reproduce the properties of the first Nucleon-Nucleon scattering and bound states. The best performing models to date are the Argonne v18 [54] (a momentum space version was very recently published, [55]) and the CD-Bonn [56]. The latter was used in all the Nuclear Matter calculations presented.
The Many Body Problem is then the solution of the Schrödinger equation for the static Hamiltonian H^{NM}:

$$H^{\mathrm{NM}}\Phi_k(q_1, q_2, ..., q_A) = E\Phi_k(q_1, q_2, ..., q_A) \tag{3.2}$$

i.e. the complete set of Wavefunctions Φ_k, depending on an appropriate set of space-coordinates q_i for the $i-$th particle and the corresponding energy

eigenvalues E_k, specifying the total energy of the system that depends from the many particle-configuration.

§ **3.1.1. Fermi Gas.**— One of the most simple thermodynamic applications of a trivial solution of such a quantum-mechanical problem is the Free Fermi Gas at $T = 0$. The term "free" here refers to the procedure of dropping down the interaction term in eq. (3.1), thus working with the H_0 defined on the right-hand side. Such a problem is characterised by a trivial Hamiltonian, whose only action on the many-body wavefunction Φ_k is mediated by the momentum operator p:

$$H_0 = \sum_{i=1}^{A} \frac{p_i^2}{2m}. \tag{3.3}$$

The single particle problem of Hamiltonian H_i is very easy to solve; the s-th eigenfunction is the plain wave $e^{i\,p_k r}$ and the corresponding single particle energy is $\epsilon_k = p_k^2/2m$, with quantised *momenta* p_k appearing due to translational invariance and subsequent use of periodic boundary conditions; classically s can be interpreted as the number of nodes of a string of fixed length.
In this particular case a Many-Body solution of the Fermi Gas of Hamiltonian (3.3) is simply found filling the single particle levels in a box with two nucleons per level k (accounting for two opposite spin degeneracy), up to the so-called Fermi Energy, the level of the last particle with $k = k_F$. The total ground state (gs) energy of the system is then a simple sum over single particle states:

$$E_0 = 2 \sum_{k=1}^{A/2} \epsilon_k \tag{3.4}$$

the role of $T = 0$ temperature here is to ensure the degeneracy of system: the total energy is then the Fermi Energy and it is simply given by a sum of the single particle states, as the nucleons do not interact with each other. A much desirable property for a many-nucleon system! Before going on with the discussion it is necessary to make two remarks, that demand for a powerful formalism in order to be treated.

- **Statistical thermodynamics:** at the Thermodynamical Limit the first excited levels strongly depend on the (T, μ) environment: thermodynamics kicks in with a classy generalisation of the theory given in

Chapt. 2. The properties of a system of many particles, in which $A \gg 0$, can be described recurring to the Gibbs grand-canonical ensemble and the various observables calculated by means of a suitable quantum grand-canonical partition function $Z(T, \mu, V)$:

$$\begin{aligned} Z(T,\mu,V) &= \mathrm{Tr}\,[e^{-(H^{\mathrm{NM}}-\mu N)/T}] \\ &= \sum_{n_1,...,n_\infty} \langle n_1, n_2, ..., n_\infty | e^{-(H^{\mathrm{NM}}-\mu N)/T} | n_1, n_2, ..., n_\infty \rangle, \quad (3.5) \end{aligned}$$

in which now a many-body state is specified in terms of the occupation numbers $n = \{0, 1\}$ (for fermions) of an indefinite number of particles $i = \{0, 1, ..., \infty\}$, represented by the operator N, rather than by the space coordinates of A labeled particles q_i. Many fermion-states in occupation number representation obey the simple relation:

$$|n_1, n_2, ..., n_\infty\rangle = |n_1\rangle|n_2\rangle...|n_\infty\rangle, \quad (3.6)$$

that in turn lets the factorisation eq. (3.5), $Z = \prod_{i=1}^{\infty}(1 + e^{-(\epsilon_i-\mu)/T})$, in terms of the single particle energies ϵ_i. The thermodynamics can be calculated starting from the grand-canonical potential:

$$\Omega = -\frac{T}{V} \ln Z(T,\mu,V) = -T \sum_{i=1}^{\infty} \ln\,(1 + e^{-(\epsilon_i-\mu)/T}) \quad (3.7)$$

by means of the First Principle and Maxwell relations. Any Ensemble average for a generic observable O can be evaluated as $\langle O \rangle = \mathrm{Tr}(\rho_{\mathrm{GC}} O)$, by means of the statistical operator:

$$\rho_{\mathrm{GC}} = Z^{-1} e^{-(H-\mu N)/T}. \quad (3.8)$$

As an example, for the average number of fermions $\langle N \rangle = \mathrm{Tr}(\rho_{\mathrm{GC}} N)$:

$$\langle N \rangle \equiv -\frac{\partial \Omega}{\partial \mu} = \sum_{i=1}^{\infty} \frac{1}{1 + e^{-(\epsilon_i-\mu)/T}} \equiv \sum_{i=1}^{\infty} n_i^0, \quad (3.9)$$

thus making the average number of particles as the sum of the statistical occupation numbers n_i^0, that represents the probability of occupying the single particle level i at (T, μ), in terms of the Fermi-Dirac statistics.

- **Indistinguishability of particles:** this fundamental quantum postulate is manifestly violated by the Hamiltonians (3.1),(3.3), that contain labels i, j for the particle coordinates. An elegant way to overcome this

difficulty is to switch to second-quantisation, in order to exploit the occupation number representation of many-particle states compactness, in a form particularly desirable for statistical approaches. The starting point is the Many-Body wavefunction, that must be expressed as an Antisymmetrized product of single particle states $\phi_k(q)$, solution of a 1-particle Schrödinger problem. This is obtained with the so-called Slater determinants:

$$\Phi(q_1, ..., q_A) = \frac{1}{\sqrt{A!}} \begin{vmatrix} \phi_1(q_1) & \phi_2(q_1) & \cdots & \phi_A(q_1) \\ \phi_1(q_2) & \phi_2(q_2) & \cdots & \phi_A(q_2) \\ \vdots & \vdots & \ddots & \vdots \\ \phi_1(q_N) & \phi_2(q_N) & \cdots & \phi_A(q_N) \end{vmatrix}, \tag{3.10}$$

a way to develop wavefunctions of indistinguishable A-body states without violating Pauli Blocking. It is possible to prove that the given determinant changes sign for the exchange of two particles q_i, q_j. The next step is to promote the wavefunctions to field operators (again temporarily denoted by hats, just to show the difference with c-numbers):

$$\hat{\Phi}(q) = \sum_k \hat{a}_k \phi_k(q), \tag{3.11}$$

with index k running over the quantum numbers of the set of eigenstates ϕ_k and $\hat{a}_k$, $\hat{a}_k^\dagger$ the annihilation/creation operators, that, applied to eigenstates of the system, destroy/create a particle with quantum numbers k. The procedure, called "second quantisation", leads to the imposition of the following anti-commutation relations among the fields:

$$[\hat{\Phi}(q), \hat{\Phi}^\dagger(q')]_+ = \delta(q - q') \tag{3.12}$$

$$[\hat{\Phi}(q), \hat{\Phi}(q')]_+ = [\hat{\Phi}^\dagger(q), \hat{\Phi}^\dagger(q')]_+ = 0, \tag{3.13}$$

that in turn imply analogous equations for the a, $a^\dagger$ operators of usual quantum mechanincs. By means of this representation one can build all the states of the single-particle problem, provided it's solvable.

Under this assumptions, the Hamiltonian for Nuclear Matter can be written in second quantisation as:

$$H^{\mathrm{NM}} = \sum_{ij} \langle i|T^c|j\rangle a_i^\dagger a_j + \frac{1}{2} \sum_{ijkl} \langle ij|u|kl\rangle a_i^\dagger a_j^\dagger a_l a_k, \tag{3.14}$$

and in this form it is the starting point of the Many Body problem of interacting Nuclear Matter and it must be applied - by means of the Schrödinger equation - to Antisymmetrized products of single-fermion wavefunctions.

§ **3.1.2. Basics of Landau approach: quasiparticles.**— A way to introducing the quasiparticle concept when solving for static properties is the use of Landau semi-phenomenological theory for Normal Fermi liquids. This includes a review of the stated many particle formalism in the case of a system at thermodynamical limit, that is composed, as $A \to \infty$, by an arbitrarily high number of constituents, so that the Hamiltonian for a Free Gas:

$$\sum_k \frac{p_k^2}{2m} a_k^\dagger a_k ... \quad \to \quad \frac{V}{(2\pi)^3} \int p^2 \mathrm{d}p \, ... \tag{3.15}$$

with corresponding need to switch to the distribution formalism. The total energy $E[n_k(q,t)]$ of the system is thus a functional of the distribution n_k; so that in this easy case, to any infinitesimal variation δn_k, corresponds a:

$$\delta E_{\mathrm{gas}} = \sum_k \epsilon_k^0 \, \delta n_k \tag{3.16}$$

which, due to the simple dispersion relation, is simply a sum of the single particle states $\epsilon_k^0 = p^2/2m$, as in the case discussed in the previous section. Following then the original intuition by Landau and his coworkers, the interaction is adiabatically switched on, transforming the single particle states of the free particles in a Fermi gas into the energy levels of an interacting quantum liquid. Indeed, after a new equilibrium is reached, each particle carries the same spin, charge and momentum that it used to carry; the total number of particles $N_{\mathrm{part}} = A$ remains constant, so that every quasiparticle is the dressing of a bare particle, and a state of the whole system is still obtainable by a careful counting of the occupation numbers through the distribution n_k; a deviation from the ground-state equilibrium distribution n_k^0 to first order in δn, yields a change in the energy distribution:

$$\delta E_{\mathrm{liq}} = \sum_k \epsilon_k \, \delta n_k \tag{3.17}$$

in which the label k has the same role as before, with ϵ_k now defined as the functional derivative of E with respect to the change in the distribution n (due to an interaction), and corresponding to the quasiparticle energy. This time though, differently from the free gas case, nothing can be said on the

total energy, as the definition of quasiparticle energy makes sense only around the Fermi surface. The Fermi energy ϵ_F is the energy acquired by the system for adding a particle on top of the Fermi level. Expanding to second order in δn:

$$\delta E_{\rm liq} = \sum_k \epsilon_k \, \delta n_k + \frac{1}{2} \sum_{kk'} f(k,k') \, \delta n_k \delta n_{k'} \tag{3.18}$$

in which appears a two-particle function f, the interaction energy between two particles. At low temperatures, with Pauli blocking limiting most of the particle/hole excitations around ϵ_F, the excitation of the system is related to the deviation from the ground state:

$$\delta n_k = n_k - n_k^0. \tag{3.19}$$

Furthermore, expanding $\epsilon - \epsilon_F$ in powers of $p - p_F$ around the Fermi surface, one obtains:

$$\epsilon - \epsilon_F \approx v_F (p - p_F) \tag{3.20}$$

where $v_F = [\partial\epsilon/\partial p]_{p=p_F}$ is the Fermi velocity of a particle around the corresponding surface; recalling the case of a noninteracting gas, in which particles and quasiparticles coincide, $\epsilon = p^2/2m$ and $v_F = p_F/m$; by analogy then, for a Fermi liquid one defines:

$$m^* = \frac{p_F}{v_F}, \tag{3.21}$$

obviously different from the bare mass m of the particles, yet meaningful as an "effective mass". Its value can be in principle measured from the system by means of the Landau-parameters, essentially the coefficients of a Legendre Polynomials expansion of the interaction energy f between two quasi-particles. Its physical meaning is quite clear: the excitation of degrees of freedom around the Fermi surface is sketched as a few, noninteracting quasiparticles that move freely as if they had a different mass m^*. This semi-phenomenological theory is now put aside to calculate static properties with the Hartree-Fock method.

§ 3.1.3. Hartree Fock.— The effective mass will be here calculated with a microscopic method developed by Hartree, and successively perfected by Fock and Slater. It was initially used in the treatment of the atomic Many-Body problem coupled to the variational approach, using Slater determinants as trial functions. During the 60s the method received new attention and was generalised for the case of perturbative approaches.

The core idea of the Hartree-Fock method is to replace the four Fermi interaction term in the second quantised Hamiltonian of eq. (3.14) with a sum of all possible free particle-like two-body term. Due to translational invariance,

$$H^{\mathrm{NM}} = \sum_k \frac{p_k^2}{2m} a_k^\dagger a_k + \frac{1}{2} \sum_{kk',q} \tilde{u}(p) a_k^\dagger a_{k'+q}^\dagger a_{k'} a_{k+q}, \tag{3.22}$$

in which - working in momentum space - a Fourier transform $\tilde{u}$ of the potential u was performed. Without entering the details, the substitution is obtained essentially by means of a linearisation, averaging pairs of operators:

$$a_1^\dagger a_2^\dagger a_3 a_4 \simeq -\langle a_1^\dagger a_3 \rangle a_2^\dagger a_4 - \langle a_2^\dagger a_4 \rangle a_1^\dagger a_3 + \langle a_1^\dagger a_4 \rangle a_2^\dagger a_3 + \langle a_2^\dagger a_3 \rangle a_1^\dagger a_4, \tag{3.23}$$

in which the signs come from fermionic orderings by means of anti commutation relations; terms like $\langle a^\dagger a^\dagger \rangle$ or $\langle aa \rangle$ were dropped, as they violate baryon number conservation. In principle one should ensure that the performed operation leads to an effective minimisation of the energy. The procedure substitutes a two-body term with an average field that, summated over all the particle states, acts as a "mean field" that takes into account the *medium* behaviour:

$$\langle a_k^\dagger a_{k'} \rangle = \langle a_k^\dagger a_k \rangle \delta_{kk'} \equiv n_k \delta_{kk'} \tag{3.24}$$

such a mean field term finally depends on n_k, the average number of particles in the k state; when substituted in the interaction term of the Hamiltonian (3.14), yields an average interaction due to all the other particles. After some easy algebraic passages and applying repeatedly eq. (3.24):

$$u_{\mathrm{HF}} = \sum_k \left[-\sum_q n_{k-q} u + nu \right] a_k^\dagger a_k \equiv \sum_k \Sigma_{\mathrm{HF}}(p) a_k^\dagger a_k, \tag{3.25}$$

that finally is a one-body operator; n is the total density as sum of the mean occupation numbers. The Hartree-Fock potential is sum of two terms, a "direct" term, due to Hartree, that averages the interaction on one particle due to a mean field generated by all the others; and an "exchange" term, due to Fock, that essentially performs a momentum shift.

The method has been generalised to be employed in perturbative Many-Body approaches, in which the Scrhödinger problem is solved by means of Dyson expansions of Green functions. Providing that a proper set of Feynman rules is specified, the exact Green function, solution of the Many-Body problem, can be diagrammatically represented as a sum of the unperturbed Green

function plus all connected terms with a free Green function at one end. This is usually defined as "Proper Self-Energy" and is indicated as Σ^*. The Hartree-Fock approximation consists in stopping the expansion for Σ^* at the two first order contributions.
A very important remark must be here made: the method implies the so-called "self-consistency", as the matrix elements of $u_{\rm HF}$ are calculated by means of the auto-functions, that in turn are unknown and to be determined. The problem is then solved iteratively and numerically, starting from some guess-solution that should converge, after a given number of cycles - to the desired solution. Once this happens the system will be a collection of quasiparticles with a new dispersion relation:

$$E^{\rm HF} = \langle\Phi|H^{\rm HF}|\Phi\rangle = \langle\Phi|\sum_k \left(\frac{p_k^2}{2m} + \Sigma_{\rm HF}(p)\right) a_k^\dagger a_k|\Phi\rangle; \tag{3.26}$$

the $\Sigma_{\rm HF}$ term can be included inside a renormalised mass m^*: the energy spectrum has the form of a Free Gas spectrum, whose static properties can be calculated quite easily.
The method is obviously non exact and works well in all those systems in which correlations are not too important. A good example are Pauli-blocked dense systems at $T \to 0$, in which the main contribution to the first excited states energy comes from a few quasiparticles at the Fermi surface - as extensively discussed - leading to a huge suppression of any other two-body correlation.

§ 3.1.4. Thermodynamical consistence.— The effect of the Hartree-Fock method is thus to change the dispersion relation; it must be kept well in mind that in a thermodynamic scheme the system properties are regulated by the parameters T and ρ_B, both appearing in the Fermi-Dirac distribution - the latter being related to the chemical potential μ_B. The quasinucleon dispersion relation is thus *medium* dependent through the average occupation numbers n_k. In the $T \to 0$ limit, this can be sketched as:

$$\omega^*(p, \mu_B) = \frac{p^2}{2m} + \Sigma_{\rm HF}(p, \mu_B). \tag{3.27}$$

Such a *medium* dependence actually destroys thermodynamic consistence. The Free Gas, extensively treated, has a dispersion relation $\omega = \omega(p)$; its

Hamiltonian and Partition Functions are:

$$H^{\mathrm{FG}} = \sum_k \omega(p) a_k^\dagger a_k \tag{3.28}$$

$$Z(T,\mu,V) = \mathrm{Tr}\,[e^{-(H^{\mathrm{FG}}-\mu N)/T}]; \tag{3.29}$$

the energy density $\epsilon(T,\mu)$ can be calculated either from the partition function, or from the thermodynamical identity $\epsilon = Ts + \mu n - P$, from other thermodynamical relations, and the result would obviously be the same.
The same does not apply for a system that - for the sake of generality - holds a single particle dispersion relation $\omega^* = \omega^*(p,T,\mu)$: in such a case the effective Hamiltonian becomes *medium* dependent; when calculating the energy density from the partition function one ends up with the same form of the free-gas:

$$\epsilon(T,\mu) = \frac{1}{V}\frac{1}{Z(T,\mu,V)}\,\mathrm{Tr}\,[H^{\mathrm{FG}} e^{-(H^{\mathrm{FG}}-\mu N)/T)}], \tag{3.30}$$

but this time the definition of any observable from the first principle of thermodynamics would contradict the free gas case, as any derivative of the thermodynamical functions yields new terms due to the *medium* dependence of the Hamiltonian.
The inconsistency does not prevent the use of such models, but breaks the "Quasiparticle scheme", so that a careful use of thermodynamics is advised; a formal solution was given independently in many approaches, until M. Gorenstein and S. Yang proposed a unified scheme to treat the issue [57]. According to their work, when dealing with Effective Hamiltonians $H_{\mathrm{eff}}(c_1,c_2,...)$ depending on a certain number of phenomenological parameters $c_i = c_i(T,\mu)$ - like the renormalised mass, $m^* = m^*(T,\mu)$ - one should be sure that for the corresponding pressure $P = P(T,\mu,c_1,c_2,...)$ the following conditions do hold:

$$\left(\frac{\partial P}{\partial c_1}\right)_{T,\mu,c_2,...} = 0, \quad \left(\frac{\partial P}{\partial c_2}\right)_{T,\mu,c_1,...} = 0, ... \tag{3.31}$$

so that any additional term is suppressed and the validity of the thermodynamical identity $\epsilon = Ts + \mu n - P$ is recovered. This is equivalent to adding a *medium*-dependent zero point energy $E_0^* = E_0(c_1,c_2,...)$ to the Effective Hamiltonian. This prescription was devised for high temperature QGP Equations of State, such as quasi-gluon models based on Lattice QCD data [58].

3.2 Brueckner Theory

K. A. Brueckner begun working on Nuclear Matter during the 1950s [59]; his studies were later on continued by J. Goldstone and H. A. Bethe (for example [60]). Since then the theory - that nowadays carries his name, Brueckner theory - has gained much attention, as it was employed also in finite nuclei calculations; it was highly remarkable that an *ab initio* microscopic approach, whose only input was the Nucleon-Nucleon potential in the *vacuum*, could reproduce the nuclear saturation point, despite the fact that the theory was far from being trustworthy due to internal inconsistencies and numerical difficulties. The challenge was taken back in the 1980s, with the first relativistic Dirac-Brueckner approaches on one side, formulated by C. M. Shakin [61] in a first moment, and by R. Brockmann and R. Machleidt later [62, 63]; on the other side the Catania group of M. Baldo, U. Lombardo and G. Giansiracusa and the Liége group of J. Cugnon and A. Lejeune took back the bulk of Brueckner theory, could finally elucidate the correct single-particle potential choice [64] and improve the prediction adding contribution from three body forces [65].
Technically speaking, Brueckner Many-Body theory is based on a Goldstone expansion, whose diverging ladder diagrams are carefully resummed, defining a scattering G-matrix *in medio*; this new physical quantity is non-divergent and thus exploitable in Nuclear Matter calculations.

§ **3.2.1. Goldstone expansion.**— Brueckner theory is based on the Goldstone expansion [66], a perturbative series of linked-cluster diagrams, for the ground state of a Many Body system, Nuclear Matter, under the condition that it is non-degenerate. Recalling the formalism presented in the last section, the starting point is the Hamiltonian of eq. (3.1), in which a single particle potential U_i is inserted in a way that makes the final result independent from its choice:

$$H^{\mathrm{MN}} = \sum_{i=1}^{A}(T_i^c + U_i) + \left(\sum_{i<j}^{A} u_{ij} - \sum_{i=1}^{A} U_i\right); \tag{3.32}$$

this is done in order to accelerate the series convergence. A brief discussion on its choice will be presented in the next paragraphs. The unperturbed ground state Φ_0 comes from the solution of the Schrödinger problem of Hamiltonian H_0; this is expressed as a Slater determinant in eq (3.10), and is supposed non-degenerate. The associated energy ϵ_0, eigenvalue of the $H_0\Phi_0 = \epsilon_0\Phi_0$

problem, is thus obtainable from the free-single particle contributions.
Now one switches to the full $H\psi = \epsilon\psi$ problem for the ground state ψ of the interacting system; the total energy ϵ is evaluated by means of perturbative theory, as an expansion up to third order in H_1:

$$\begin{aligned}\epsilon = \epsilon_0 &+ \langle\Phi_0|H_1|\Phi_0\rangle + \langle\Phi_0|H_1(\epsilon_0 - H_0)^{-1}PH_1|\Phi_0\rangle \\ &+ \langle\Phi_0|H_1(\epsilon_0 - H_0)^{-1}PH_1(\epsilon_0 - H_0)^{-1}PH_1|\Phi_0\rangle \\ &- \langle\Phi_0|H_1|\Phi_0\rangle\langle\Phi_0|H_1(\epsilon_0 - H_0)^{-2}PH_1|\Phi_0\rangle + \dots \end{aligned} \tag{3.33}$$

where $P \equiv 1 - |\Phi_0\rangle\langle\Phi_0|$ is the Projection operator on $|\Phi_0\rangle$, used for formal purposes. The diagrammatic form of this expansion can be built provided that a suitable set of generalised Feynman rules is specified, starting from the second quantised form of H_1, represented by eq. (3.14) upon the adding of the single particle potential U. The $\hat{a}^\dagger, \hat{a}$ operators - as stated - must satisfy the anti-commutation relations for fermions:

$$[\hat{a}_r, \hat{a}_s]_+ = 0, \quad [\hat{a}_r^\dagger, \hat{a}_s^\dagger]_+ = 0, \quad [\hat{a}_r^\dagger, \hat{a}_s^\dagger]_+ = \delta_{rs}, \tag{3.34}$$

while the matrix elements are calculated in the same functional space in which the Many-Body wavefunctions are defined (Fock space). The sums are performed on the single-particle states rather than on the particles and careful avoiding of double counting is advised (the elements symmetric under the $pq \to rs$ exchange are dropped).
The contributions at the various perturbative orders are calculable by means of the specified diagrammatical representation; for example, the second order of eq. (3.33) is:

$$\langle\Phi_0|H_1(\epsilon_0 - H_0)^{-1}PH_1|\Phi_0\rangle; \tag{3.35}$$

starting from the right, it is instructive to check the action of the various operators that appear on the unperturbed ground state $|\Phi_0\rangle$: the first term of H_1, that is of the form $\langle ab|v|lm\rangle\, \hat{a}_a^\dagger \hat{a}_b^\dagger \hat{a}_m \hat{a}_l$, destroys the particles occupying the l, m states of the Dirac sea and creates two particles in the states a, b above the Dirac sea, due to the effect of the creation and annihilation operators. With this procedure one ends up with a new Φ' Slater determinant with two particle and two hole states, whose pictorial representation lies in the (a) panel of 3.1: the matrix element, representing the interaction, is drawn as a dashed line; the usual continuous lines are used for fermions. The starting point, below the diagram, is the unperturbed state Φ_0.
Proceeding towards the right hand side in eq. 3.35, it is the turn of $(\epsilon_0 - H_0)^{-1}$

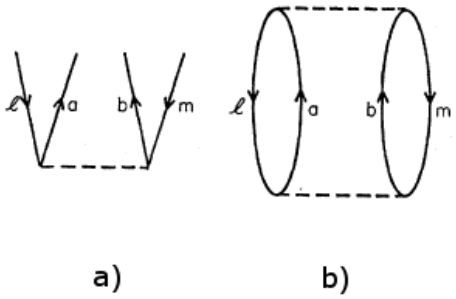

Figure 3.1: (a) Action of the first term in H_1 on the unperturbed Ground State Φ_0 - (b) A diagram contributing to the second order of the perturbative expansion 3.35. Both pictures are taken from ref. [67].

to be applied on the new determinant Φ', obtaining the reciprocal of the energy difference among the two states; its contribution is $-(E_a + E_b - E_l - E_m)^{-1}$, in which the various E_i are the single particle energy eigenstates of the free problem. The term is called "Energy Denominator".
Finally applying H_1, one ends up with Φ_0 again. The only H_1 terms to be used are those that transform $\Phi' = \hat{a}_a^\dagger \hat{a}_b^\dagger \hat{a}_m \hat{a}_l \, \Phi_0$ back in Φ_0; there is more than one way to topologically perform this taks, that anyway involves the use of diagrams of the kind shown in the (a) panel of fig. 3.1. An example of a suitable diagram, satisfying all the discussed requirements, is given in the (b) panel of the same figure, evidently composed from two diagrams of the (a) kind. A typical second order diagram contribution is composed by the product of the two-body matrix elements, form the energy denominator and from the expectation value:

$$\langle \Phi_0 | \hat{a}_l^\dagger \hat{a}_m^\dagger \hat{a}_b \hat{a}_a \hat{a}_a^\dagger \hat{a}_b^\dagger \hat{a}_m \hat{a}_l | \Phi_0 \rangle, \tag{3.36}$$

which, depending on the particular action of the $\hat{a}$ operators, is valued ± 1. For the considered (b)-diagram, the contribution is proportional to:

$$\sum_{ablm} \langle lm|v|ab\rangle (E_a + E_b - E_l - E_m)^{-1} \langle ab|v|lm\rangle \tag{3.37}$$

where the sum is extended to the states a, b above the Dirac sea and to the l, m populating the Dirac sea.
An excellent review of the development of such a diagrammatical tool for the perturbative calculations by means of the Goldstone expansion can be found in a report by D. Day [67]; the pictorial method is very powerful when it comes to write all the contributions at a given order of the expansion (3.33).

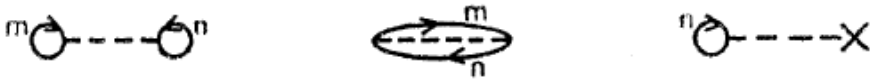

Figure 3.2: First order diagrams relative to the contributions of eq. (3.38) for the Goldstone expansion [67].

The discussed example is only one of such contributions for the second order; it is presented in order to give a minimum insight on the applied method and of its physical meaning. The correct prescription states that only the topologically connected diagrams must be picked up at a certain order, as the disconnected ones exactly cancel their contributions at all orders of the expansion.
The diagrams contributing to Leading Order (first) are reported in fig. 3.2; their contributions are:

$$\epsilon = \sum_{n \leq A} \langle n|T|n\rangle + \frac{1}{2} \sum_{m,n \leq A} \langle mn|v|mn\rangle_{\mathcal{A}}, \tag{3.38}$$

in which appears the U-term dependence that enters the unperturbed problem. The second term has been written in a compact form by means of the Anti-symmetrising operator $\mathcal{A}$:

$$|mn\rangle_{\mathcal{A}} = |mn\rangle - |nm\rangle; \tag{3.39}$$

eq. (3.38) contains the v potential and is thus divergent due to the presence of the hard-core in nuclear forces; this problems makes the discussed Goldstone expansion unusable in calculations. The problem can be overcome by a smart resummation of classes of ladder diagrams.

§ **3.2.2. Resummation and G Matrix.**— The Goldstone expansion, as it is formulated, is composed by diverging terms and thus cannot converge. But this difficulty, that the approach shares with many other perturbative approaches for the strong interaction, whose structure constant is typically $\alpha_s \sim 1$ in nuclear applications, can be overcome defining the G-matrix as the *in medio* scattering matrix and converting a series in v in one in G, noting that the latter has a non-singular behaviour for potentials that contain a hard-core, such as the nuclear one. Surprisingly enough - it can be proven that all the terms of the new Brueckner-Goldstone expansion are finite and of the appropriate order of magnitude for perturbative use.

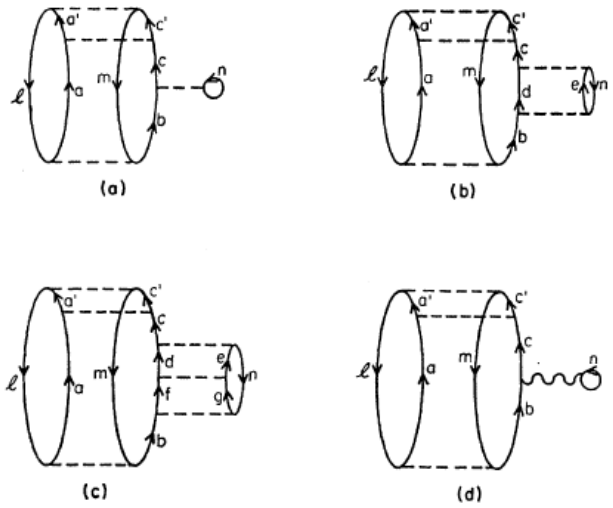

Figure 3.3: Example of ladder-diagrams risummation for the definition of the G-matrix. The (d) diagram is the sum of the (a,b,c) and of the infinite diagrams of the following orders that belong to the same class. Taken from ref. [67].

The physical intuition that lies at the base of such a procedure can be understood thinking at two interacting nucleons in the *vacuum*: the first order scattering amplitude in Born approximation yields a large, inaccurate value. But calculating all the orders contributions - or solving the corresponding Scrhödinger equation, the correct result is found. On the same grounds, a careful re-ordering of the diagrams is here performed, so that every matrix element in v is substituted by an infinite series including the two-body interaction at all orders.

A practical example can be made looking at the diagrams of fig. 3.3, in particular the first (a) and therein the v interaction ending in a bubble on its right: c and n are the outgoing lines, while b and n are the ingoing. The corresponding matrix element is $\langle cn|v|bn\rangle$; this diagram, accounting for the bubble-interaction at first order, must be added the following order diagrams (b), (c), and all the infinite obtainable by adding further dashed-interaction lines under the existing ones.

It is useful to define the "starting energy" as the energy denominator $W = E_l + E_m + E_n - E_a$, observing that it is the energy of the prototype diagram of the class with only three v interactions (obtainable by cutting the bubble interaction in diagram (a) of fig. 3.3). With this prescription, the

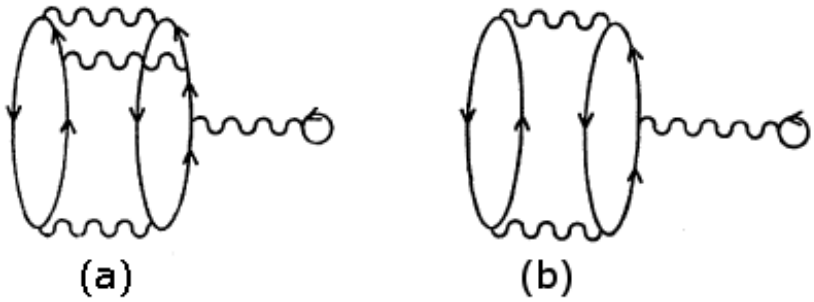

Figure 3.4: (a) Diagram redundant for the definition of G - (b) Correct diagram contributing to the definition of G [67].

contributions relative to the second (b) and third (c) order diagrams are:

$$-\sum_{d,e>A}\langle cn|v|de\rangle\,(E_d+E_e-W)^{-1}\langle de|v|bn\rangle$$
$$\sum_{defg>A}\langle cn|v|de\rangle\,(E_d+E_e-W)^{-1}\langle de|v|fg\rangle\,(E_f+E_g-W)^{-1}\langle fg|v|bn\rangle.$$

The correct classes of resummed diagrams are built with a few simple prescriptions, formulated in order to avoid redundance:

- **The initial energy must be constant:** new interactions are inserted all in the same point each following its predecessor, with the rest of the diagram never changing, so that the initial energy stays constant;
- **Cutting particle lines:** new interactions must always be inserted cutting particle lines;
- **Hole-lines number:** the number of vertex-ingoing hole-lines must be kept constant in all diagrams.

Following this rules the sum of all the infinite ladder diagrams defines the G-matrix, represented as a wiggly line in the (d) diagram of fig. 3.3. But the procedure, even on resulting diagram (d) is far from being complete, and must be then applied again for the two top interactions, i.e. the second order in v resummation, and for the bottom interaction, that is a first order. Again this must be done avoiding any redundance: looking at fig. 3.4, the correct result is not the (a), but the (b) diagram. Again, this was presented as an example and is only part of the complete procedure of building the relevant diagrams at a given order of the G-matrix expansion.

The ordering criterion of resummed diagram is thus the equal number of hole-lines. The interactions, inserted in particle lines, compose the ladder diagrams. This procedure finally yields the correct contributions at the desired order. The underlying physical lead is that two particles are strongly correlated - i.e. the ψ state is considerably different from the unperturbed Φ - only when the distance between them is smaller than some characteristic correlation parameter. In the case of nuclear forces, such a scale length is of the same order of the hard-core, $c \approx 0.4\,\mathrm{fm}$. The average spacing r_0 among the nucleons can be estimated at every value of ρ_B: within a sphere of radius r_0 one can find one particle in average; the probability that it is strongly correlated is of the order of $P \sim 4\rho\pi c^3$; a second correlated particle can be found with probability P^2, a third with probability P^3, and so on. The probability of finding strongly correlated particles within the hard-core range is thus a good perturbative parameter to obtain converging expansions and can be found once per hole-line in the diagrams; the rough estimate given is a good tool to understand the success probability of the Brueckner-Goldstone expansion.
The new G-matrix series can be analytically defined introducing the Q, e operators:

$$Q|p\,q\rangle = \begin{cases} |p\,q\rangle & \text{if } p > A \text{ and } q > A, \\ 0 & \text{elsewhere;} \end{cases} \tag{3.40}$$

$$e|p\,q\rangle = (E_p + E_q - W). \tag{3.41}$$

respectively responsible of the forbidding of the interaction for particles that are not above the Dirac sea, and of stating the correct energy determinant for every ladder-diagram class. By means of their use, the G-matrix can be expanded as:

$$G(W) = v - v(Q/e)v + v(Q/e)v(Q/e)v - \ldots; \tag{3.42}$$

the label "matrix" used so far must recall the generalisation of the T-matrix scattering in the *vacuum*, recalled when eliminating the Pauli-blocking with the position $Q = 1$. But the G-matrix is an operator defined in infinite dimensional spaces, so it admits a continuous representation by means of the Bethe-Brueckner-Goldstone (BBG) integral equation:

$$G(W) = v - v(Q/e)G(W) = v - v\sum_{k,k'} \frac{|kk'\rangle\, Q_{k,k'} \langle kk'|}{W - e(k) - e(k')}\, G(W); \tag{3.43}$$

the right hand side is the form commonly used in the applications; a sum is shown instead of the proper integral: this is due to the fact that the integral equation is commonly solved approximating the Fredholm method, thus discretising the momentum-space and substituting the integral Kernel with a finite dimensional matrix, and an integral equation with a very large system of coupled algebraic equations.
When turning to practical calculations, the matter of specifying a proper single particle potential U comes back. It is very important as it appears in the single quasi-particle spectrum:

$$\epsilon(p) = \frac{p^2}{2m} + U(p). \tag{3.44}$$

A proper choice of U is very important in accelerating the convergence of the series, as it is responsible for the cancellation of a given class of diagrams in the G-matrix expansion. But this is not the only point to look at when going to actual calculations: it is necessary to study the character of the series and to choose at which order to stop the expansion to obtain reliable results.

§ **3.2.3. Brueckner Hartree-Fock.**— The three points stated in the end of the previous paragraph can be treated separatedly, in order to give the guidelines of a reliable calculation scheme for Nuclear Matter applications. Briefly, the Leading Order is the first; the correct choice for U is the Hartree-Fock single particle potential; the convergence of the expansion was proven numerically.

- **No NLO contributions:** the second order diagrams do not give any contributions to the expansion. This is due to a peculiar property of Nuclear Matter: an infinite system of interacting nucleons with boundary periodic conditions has plane waves as single particle wavefunctions [→ § 3.1.1]. It can be proven that p is a cyclic coordinate for the Hamiltonian (3.32) and that any consequent Slater determinant must thus have vanishing total momentum, i.e. the Dirac vacuum, in which every particle is counterbalanced by an anti-particle of inverse momentum. Even the diagrams that would give non-zero contributions, like the (b) diagram of fig. 3.4 when carefully removing the bubble on the right, are redundant in the G-definition: this particular example is already included in the (a) diagram of fig. 3.5, that pertains to the first order of the BG series.

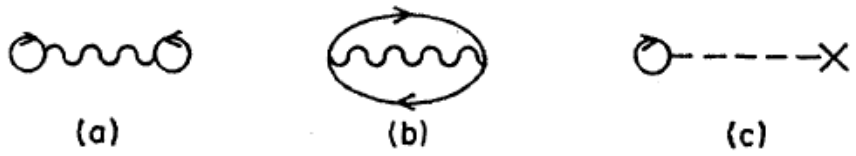

Figure 3.5: First order diagrams in the hole-line BBG expansion; (a,b) Hartree-Fock approximation relevant diagrams - (c) diagram dropped due to the $U_{\rm HF}$ choice. Taken from ref. [67].

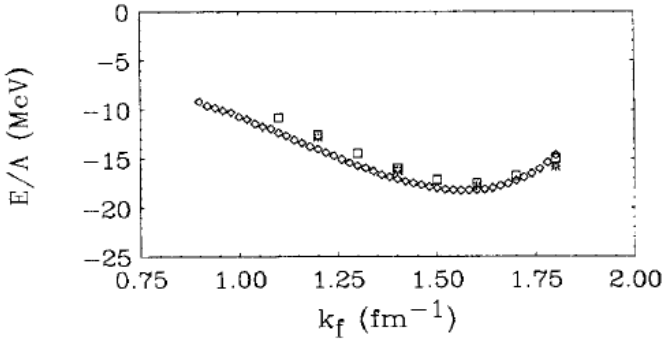

Figure 3.6: Symmetric matter Equation of State: the diamonds are the LO calculations; the squares are the NNNLO calculations (fourth order in the hole-line number). Taken from ref. [64].

- **Hartree-Fock:** back in the early times of Brueckner Theory, many single particle potential U choices have been discussed. Nowadays calculations are always performed - or at least begun - with the Hartree-Fock choice. This particular choice cancels all the diagrams in which a bubble line is attached to a hole line, thus all the diagrams carrying one or more interactions and bubble-interactions exchange. The choice corresponds to the form:

$$U(p_m) = \sum_{n \leq A} \langle mn|G(W)|mn\rangle_{\mathcal{A}} \tag{3.45}$$

  clearly leading to a self-consistency, as discussed in § 3.1.3, when inserted in the BBG equations. The scheme consequently takes the name "Brueckner Hartree-Fock" (BHF).

- **Convergence:** a series of works on this issue was produced by the Catania group during the 1990s, whose results are summarised in the work [64](1998), appeared on Physical Review Letters. The convergence of the series was therein numerically proved; the Leading Order

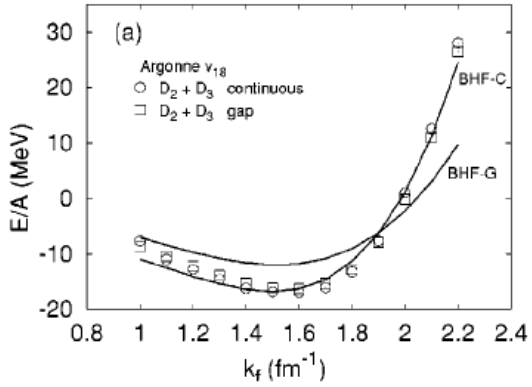

Figure 3.7: Equation of State for Symmetric Nuclear Matter with the Argonne v18 realistic potential [54]. The solid lines represent respectively gap and continuous choice BHF approximations, while the dots show the contributions up to NNLO. Taken from ref. [68].

was fixed already at the first, as the second order diagrams do not give any contribution and the third diagrams contributions can be neglected; the results have an accuracy of $1 \div 2$ MeV: this can be checked in the bottom panel of fig. 3.6. Finally, the authors proved the validity of a procedure in which the energy contributions are summed even above the Fermi surface $k > k_F$, called "continuous choice", against the common scheme, called "gap choice", that led to the cancellation of a higher number of high-order diagrams.

§ **3.2.4. Three-Body Forces.**— A rapid eye at figs. 3.6-3.7 can better explain the point stated in the introduction: Brueckner theory successfully reproduces the nuclear saturation behaviour starting from Nucleon-Nucleon bare interactions. The presented scheme however fails in reproducing good quantitative results, as required by the observations reported in eq. (2.16). Furthermore, slightly above saturation it shows too much attraction. This is due to the fact that the realistic NN forces describe the nucleon as a point-like particle. To overcome this problem, contributions due to three and four-body forces were included, recovering an idea due to D. Day [67], in order to take into account for the possible internal structure of the nucleon, responsible for resonances or nucleon/anti-nucleon vacuum polarisations. In a seminal work by the Liège group [65], the three-body diagrams of fig. 3.8 were added in a microscopic fashion, then treated as a two body effective interaction by means of a Wick contraction and summed to the usual v potential.

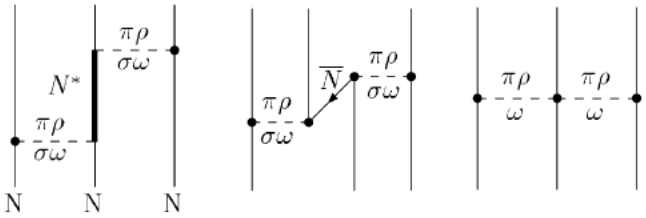

Figure 3.8: Three body-forces contribution diagrams: nucleonic resonance, virtual $N, \bar{N}$ vacuum excitation and two meson-exchange [69].

The contributions used in this thesis come from the more recent work by W. Zuo et al. [69], in which the three-body forces are constructed consistently with the Bonn and Nijmegen NN potentials, to pair up the input of the microscopic calculations.

§ 3.2.5. Thermodynamic consistency.— Brueckner Hartree Fock calculations end up modifying the single particle energy spectrum, like predicted in § 3.1.4, as the nucleon bare mass is renormalised due to the mean field interaction. The first calculations by Brueckner showed a similar thermodynamic inconsistence, that led N. M. Hugenholtz and L. van Hove to the formulation of a theorem [70]:

> For a system with zero pressure (i.e. a Fermi liquid at absolute zero) the Fermi energy ϵ_F is equal to the average energy per particle E_0/N of the system. This result should apply both to liquid ^{3}He and to nuclear matter.

that can be seen as a generalisation to Nuclear Matter of a famous theorem by T. Koopmans for the closed shell states in Hartree-Fock theory [71], according to which the first ionization energy of a molecular system is equal to the negative of the orbital energy of the highest occupied molecular orbital. According to the authors, the problem arose from the fact that Brueckner neglected important cluster terms contributing to the single particle energy; a good calculation asset was found by M. Baldo et al. [72], in the framework of an approximation scheme which includes single-particle correlations, finally satisfying the Hugenholtz-van Hove theorem. Furthermore, it can be formally proven that the problem lies in the choice of the single particle potential, because Brueckner theory satisfies the Hugenholtz-van Hove theorem at Hartree Fock level for any potential not depending on density; a concise proof is given in the appendix of ref. [73].

3.3 Quark Matter

The approach to describe Quark Matter is analogous to the hadronic case; its properties are unconstrained though, due to the lack of empirical observations of free coloured systems. Recalling the discussion of § 2.1.4, Bulk strange-Quark Matter is an infinite aggregate of u, d, s quarks at the Thermodynamic Limit, thus with net baryon number $A_q \to \infty$, in a global colour singlet state, and within a volume $V \to \infty$, so that the quark density $\rho_q = A_q/V$ is a well-defined finite real number. Clearly the "bulk" label refers to the absence of any surface effect, plausible assumption for large Macroscopic-scale systems as the interior of Neutron Stars.
The starting point is the Gibbs Grand-potential $\Omega_q = \Omega_q^0 + \Omega_q^{\rm int}$, sum of a free-gas term plus an interaction term. The latter should come from a QCD-Many Body problem; the difficulties in solving the Gauge Theory of Strong Interactions in non-perturbative regime makes necessary to use some effective theories that reproduce a basic set of the full QCD properties.

§ **3.3.1. MIT Bag Model.**— The first, and most crude approach, is what nowadays is referred as the "MIT Bag Model" [74], briefly used in § 1.2.1 to calculate the Equation of State of quarks; its whose basic idea is to suppose that quarks are confined within a spherical region, called "bag", of the QCD vacuum. Outside the bag, lies the true QCD vacuum; inside the quarks interact weakly, so that they are immersed in some perturbative vacuum, an excited state of the true QCD vacuum, characterised by a constant energy density B, called "Bag Constant", accounting in a phenomenological way for the non-perturbative aspects of QCD. The quarks in such scheme exert an outgoing pressure on the surface of the bag with their Fermi motions, while the different vacuum energy density gives rise to an inward counterterm $P_B = -B$. In principle quark dynamics inside the bag can be calculated by means of perturbative QCD, so that the thermodynamic potential can be calculated from two contributions: $\Omega_q^{\rm int} \simeq \Omega_q^{\rm NP} + \Omega_q^{\rm AF}$, one Non-Perturbative, the other in Asymptotic Freedom regime.
As a first, crude approximation is to treat neglige any interactions among the quarks, thus treating them as the free-flavours of a Fermi Gas, and to approximate the non perturbative effects as:

$$\Omega_q^{\rm int} = \Omega_q^{\rm NP} = B; \tag{3.46}$$

this prescription lies at the base of the Bag Model. The assumption, despite being extremely simplistic, is thought to be reasonable at very high densities, while obviously fails at the density regimes typical of hadron formation, i.e. around the first-order phase transition of colour confinement / chiral symmetry breaking.
In this thesis - having in mind a comparison with Nambu-Jona Lasinio results - the three flavours are treated in exact $SU_f(3)$ chiral symmetry - i.e. the quarks are massless. From the Free Gas theory of § 3.1.1, the potential reads:

$$\Omega_q^0 = -\sum_i \frac{1}{(\hbar c)^3}\frac{1}{4\pi^2}\mu_i^4, \tag{3.47}$$

where the flavour index $i = \{u, d, s\}$; correspondingly, one can calculate from thermodynamics the flavour densities:

$$\rho_i = -\left(\frac{\partial \Omega_i}{\partial \mu_i}\right)_{T,V}, \tag{3.48}$$

so that the total quark density is $\rho_q = \sum_i \rho_i$. The Equation of State has the very simple form:

$$P(\mu_u, \mu_d, \mu_s) = -\Omega_q^0 + \sum_i \frac{1}{(\hbar c)^3}\frac{1}{4\pi^2}\mu_i^4 - B \tag{3.49}$$

$$\epsilon_q(\mu_u, \mu_d, \mu_s) = +\Omega_q^0 + \sum_i \mu_i \rho_i + B. \tag{3.50}$$

The last step comes applying the proper relations for the quark matter β-stability:

$$d \to u + e^- + \bar{\nu}_{e^-}, \qquad s \to u + e^- + \bar{\nu}_{e^-}, \qquad s + u \to d + u,$$

that leads - in the considered case - to degenerate quark-flavour densities and chemical potentials, and to a total suppression of the electron density. The Equation of State can thus be expressed by means of the total quark density ρ_q analogously to the hadronic case.

The assertion that a theory is the only correct one can only be an expression of our subjective conviction that there can be no other equally simple and equally fitting picture.

L. E. Boltzmann

4 Viscosity

The term "fluid" comes from the ancient greek verb φλύειν, literally meaning "to bubble up", describing a liquid that overflowed the recipient in which it was boiling. Physics speaks of "fluids" referring to a subset of the phases of matter that do not have a definite shape; a substance has a fluid behaviour when it continually deforms under an applied shear stress. Viscosity is a key property of a fluid, representing a measure of its dissipative behaviour. A liquid, for example, flows in layers so that a force applied on the upper layer is transferred to the next with a small defect due to friction. In this setup Shear Viscosity η is defined in terms of the friction force F per unit area A created by a shear flow with transverse flow gradient $\nabla_y v_x$:

$$\frac{F}{A} = \eta \nabla_y v_x, \tag{4.1}$$

and is measured in the S.I. of units as Pa·s=kg·m^{-1}·s^{-1}. A discussion about its conversion in other unit systems can be found in the Appendices [→ App. A.2]. The relative importance of inertial vs. viscous forces in given flow conditions for different systems is expressed by the Reynolds number Re, a dimensionless parameter, as the ratio:

$$\mathrm{Re} = \frac{vL}{\nu} \tag{4.2}$$

between a property of the fluid, the kinematic viscosity $\nu = \eta/\rho$ and a property of the flow, expressed in terms of the product between a characteristic velocity v and a characteristic length of the system L. For example in a pipe the characteristic length $L \sim D$ is of order of the diameter D; experimental observations show that laminar flow occurs when $Re_D < 2300$ and turbulent flow occurs when $Re_D > 4000$.
But the macroscopic properties of a fluid are very sensitive of the microscopic

interactions among their corpuscular constituents. This leitmotiv is carried out throughout this thesis, it can be seen as a sort of underlying principle: again, hydrodynamics and transport theory will be the microscopic frameworks that link the sketching of the interactions by means of many body theories, to devise thermodynamical and macroscopic properties of a fluid. Recent discoveries by RHIC show that the Quark-Gluon Plasma produced in heavy ion collisions is the most perfect liquid ever observed [→ § 1.3.2]; in the low T, finite μ regime the properties of QGP are unconstrained, so the calculations presented in this work are meant to give some insight in this very open field of Physics. General arguments come from the textbooks of P. Nozieres [41], G. Baym and C. Pethick [42] on Normal Fermi liquids, and from the excellent review article by T. Schäfer and D. Teaney [75].

4.1 Hydrodynamics and Transport Theory

For illustrative purposes, Hydrodynamics here will be briefly sketched in the case of a one-component non-relativistic fluid of Equation of State at thermal equilibrium $P = P(\epsilon, \rho)$. The idea is to give the general guidelines to solve a transport problem for dynamical properties. In such a picture, five conservation laws $(2 + 3)$ are given:

$$\frac{\partial \epsilon}{\partial t} + \nabla \cdot j^{\epsilon} = 0 \tag{4.3}$$

$$\frac{\partial \rho}{\partial t} + \nabla \cdot g = 0 \tag{4.4}$$

$$\frac{\partial g_i}{\partial t} + \nabla_i \, \Pi_{ij} = 0 \tag{4.5}$$

in terms of the energy density ϵ and its relative current j^{ϵ}, of the mass-density ρ, of the three *momentum*-density g_i components, and of the stress tensor Π. These equations fundamentally rule the dynamical evolution of the fluid, whose properties are expressed by means of "constitutive relations" that relate derivatives of the flow velocity v and thermodynamic variables (such as ϵ, P, ρ, etc.) with the conserved currents (j^{ϵ}, g, etc.).
In practical matters the currents are expanded with respect to their associated thermodynamical variables so that the contributions at the various order, plugged inside the evolution relations, describe fluids in different regimes; the first two orders account for most of the known physical systems. Viscosity appears at second order as a dissipative effect.

§ **4.1.1. Ideal fluid.**— Ideal hydrodynamics is the result of constitutive equations stopped at the Leading Order in the thermodynamic relations; they describe the behaviour of a fluid that has no dissipative term. This represent an extremely simplified model and is suitable for few applications to real systems. The corresponding constitutive relations are fixed by Galilean invariance, rotational invariance and conservation of entropy as:

$$j^{\epsilon} = v(\epsilon + P) \tag{4.6}$$

$$g = \rho\, v \tag{4.7}$$

$$\Pi_{ij} = P\delta_{ij} + \rho\, v_i v_j \tag{4.8}$$

with $\epsilon = \epsilon_0 + \frac{1}{2}\rho\, v^2$ depending on the energy (density) in the rest frame of the fluid. This equations, together with the Equation of State $P(\epsilon, \rho)$ must be coupled with the conservation equations:

$$\frac{\partial \rho}{\partial t} + \nabla \cdot (\rho v) = 0 \tag{4.9}$$

$$\frac{\partial v}{\partial t} + (v \cdot \nabla)v = -\frac{1}{\rho}\nabla P \tag{4.10}$$

$$\frac{\partial s}{\partial t} + \nabla \cdot (vs) = 0; \tag{4.11}$$

the first is called "continuity equation" and the second describes *momentum* conservation; the third replaces the energy conservation equation, that can be rewritten at leading order in terms of entropy conservation. The set of first-order constitutive relations (4.6),(4.7) and (4.8) substituted inside the conservation equations specify completely the fluid-thermodynamics; they are named "Euler equations" and describe the evolution of a "perfect", i.e. non viscous fluid.

§ **4.1.2. Dissipative fluid and definition of viscosity.**— Dissipative contributions arise at the next order, and are called "transport coefficients". To the next order then, the constitutive relations become:

$$\Pi_{ij} = P\delta_{ij} + \rho\, v_i v_j + \delta\Pi_{ij} \qquad \text{in which:} \tag{4.12}$$

$$\delta\Pi_{ij} = -\eta(\nabla_i v_j - \nabla_j v_i - \frac{2}{3}\delta_{ij}\nabla \cdot v) - \zeta\, \delta_{ij}(\nabla \cdot v), \tag{4.13}$$

depending on the two viscosities: the first (or shear) η and the second (or bulk) ζ. The energy current becomes:

$$j^{\epsilon} = v_i(\epsilon + P) + v_j\, \delta\Pi_{ij} + Q_i, \tag{4.14}$$

in which appear a contribution of the temperature gradient $Q = -\kappa \nabla T$, mediated by the thermal conductivity κ. The third relation remains simply $g = \rho v$, and this is set by Galilean invariance, whose breaking cannot be coupled to any observable effect. The three transport η, ζ and κ coefficients are constrained to be positive from the second principle of thermodynamics. The equations of evolution including the new terms describe the hydrodynamics of a dissipative viscous fluid; they are a system of coupled Partial Differential Equations called "Navier-Stokes equations".

§ **4.1.3. Transport Theory.**— L. Boltzmann pioneered the studies of non-equilibrium Statistical Mechanics being the first to study the dynamical features of dilute-gases by means of his "Transport Equation". The derivation comes from the set of assumptions:

- **Dilute system:** The gas consists of a large number N of hard elastic spheres occur; the system is dilute, so that only binary elastic collision are relevant for its dynamics.

- **Distribution function:** at the time instant t^*, a state of the gas is represented by the distribution function f, so that:

$$f_k(q, t^*)\delta p \delta q = \frac{1}{N}, \tag{4.15}$$

  where N is the number of particles in the infinitesimal configurations-space volume $\delta p \delta q$.

- **Stosszahl-ansatz:** later justified by Boltzmann as a "Molecular Chaos assumption", is the statement that at every time instant t, the number of particle-pairs that are going to collide in the time interval $t + \delta t$ is:

$$\frac{N^2}{m} f_k(q, t) f_{k'}(q', t) \, |p_k - p_{k'}| \, \delta t \, \delta \Omega \tag{4.16}$$

  expressed in terms of the infinitesimal solid angle variation $\delta\Omega$. The label k accounts for *momentum* quantisation - as in the case of Fermi liquids.

The third assumption is essentially introduced to treat collisions in a simplified and non-realistic way, as if it breaks time-reversal. Subsequent studies from Jeans (1902) tried to justify it in the context of statistical mechanics,

reformulating the Stosszahl-ansatz as an independent particle approximation for the two-body distribution function:

$$f(p_k, q, t; p_{k'}, q', t) \approx f_k(q,t)\, f_{k'}(q',t), \tag{4.17}$$

not overcoming anyway the problem of time-reversal symmetry breaking. For the non relativistic fluid sketched in this section, the three energy, *momentum* and stress-tensorial currents are given in components by:

$$j_i^{\epsilon}(q,t) = \int \frac{\mathrm{d}^3 p}{(2\pi^3)}\, \epsilon_k\, v_{k,i}\, f_k(q,t) \tag{4.18}$$

$$g_i(q,t) = \int \frac{\mathrm{d}^3 p}{(2\pi^3)}\, m\, v_{k,i}\, f_k(q,t) \tag{4.19}$$

$$\Pi_{ij}(q,t) = \int \frac{\mathrm{d}^3 p}{(2\pi^3)}\, m\, v_{k,i} v_{k,j}\, f_k(q,t) \tag{4.20}$$

in which the label k is relative to the single-particle energy spectrum ϵ_k and $v_{k,i} = \partial\epsilon_k/\partial p_i$ is the quasiparticle velocity. The equation of motion for the distribution function is the Boltzmann Transport Equation:

$$\frac{\partial f_k}{\partial t} + v \cdot \nabla f_k + F \cdot \nabla_k f_k = I[f_k] \tag{4.21}$$

where F is the contribution for external forces and $I[f_k]$ is the collision term, that accounts for quasiparticle collisions, suddenly changing their *momenta*. Thanks to the Stosszahl-ansatz, the collision term can be expressed as:

$$I[f_{k'}] = \frac{N}{m} \int [f_k(q,t) f_{k'}(q',t) - f_k(q_f,t) f_{k'_f}(q'_f,t)]\, |p_k - p_{k'}|\, \delta\Omega \tag{4.22}$$

in which the subscript f refers to the final coordinates of the outgoing particles after a collision, so that $f(q)f(q') \rightarrow f(q_f)f(q'_f)$. The distribution function is determined by the local temperature, chemical potential and flow velocities as:

$$f_k^0(q,t) = \frac{1}{e^{(\epsilon_k - v\cdot p - \mu)/T + 1}} \tag{4.23}$$

as the usual Fermi-Dirac distribution, describing the statistic behaviour of fermions. The Transport equation in absence of collisions is just the continuity equation (4.4) for the distribution function f_k; it was applied to many systems and generalised to include quantum effects or to describe relativistic systems. One of the most famous generalisations is briefly presented here, as it leads to the calculation of the transport coefficients for a Normal liquid.

§ 4.1.4. The Landau-Boltzmann approach for Fermi Liquids.— The Boltzmann approach in this formulation was found by Landau to be unsuitable to describe the properties of weakly interacting quantum liquids. His generalisation of the theory started from a fluid-dynamical analogy between a dilute gas and a normal liquid, that lead to a more refined approach: the basics of Landau Normal Fermi liquid theory were given in Chapt. 3 [→ § 3.1.2] to elucidate how the concept of quasi-particle arises in a free system with an adiabatic switch-on of the interaction. If the interactions met the requirements of Landau theory then the fluid can be described in terms of weakly interacting quasiparticles around the Fermi surface and the hydrodynamic variables can now be written in terms of quasiparticle distribution functions $n_k(q,t)$ in coordinate space, substituting the particle distribution functions $f_k(q,t)$ of Boltzmann dilute gas theory. New degrees of freedom are thus quasiparticles, for which one can define velocity and *momentum* variation as the time derivatives of 3-position q and 3-*momentum* p coordinates. The assumption of quasiparticle kinetic theory is that ϵ_k, the single particle spectrum, plays the role of quasiparticle Hamiltonian; the usual quasiparticle velocity term is now put alongside with a new force-term F_k, that is very important in actual calculations of quantum liquid properties:

$$v_k(q,t) = +\nabla_k \epsilon_k(q,t) \tag{4.24}$$

$$F_k(q,t) = -\nabla_q \epsilon_k(q,t); \tag{4.25}$$

This aspect is later discussed in the case of the insertion of an external potential U. Under this ansatz, the Boltzmann-Landau classical equation can be written as:

$$\frac{\partial n_k(p,t)}{\partial t} - \{\epsilon_k(q,t), n_k(q,t)\} = \mathrm{I}[n_k], \tag{4.26}$$

where the symbol $\{\cdot,\cdot\}$ stands for the usual Poisson brackets of Analytical Mechanics. The right hand side is again a term taking into account the role of quasiparticle collisions in determining the time evolution of the quasiparticle distribution function n_k. Thus, again ignoring spin degrees of freedom, an elastic collision between two quasiparticles from the initial states $1+2 \to 3+4$ to the final would yield a rate of events in the system that in general depends on some quantum collision probability $W(12;34)$, on some fitting Dirac delta $\delta(\epsilon_i)$, $\delta(p_i)$ to impose energy and *momentum* conservation in a given volume V, and on the relative populations of the quasiparticle

states n_i, with $i = \{1, 2, 3, 4\}$:

$$R_{12\to 34} = \frac{1}{V^2} W(12;34)\, \delta_{p_1+p_2,p_3+p_4}\, \delta(\epsilon_1 + \epsilon_2 - \epsilon_3 - \epsilon_4)\, n_1 n_2 (1-n_3)(1-n_4); \tag{4.27}$$

the collision term $\mathrm{I}[n_k]$ is the net rate at which two-body collisions increase the occupation of the state p_1; this is given by:

$$\mathrm{I}[n_k] = \sum_{2,3,4} R_{34\to 12} - R_{12\to 34} \tag{4.28}$$

as the difference of the collisions populating the $1, 2$ states and those that depopulate them, summed over any quasiparticle *momentum* states $2, 3, 4$. The full term becomes:

$$\frac{1}{V^2} \sum_{2,3,4} W(12;34)\, \delta(\epsilon)\delta(p)\, [n_3 n_4 (1-n_1)(1-n_2) - n_1 n_2 (1-n_3)(1-n_4)]; \tag{4.29}$$

the quantum transition amplitude matrix is supposed symmetric. An additive δ accounting for spin angular *momentum* conservation completes the picture (supposing that the interactions is spin-independent). The new transport equation (4.26), with collision term specified by eq. (4.29), includes two interesting features: the first is a dependence on position and time for the quasiparticle velocity $\nabla_k\, \epsilon_k$; the second is related to the inclusion of effective field contributions in the force field $\nabla_q\, \epsilon_k$. Indeed, upon the insertion of an external scalar potential U acting on the system, the total energy acquires a term:

$$\int \mathrm{d}^3 q\, U(q,t)\, n_k(q,t), \tag{4.30}$$

so that the quasiparticle spectrum ϵ_k is shifted by U. This in turn yields an additional term when one computes the term $\nabla_q\, \epsilon_k$:

$$\nabla_q\, \epsilon_k = \nabla_q\, U + \int \frac{\mathrm{d}^3 p'}{(2\pi^3)}\, f_{pp'} \nabla_r\, n_{k'}; \tag{4.31}$$

the first term is also present in the dilute gas equation (4.17), while the second appears only in the present case and acts as a mean-field term, responsible for many of the Fermi Liquid properties.

§ 4.1.5. Linearisation and Momentum Relaxation.— In practical applications, the Landau-Boltzmann transport equation (4.26) is very hard to

solve for analytical solutions, due to the complexity of the collision term specified by eq. (4.29). The first solution for the shear viscosity of a low temperature Normal Fermi liquid were given by A. A. Abrikosov and I. M. Khalatnikov by means of a variational estimate [76]; a full analytic solution was finally devised by G. Brooker and J. Sykes [77] that could finally solve the integral equations of Abrikosov-Khalatnikov. Before any solution is sought, it is clever to follow the historical methods of the cited authors, linearising the transport equation and simplifying further the collision term by means of the "Relaxation time approximation". The details about the first task will be skipped, as the calculation is tedious and can be found in the textbooks cited at the beginning of the chapter. It is much more interesting to present the physical idea, that recalls the small oscillation studies in the static part of classical mechanics. In many applications the system is almost at equilibrium on small scale, i.e. the distribution function differs only by an infinitesimal amount δn_k from its value n_k^0 in uniform equilibrium. The transport equation must then be linearised in δn_k, introducing a first-order linear deviation:

$$\begin{aligned}\delta\bar{n}_k &\equiv \delta n_k - \frac{\partial n_k^0}{\partial \epsilon_k}\,\delta\epsilon_k \\ &= \delta n_k - \frac{\partial n_k^0}{\partial \epsilon_k}\int \frac{\mathrm{d}^3 p'}{(2\pi)^3}\, f_{kk'}\,\delta n_{k'},\end{aligned} \tag{4.32}$$

as the linear deviation of the distribution function from the value it would have for a quasiparticle of energy $\epsilon(q,t)$ in a system in equilibrium. Under this assumption the Boltzmann-Landau linearised equation is:

$$\frac{\partial \delta n_k}{\partial t} + v_k \cdot \nabla_q\, \delta\bar{n}_k = \mathrm{I}_l[n_{k'}], \tag{4.33}$$

in which the linearised collision term is evaluated with the same prescription in terms of a local equilibrium, and reads as:

$$-\frac{1}{TV^2}\sum_{2,3,4} W(12;34)\,\delta(\epsilon)\delta(p)\,n_1 n_2(1-n_3)(1-n_4)[\Phi_1+\Phi_2-\Phi_3-\Phi_4], \tag{4.34}$$

with all the appearing n_k, ϵ_k and W have their local equilibrium values and the Φ can be defined from a prescription similar to eq. (4.32) but in the much more complicated formalism of local equilibrium:

$$\delta\bar{n}_i^{\text{l.e.}} \equiv -\frac{\partial n_k^0}{\partial \epsilon_k}\,\Phi_i, \tag{4.35}$$

due to the generally complex relation between local equilibrium and global equilibrium, clearly beyond the scope of this treatment (the details can be found in [42], pag. 27).
The linearised collision term, expressing the microscopic complexity of the system, has a full energy dependence that is anyway to hard to be treated in a large number of practicals matters, so that often a further simplification is introduced:

$$\mathrm{I}[n_k]_{\mathrm{R.T.}} = -\frac{\delta\bar{n}_1^{\mathrm{l.e.}}}{\tau} \tag{4.36}$$

known as "Relaxation Time approximation": the collision term does not include anymore a complex quantum-collisional scheme of single-particle level population, but simply describes the effects of collision as a restoration of the equilibrium function n_k^0 from the non-equilibrium n_k on a timescale τ, independent of the particle energy.

§ **4.1.6. Viscosity of Normal Fermi liquids.**— Shear Viscosity in a Normal Fermi liquid at low temperature can thus be calculated by means of the linearised Boltzmann-Landau equation (4.33) for the quasiparticle local distribution function $\delta\bar{n}_i^{\mathrm{l.e.}}$, that in turn are inserted in eq. (4.20), valid also in Landau scheme by making the substitution $f \to n$; the shear stress tensor components are defined in eq. (4.13) by its second-order dissipative expansion in terms of P, ρ, v and obviously of the shear η and bulk ζ viscosities. The hypothesis here is that the system is in local equilibrium, with small spatially varying fluid velocity v; under this assumption the term $\rho\, v_i v_j$ - of second-order in v - can be dropped in eq. (4.13), that reads:

$$\Pi_{ij} = P\delta_{ij} - \eta(\nabla_i v_j - \nabla_j v_i - \frac{2}{3}\delta_{ij}\nabla\cdot v) - \zeta\,\delta_{ij}(\nabla\cdot v); \tag{4.37}$$

a small deviation δn_k of the distribution function from global equilibrium yields a change in the stress tensor Π_{ij}:

$$\delta[\Pi_{ij}] = \int \frac{\mathrm{d}^3 p}{(2\pi^3)}\, p_{k,i} v_{k,j}\, \delta\bar{n}_k; \tag{4.38}$$

once $\delta\bar{n}_k$ is expanded in terms of the corresponding quantity for local equilibrium $\delta\bar{n}_k^{\mathrm{l.e.}}$ yields a term accounting for pressure variation, plus a term:

$$\delta\Pi_{ij} = -\int \frac{\mathrm{d}^3 p}{(2\pi^3)}\, p_{k,i} v_{k,j}\, \delta\bar{n}_k^{\mathrm{l.e.}}. \tag{4.39}$$

Here $\delta\Pi_{ij}$ refers to the second order dissipative contribution to the hydrodynamical shear stress current of tensorial components Π_{ij}, while the previous notation $\delta[\cdot]$ refers to the functional derivative of the tensor components with respect to the small variation δn_k. Shear Viscosity can be computed from this equation retaining only the $ij = xy$ components, i.e. assuming that v is in the x direction and that $v_x = v_x(y)$:

$$\delta\Pi_{xy} = \eta\frac{\partial v_x}{\partial y} = -\int \frac{\mathrm{d}^3p}{(2\pi^3)}\, p_{k,x} v_{k,y}\, \delta\bar{n}_k^{\mathrm{l.e.}}. \tag{4.40}$$

The problem is solved by integrating the linearised Landau-Boltzmann equation (4.33) for the quasiparticle local equilibrium distribution variation $\delta\bar{n}_k^{\mathrm{l.e.}}$; this was approximately estimated by Abrikosov and Khalatnikov with a variational approach and exactly calculated by Brooker and Sykes, whose full result reads [77]:

$$\eta = \frac{64}{45}\frac{\hbar^3 p_0^5}{m^* k_B^2 T^2}\left[\int \frac{\mathrm{d}\Omega}{2\pi}\frac{\omega(\theta,\phi)}{\cos(\theta/2)}(1-\cos\theta)^2\sin^2\phi\right]^{-1} C(\lambda); \tag{4.41}$$

in which appear back the constants $\hbar$ and k_B; $C(\lambda)$ is a correction factor for the Abrikosov-Khalatnikov form. Aside from the very complex integral, arising from the complex-energy dependencies of the collision factor, at low temperature the Shear Viscosity of a Normal Fermi liquid goes like $\eta \sim T^{-2}$.

§ 4.1.7. Nuclear Matter calculations.— The Shear Viscosity for Nuclear Matter was calculated in the framework of Brueckner Theory by U. Lombardo et al. [78] simply extending the Brooker and Sykes result of eq. (4.41) for a multicomponent system of asymmetric constituents in β equilibrium. The corresponding equations are:

$$\eta\, T^2 = \frac{1}{20}\rho_B\, v_F^2\, W(\rho_B)^{-1}\, C(\lambda) \tag{4.42}$$

where ρ_B is the density, $v_F = p_F/m^*$ is the Fermi velocity of the system calculated in terms of the effective mass m^* and:

$$W(\rho_B) = \frac{1}{2\epsilon_F}\int_0^{4\epsilon_F}\mathrm{d}E\int_0^{2\pi}\frac{\mathrm{d}\theta}{2\pi}\frac{1}{\sqrt{1-E/4\epsilon_F}}\,\sigma(E,\theta) \tag{4.43}$$

to be evaluated in terms of the *in medio* cross section $\sigma(E,\theta)$, function of the energy in the laboratory frame and of the scattering angle in the center-of-mass system; the upper integration limit $4\epsilon_F$ restricts the quasi-nucleon

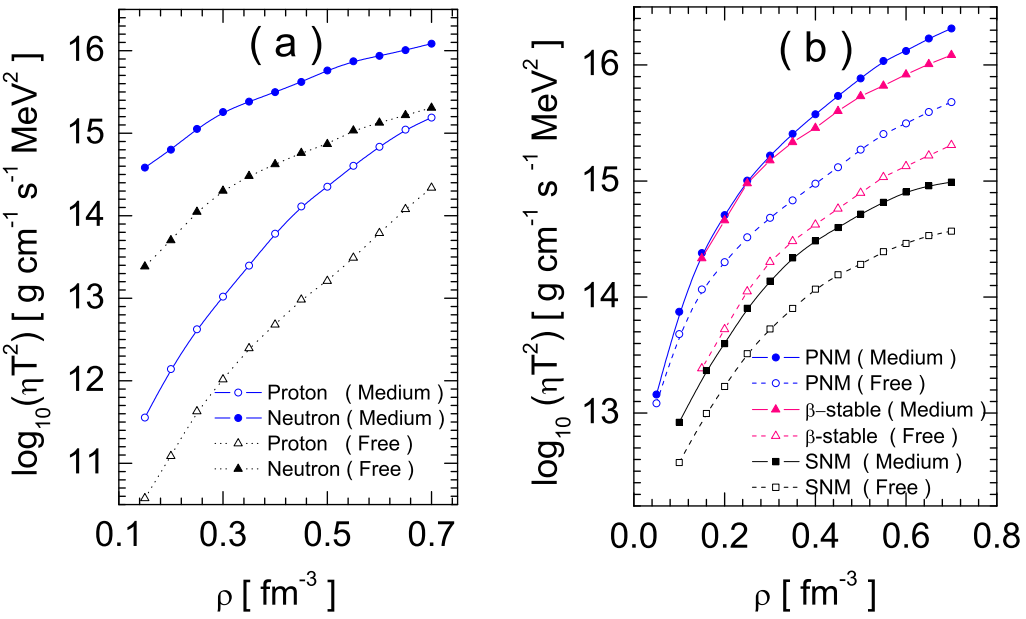

Figure 4.1: Shear Viscosity of Nuclear Matter. *Left:* Proton and Neutron matters: comparison between the free result and the *in medio* calculation. *Right:* Calculation for Asymmetric Nuclear matter in β equilibrium, confronted with Symmetric Nuclear matter and Proton Matter. Taken from ref. [78]

excitations to the Fermi surface. In Brueckner theory the in-medium cross section can be evaluated separately for two scattering channels starting from the effective mass m^* - arising from the mean field treatment of interactions and here defining the single-particle level densities in the pre-factor - and from the G-scattering matrix in the *medium* for the S wave channel, defined by the integral eq. (3.43) in terms of the bare potential u_{NN}. The corresponding cross-sections for neutron-neutron and neutron proton scatterings are:

$$\sigma_{nn}(E,\theta) = \frac{m^{*2}}{16\pi^2\hbar^4} \sum_{SS_zS_z'} |G^S_{S_zS_z'}(\theta) + (-1)^S G^S_{S_zS_z'}(\pi-\theta)|^2 \tag{4.44}$$

$$\sigma_{np}(E,\theta) = \frac{m^{*2}}{16\pi^2\hbar^4} \sum_{SS_zS_z'} |G^S_{S_zS_z'}(\theta)|^2. \tag{4.45}$$

But, as stated, in practical matters Nuclear Matter is an asymmetric two-component system in β equilibrium. The two given relations lead to calculations that cannot be combined to yield the viscosity in asymmetric matter, so that a third calculation must be performed for future use in calculations:

$$\sigma_{np}(E,\theta) = \frac{1}{16\pi^2\hbar^4} \left(\frac{2m_n^* m_p^*}{m_n^* + m_p^*}\right)^2 \sum_{SS_zS_z'} |G^S_{S_zS_z'}(\theta)|^2, \tag{4.46}$$

containing a term that accounts for the blending of neutrons and protons by means of their effective masses m^*. The results for the discussed limits are reported in fig. 4.1.

4.2 Shear Viscosity in Quark-Gluon Plasma

During the first years of the 1990s G. Baym, C. J. Pethick and H. Heiselberg spent many efforts on a model for the solution of the transport problem in a Quark-Gluon Plasma based on the "dynamical screening" of transverse interactions at small *momenta* [79–81]. The model was developed for high temperatures, i.e. much larger $T \gg \mu_q$ than the typical quark-chemical potential and the *momentum* relaxation rates were calculated by means of a perturbative approach in which the gluon propagator is dressed with a Debye *in medio* mass $m_D^2 \sim g^2 T^2$; when applied to the $T \sim 200$ MeV situation, clearly $T \sim \Lambda_{\rm QCD}$ and non-perturbative effects become non-negligible as $\alpha_s = 0.6$, but analogously to QCD Lattice studies, the $\eta/s \sim 0.2$ ratio is estimated to be safely within a factor 2 from experimental evidences and more sophisticated calculations.
Later, in 1993, C. J. Pethick and H. Heiselberg extended the model to the complementary regime $T \ll \mu_q$ [82], describing two further physical situations arising in dependence of the relative values of T and of the dressed gluon mass $m_D^2 = g^2 N_q \mu_q^2 / 2\pi^2$. In conditions sketched in Chapt. 2, $T \ll m_D$ so that the shear viscosity is found to be:

$$\eta_Q \, T^2 \; = \; \frac{\mu_q^4}{40\pi \, \alpha_s^2} \frac{m_D^{-1}}{\left[\pi^3/4 + a \, (T/m_D)^{-1/3}\right]}, \tag{4.47}$$

in term of the constant $a = \Gamma(\frac{8}{3})\zeta(\frac{5}{3})(2\pi)^{2/3}/6 \sim 1.81$ and significantly deviating from the $\eta \sim T^{-2}$ behaviour of Normal Fermi liquid theories (4.41). This can be explained by the fact that the Fermi Liquid behaviour is computed assuming a constant scattering cross-section: any realistic calculation thus should deviate from this behaviour, and the present case does particularly at low T.

§ 4.2.1. Dynamical Screening of Transverse Interaction.— As briefly anticipated, the problem of calculating transport parameters in the $T \ll \mu_q$ limit is complicated from the fact that although almost no thermal gluons are present in degenerate quark matter, there effects of dynamical screening

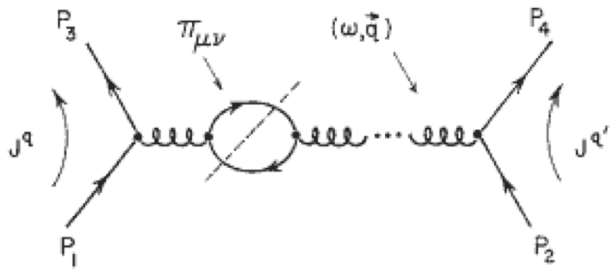

Figure 4.2: Feynman diagram for quark-quark scattering including the gluon self-energy $\Pi_{\mu\nu}$, of which the leading order is just the qq bubble. Putting intermediate states in the bubble on the energy shell gives the imaginary part of $\Pi_{\mu\nu}$ due to absorption of the exchanged gluon by scattering on a quark (Landau damping). [82].

are more pronounced and there are three scales T, μ_q and m_D.
The starting point is the Boltzmann equation (4.21) with collision term (4.29) written for a three-component system of free, relativistic massless u, d, s quarks. Any quasiparticle effects of the Landau-Boltzmann approach can be neglected. No particular colour-spin channel is relevant in calculations, so that the probability $W(12;34)$ is summed over final states and averaged over the initial ones $\langle W \rangle$. The relevant scattering process is depicted in fig. 4.2 and it yields two contributions that, in terms of the Mandelstam invariants, can be expressed as:

$$\langle W(q,q') \rangle = \frac{4}{9} g^4 \frac{u^2+s^2}{t^2} \tag{4.48}$$

$$\langle W(q,q) \rangle = \frac{4}{9} g^4 \left(\frac{u^2+s^2}{t^2} + \frac{t^2+s^2}{u^2} \right) - \frac{8}{27} \frac{s^2}{ut} \tag{4.49}$$

as two singular contributions, respectively for quarks of different flavour (q, q') and of the same (q, q). The screening of interactions in the plasma is included as a polarisation insertion $\Pi_{\mu\nu}$ in the gluon propagator $D_{\mu\nu}$: this can be seen as a relativistic generalisation of the proper self-energy insertion in Many Body problems. The Dyson equation for the propagator defines a perturbative scheme:

$$D^{-1}_{\mu\nu} = g_{\mu\nu}(\omega^2 - q^2) + \Pi_{\mu\nu} \tag{4.50}$$

in terms of the metric tensor $g_{\mu\nu}$ and of the exchanged *momentum* q^2; the propagator can be split into longitudinal (l) and transverse (t) parts, according to a method devised by H. Weldon [83]; recalling that $W(q,q') = |\mathcal{M}_{qq'}|^2$,

i.e. the amplitude W is the square of the (averaged) scattering matrix $\mathcal{M}$:

$$\mathcal{M}_{qq'} = J^q_\mu \, D_{\mu\nu} \, J^{q'}_\nu = \frac{J^q_0 J^{q'}_0}{q^2 + \Pi_l} - \frac{J^q_t J^{q'}_t}{q^2 - \omega^2 + \Pi_t}; \tag{4.51}$$

the polarization insertions are then evaluated by means of the Random-Phase Approximation (RPA):

$$\Pi_l = m_D^2 \, \chi_l(x) \tag{4.52}$$

$$\Pi_t = m_D^2 \, \chi_t(x) \tag{4.53}$$

in which the χ functions are defined in terms of the variable $x = \omega/q$:

$$\chi_l(x) = \left[1 - \frac{x}{2} \ln\left(\frac{x+1}{x-1} \right) \right] \tag{4.54}$$

$$\chi_t(x) = \left[\frac{x^2}{2} + \frac{x(1-x^2)}{4} \ln\left(\frac{x+1}{x-1} \right) \right]. \tag{4.55}$$

The currents J^q_μ of fig. 4.2 are evaluated to first order in the coupling g; the spin sums are performed neglecting the magnetic moment contributions to the currents and the colour averages are performed by means of the expectation values of the Gell-Mann matrices connected with each vertex. Such manipulations plus geometrical considerations lead to the result:

$$\langle W(q,q') \rangle = \langle |\mathcal{M}_{qq'}|^2 \rangle = \frac{2}{9} g^4 \left| \frac{1}{q^2 + \Pi_l} - \frac{(1-x^2)\cos\phi}{q^2 - \omega^2 + \Pi_t} \right|^2 \tag{4.56}$$

in terms of $x = \omega/q$ and $(1-x^2)\cos\phi$ is the scalar product between the transverse velocity vectors of the incoming particles. This term is actually inserted in the Boltzmann equation to yield transport properties, and simulates a Quark-Gluon Plasma as a dynamically screened medium due to Landau damping of the exchanged gluons. The RPA treatment of the polarisation insertions yields a gluon mass term in its propagator $m_D^2 = g^2 N_q \mu_q^2 / 2\pi^2$, that behaves as a characteristic scale-length of the system.

§ **4.2.2. Transport Parameters.**— The transport problem of eq. (4.21), (4.29) cannot be solved exactly with the scheme presented in § 4.1.6 because of the singular interaction, that does not allow to decouple the integration over angles from those over particle energies. Heiselberg and Pethick solved a linearised Boltzmann problem in the assumption of local equilibrium both by variational estimate and of momentum relaxation approximation. The

two results coincide in the $T \ll m_D$ limit of interest here, so that the very simple result of eq. (4.47) is recovered.
The Boltzmann equation is linearised by expanding the distribution function for the specie $i = \{u, d, s\}$:

$$f_i = f_i^{\text{l.e.}} + \frac{\partial f_i^0}{\partial \epsilon_i} \Phi_i \frac{\partial v_x}{\partial y} \tag{4.57}$$

in terms of the local equilibrium function and of the derivative of the ground state distribution function f^0; this expression is the analogous of eq. (4.35) for Normal Fermi liquids; the procedure is carried on in the same fashion as the Landau-Boltzmann case, developed in § 4.1.5. The corresponding problem is then solved in a variational approach, like the original Abrikosov-Khalatnikov solution [42, 76]:

$$\frac{1}{\eta} \geq \left(\sum_p p_x v_y \frac{\partial f^0}{\partial \epsilon_p} \Psi_p \right)^{-2} \frac{\pi}{2T} \sum_{q p_1 p_2} \langle |\mathcal{M}_{qq'}|^2 \rangle \times \\ \times \; f_1^0 f_2^0 (1 - f_3^0)(1 - f_4^0) \delta(\epsilon) [\Psi_1 + \Psi_2 - \Psi_3 - \Psi_4]^2, \tag{4.58}$$

in which the equal sign is for the exact result $\Psi \equiv \Phi$; the complete solution for shear viscosity is thus:

$$\frac{1}{\eta} = 40\pi \, \alpha_s^2 \mu_q^{-4} \, T \, \mathrm{I}_\eta(T/m_D) \tag{4.59}$$

in which μ_q is the degenerate quark chemical potential and $\mathrm{I}_\eta(T/m_D)$ is the following integral:

$$\mathrm{I}_\eta(T/m_D) = \int_0^\infty \frac{\mathrm{d}\omega}{\omega} \left[\frac{\omega/2T}{\sinh(\omega/2T)} \right]^2 \int_0^1 \mathrm{d}x \int_0^{2\pi} \frac{\mathrm{d}\phi}{2\pi} (1 - x^2)(1 - \cos\phi) \times \\ \times \left| \frac{1}{1 + (x \, m_D/\omega)^2 \chi_l(x)} - \frac{\cos\phi}{1 + (x \, m_D/\omega)^2 \chi_t(x)/(1 - x^2)} \right|^2, \tag{4.60}$$

that cannot be solved analiticly, but can be evaluated in the two limits $T \ll m_D$ and $T \gg m_D$. In the actual calculations this was solved numerically and confronted with the relaxation time result of eq. (4.47) to test the goodness of the approximation.

Part III

Astrophysical Applications and Results

With all reserve we advance the view that a super-nova represents the transition of an ordinary star into a neutron star, consisting mainly of neutrons.

W. Baade and F. Zwicky - (1934)

5 Neutron Stars

This chapter is focused on Neutron Stars, compact astrophysical objects whose interior is very likely to be composed by bulk strongly-interacting matter. The first part is devoted to their general properties, as they are understood from actual observations and measurements. The second part contains the theoretical tools to build static stable configurations of NS starting from a well-defined Equation of State of Nuclear Matter; the results are an interesting application of Nuclear Theories and can be used to test their properties. The last part contains a discussion about the effect of Nuclear Matter viscosity on Neutron Star oscillations; this is again a very interesting test of microscopic viscosity calculations and a way to apply the resulting knowledge to observable systems. All quantities, unless differently pointed out, are supposed to be calculated in the *cgs* scheme [→ App. A]. General arguments are taken by the excellent books by S. Shapiro and S. Teukolsky [84], N. K. Glendenning [85] and from Chapt. 8 of the book by M. Baldo et al. [47], written by I. Bombaci.

5.1 Generalities and empirical facts

Neutron Stars are astrophysical objects composed by very dense matter and believed to be produced in Type II *Supernovae*, i.e. the endpoint of stars that possessed a mass between $8 \div 25\ M_\odot$ at the age they ignited thermonuclear fusion reactions in their cores or, in the stellar evolution terms, entered the Zero Age Main Sequence in Hertzsprung-Russel Radius-Luminosity diagrams. The symbol $M_\odot$ refers to the Solar mass [→ § A.2].
Typical Neutron Stars have masses of about $1.4\ M_\odot$ and *radii* of the order of $10 \div 12$ Km: the matter in their interior is among the most dense in the Universe, and generally larger than the density of stable *nuclei* $\rho_0 = 0.17\ \mathrm{fm}^{-3} = 2.8 \cdot 10^{14}\,\mathrm{g/cm}^3$, the reviewed nuclear saturation point [→ § 2.2.4].

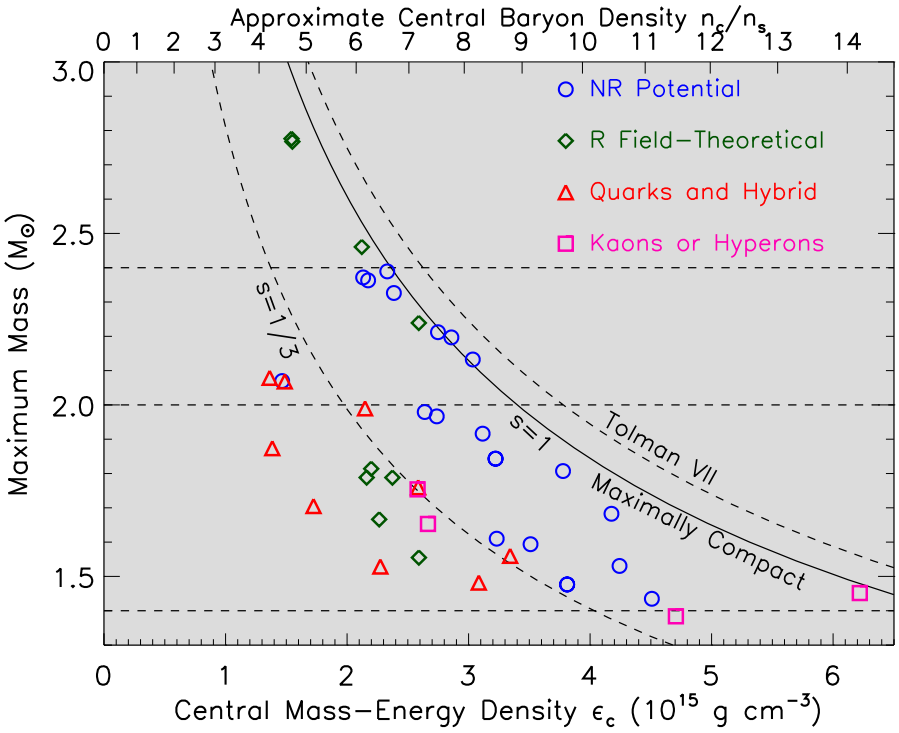

Figure 5.1: Oppenheimer-Volkoff limit calculated by means of various theoretical approaches: it is interesting to note that the inclusion of more degrees of freedom (triangles, squares) leads to smaller values of maximum mass, if compared to nucleonic matter calculations (circles and diamonds). Taken from ref. [86].

§ **5.1.1. Some History.**— The term "Neutron Star", coming from the hypothesis about their composition, was coined by W. Baade and F. Zwicky in 1934 [87], only one year after the discovery of neutrons by Sir J. Chadwick. In that paper the authors proposed for the first time that Neutron Stars could come from *Supernovae*, a name by which themselves called a the most bright non-periodic *novae*. The first theoretical calculation about Neutron-Star structure came a few years later, when R. Tolman calculated some static solutions of Einstein's Field Equations for spherical fluid configurations [88] and J. Oppenheimer and G. Volkoff, applying his results, calculated static Neutron Star configurations sketching the matter inside them as a Fermi Gas of non-interacting neutrons. They could estimate an upper mass limit around 0.8 $M_\odot$, not so far from the observed objects. Such a limit is today called "Oppenheimer-Volkoff limit", as a generalisation on neutron-degenerate compact objects of the Chandrasekhar limit.

All of this studies remained theoretical investigations until 1967 when J. Bell,

at that time Ph.D. student in Cambdridge, revealed a regularly pulsed Radio-signal with a period of 1.377 seconds, pointing at a fixed point in the space: the discovery of the first Radio Pulsar [89]. Later, in 1974, R. A. Hulse and J. H. Taylor discovered the PSR B1913+16 Pulsar binary system; they could accurately measure a period of 59 ms for B1913, and suggested that the system was losing energy due to Gravitational Wave emission, a task for which they received the Nobel Prize for Physics in 1993.
Since then a lot of Pulsars were discovered; the last striking observation was made in 2010 by P. B. Demorest et al. and published on Nature [90]; they could measure, with a technique called "Shapiro Delay", the mass of the binary millisecond Pulsar J1614-2230, finding a very precise value of $1.97 \pm 0.04\ M_{\odot}$. The discovery gave new interest to all the theoretical determinations of the Oppenheimer-Volkoff limit that predicted a value higher than $\sim 1.6\ M_{\odot}$; the situation is sketched in fig. 5.1.

§ **5.1.2. Formation.**— The intuition by Baade and Zwicky turned out to be correct: Neutron Stars indeed are originated in *Supernovae* explosions. Such phenomena are categorised into two categories by the Astrophysicists, that differentiate on the resolvable light spectrum that they send: the Type II show the typical Hydrogen lines, while the Type II don't. Stars of both classes end up their days with a spectacular explosion that enriches the surrounding space of gas and heavy elements that can in turn be stage for second-generation stars formation, but only Type II *Supernovae* leave a Neutron Star among their remnants. Further on, a large parte of Type I *Supernovae*, called Type Ia, has its origins in binary systems in which a White Dwarf absorbs mass from its companion, until its mass overcomes the Chandrasekhar Limit of $1.4\ M_{\odot}$. Type II supernovae are instead the evolutive end-product of single stars that could ignite in their core all the fusion reactions up to ^{56}Fe, thanks to their high ZAMS initial mass. The Iron core is fusion-inert, as ^{56}Fe is the last producible by fusion, as it has the highest value of Binding Energy per Nucleon among the observed *nuclei*: by contrast fusion reactions continue in the upper shell of the star, until the lack of radiation pressure cannot sustain anymore the upper layers against falling on the centre, and the system collapses creating a shockwave, with subsequent photo-disintegration reactions that leave only neutrons and a smaller percentage of protons and electrons, composing the hot Neutron Star.
The new-born Neutron Star, whose temperature is estimated to be around

$30 \div 40$ MeV, suddenly cools down in timescales of the order of 10 seconds, by suddenly becoming transparent to highly energetic neutrino emissions, that transfer part of their energy to the superficial layers of the remnant star, casting them in the space: this is a qualitative discussion to explain how a star with 15 $M_\odot$ can yield a Neutron Star of a tenth of its initial mass. The observations describe such picture as a very luminous *nebula* of fast-escaping material, with a cold Pulsar lying at its centre, rapidly rotating due to pre-collapse angular momentum conservation.

§ **5.1.3. Phenomenology.**— The actual knowledge about compact stars has been built upon the observations made of the over 1500 Pulsars discovered and catalogued in our galaxy. Their characteristics are profoundly different from common stars, yielding phenomena like 1 second-period rotation, Radio-wave emissions and high magnetisation. A comprehensive list is:

- **Rotation and emissions:** the biggest part of the known objects is catalogued as a Radio Pulsar - name coined on the crasis Pulsating Star - from the periodic Radio emission on a timespan of about 1 s; the first observation referred to this phenomenon as "Lighthouse effect" and it is believed that its origin lies in the strong magnetic fields that embeds in the surrounding space. But about 100 objects have much shorter periods, of the order of 10^{-3} s, like the discussed Hulse-Taylor Pulsar [89]. Two-hundred additional stars emit radiation up to the X-ray and gamma wavelengths in bursts: this happens in binary systems in which one the Neutron Star continuously draws hydrogen from the companion star, that deposits in 1 meter shells on its surface, whose sudden compression due to the strong gravitational field ignites very rapid fusion reactions, that end up in flashes. This phenomenon is addressed with the name "X-Ray Burst". Systematic observations of certain objects led to the discovery that the highly regular spinning periods are not constant on galactic-life timescales: they indeed slowly decrease.

- **Magnetisation:** Neutron Stars generate very intense Magnetic Fields: on their surface these can vary in the range $10^6 \div 10^{15}$ Gauss and they are responsible for the Synchrotron radiation emission.

- **Temperature:** Neutron Stars are rated as "cold objects", even if the temperature in their first stages interior is believed to reach the 10^{11} K,

decreasing of one order of magnitude within a few days due to neutrino emission, later to approach lower values of $10^5 \div 10^9$ K in elder objects. The reason has already been discussed when talking of the $T \to 0$ limit in Nuclear Matter [→ § 2.1.2]: nucleonic matter at such temperatures behaves like a liquid as Temperatures are of the order of $1 \div 10$ MeV, and the Fermi Energies of Neutron Stars approach the value of 50 MeV. Matter is thus degenerate, i.e. the constituents occupy uniformly the single particle energy levels below the Fermi Surface, in accord with the Pauli Principle.

§ **5.1.4. Internal structure.**— The internal structure of compact objects is hardly investigable and therefore explained on theoretical grounds in a model-dependent way. The success of the Oppenheimer-Volkoff scheme makes the assumption of being composed by neutron matter very reasonable, and further realistic investigations can help in giving a comprehensive systematic description. On general grounds, it is possible to infer that density grows when going towards the centre of the star, that must be formed by layers of the most thermodynamically favoured phase at every step. Here a tentative slice of NS matter is sketched:

- **Surface** ($\rho_{^{56}\mathrm{Fe}} = 7.9\,\mathrm{g/cm^3} < \rho < 10^6\,\mathrm{g/cm^3}$): below a 1 cm thick atmosphere, compressed by gravity, lies the most outward layer, about ~ 0.3 Km thick, composed by a lattice of ^{56}Fe nuclides immersed in a degenerate electron gas, remnant of the last thermonuclear reaction-product of the progenitor star.

- **Outer Crust** ($10^6\,\mathrm{g/cm^3} < \rho < \rho_n^{\mathrm{drip}} = 4.3 \cdot 10^{11}\mathrm{g/cm^3}$): this is a layer of moderate thickness composed by solid-state nuclear matter, in a lattice similar to the previous but this times with increasing number of neutrons per ion ($A > 56$) in β-equilibrium with the electron degenerate gas. This is due to the highly energetically favoured process of electronic capture $e^- + p \to n + \nu_e$, that moves the equilibrium towards neutron enrichment.

- **Inner Crust** ($\rho_n^{\mathrm{drip}} < \rho < \rho_0$): this layer begins when the neutron drip density is surpassed. From this point on the nuclear force saturation cannot anymore bind neutrons to the highly n-rich *nuclei* of the lattice, with the appearance of a free-unbound neutron gas. Highly exotic

species here appear, that could not resist to (β?) decay in normal conditions: they are kept bound by the Pauli Principle.

- **Outer Core** ($\rho_0 < \rho < \rho_{\rm exo} \approx 2.5\rho_0$): the largest part of the star mass is here concentrated. Trespassing the nuclear saturation points nucleons are the dominating degrees of freedom and no nuclide can anymore survive; thus matter is isospin asymmetric, with a lepton-bath (electrons and possibly also muons) to maintain local charge neutrality and β-stability. Some studies point out that in such conditions neutrons should be in superfluid, protons in superconducting phases.

- **Inner Core** ($\rho > \rho_{\rm exo}$): more exotic degrees of freedom should appear, including pion/kaon condensates or stable Λ, Σ and Ξ hyperons; more likely, from the discussion carried on in Chapt. 1, after a certain density the relevant degrees of freedom should be coloured quarks and gluons, i.e. hadrons should undergo a first order QCD phase transition to deconfined matter, with restoring of Chiral Symmetry.

§ **5.1.5. Mass measurement systematics.**— What are the measurable observables connected to the study of Neutron Stars? The answer to this question naturally fits in the scheme of theoretical calculations as empirical constraints that a model should reproduce in order to describe compact objects at a satisfactorily degree of accuracy. Despite being very exotic objects, their relative abundance puts mass on top of the list of the most interesting parameters, followed by the rotation frequency, temperature, *radius* and particle/radiation emissions; they are usually measured indirectly. For example Pulsar temperatures are estimated from blackbody fits of X-Ray emission spectra (found to be a fair approximation); in principle, neutrinos emitted during the cooling phase can be detected - so far, only 20 neutrinos coming from SN1987 were revealed, though these weren't originated by any Neutron Star phenomenon - but this is subdued to Type II SN explosions, that are not so frequent in the surrounding Universe. Among the stated observable the most accessible - thus the most precisely determined - is the rotation frequency.
The most successful theoretical effort is the construction of static Neutron Stars configurations. The predictions are often put in Mass-Radius diagrams such as the one reported in fig. 5.2, showing the importance of the corresponding measurements in the process of judging the quality of an Equation

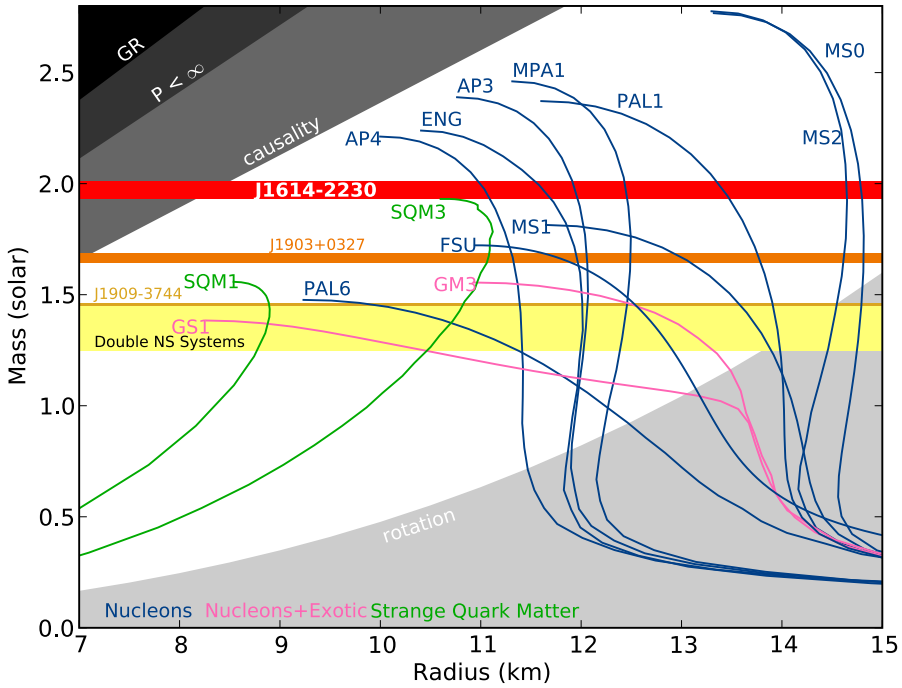

Figure 5.2: Non-rotating mass versus physical radius diagram for several Equation of State models: blue, pure nucleons; pink, nucleons plus exotic matter; green, strange quark matter. The horizontal bands show the observational constraint from different millisecond pulsars. Any EOS line that does not intersect the J1614-2230 band is ruled out by this measurement. In particular, most EOS curves involving exotic matter, such as kaon condensates or hyperons, tend to predict maximum masses well below 2 $M_{\odot}$ and are therefore ruled out. Other theoretical constraints are displayed as grey-scale shaded areas. Taken from ref. [90].

of State model. It is disappointing that no accurate measurement of *radii* exist, due to the huge difficulty in determining a length of 10 Km at a distance of 15 orders of magnitude longer. Theoretically inferred estimates exist; an example is given by a work by J. van Paradijs [91], in which the *radius* of 10 X-Ray bursters is calculated assuming that they radiate as blackbodies. The result is in average 8.5 Km, but strongly error-affected due to the simplifications introduced in the procedure.

The mass is instead measured for about 100 objects on the more than 1500 known. The first systematic work was done by S. Thorsett and D. Chakrabarty [92] in 1999; they catalogued and reviewed the measurement of 50

objects, concluding that all the measurements were consistent with a remarkably narrow Gaussian mass distribution, showing normal mass $M = 1.35 \pm 0.04\ M_\odot$. Later on their work was reprised by J. Lattimer and M. Prakash [93], that built a larger systematics including objects in Optics/X-ray, double Neutron Stars and White Dwarf/NS binary systems, calculating new averages and including large-mass candidates whose mass measurements were still propositions. They recently took up the subject again, updating with new measurements - like the very accurate result of 1.97 $M_\odot$ for PSR J1614-2230 [90] - and with high-mass candidates - like the estimated 2.4 $M_\odot$ of the so-called "Black Widow Pulsar" B1957+20. Their work [86] is reported in fig. 5.3.

§ 5.1.6. Basics of Mass measurements.— The empirical determination of Neutron Star Mass is often based on the analysis of the motion of objects in binary systems, that are indeed very common environments. The method is based on the possibility to measure with high accuracy five Keplerian parameters: the binary system revolution period P_b, the projection of the major semi-axis of the Pulsar orbit on the view line $x = a_i \sin(i/c)$, the orbital eccentricity e and finally time and longitude of the periastron, T_0 and ω_0. These parameters appear in the so-called "mass function":

$$f = \frac{(m_2 \sin i)^3}{M^2} = n^3 x^3 \left(\frac{1}{T_\odot}\right) M_\odot \tag{5.1}$$

in which $M = m_1 + m_2$ is the total mass of the system, expressed in Solar Masses units $M_\odot$ and $T_\odot = (GM_\odot)/c^3 = 4.925 \cdot 10^{-6}$ is a constant. Five more Post-Keplerian parameters come from General Relativity; the system is solved for the two single-components mass when eq. (5.1) is known together with any two of the PK parameters. One of the systematic error sources lies in the relative motion of the Solar System with respect to the Binary System, that is in general ignored. Other, more sophisticated methods can be devised when this simple scheme is not applicable. P. B. Demorest et al. [90] could measure with very high precision the mass of the binary millisecond Pulsar J1614-2230 by means of a general-relativistic increase in light travel time through the curved space-time near a massive body, known as "Shapiro delay". This method turn out to be very fruitful for highly inclined (nearly edge-on) binary millisecond radio pulsar systems.

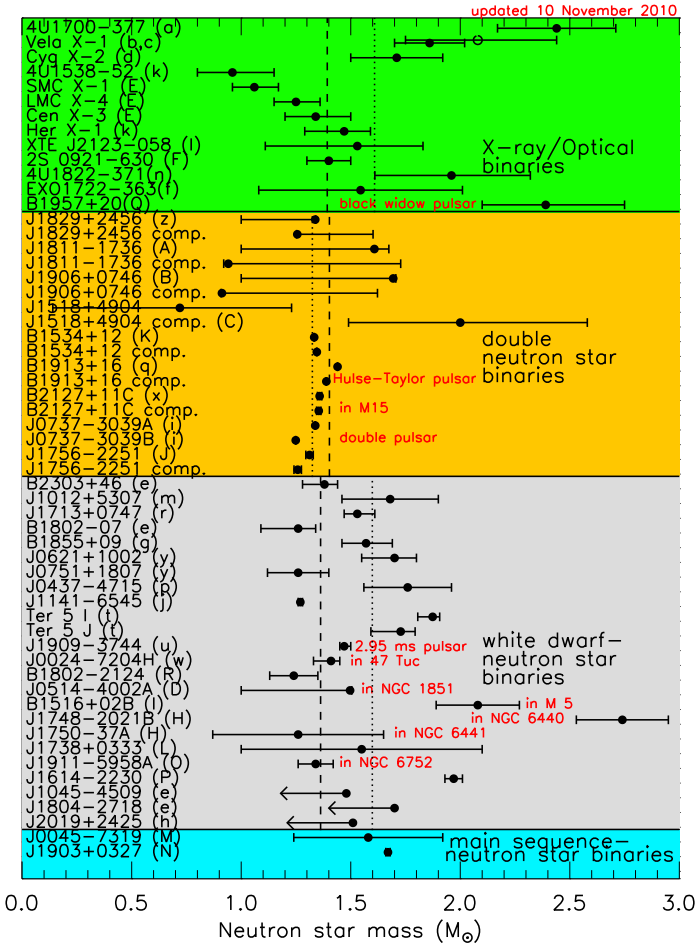

Figure 5.3: Neutron Star mass systematics by J. M. Lattimer and M. Prakash for various kinds of binary systems; vertical dashed line are the mean values for the different bins. Updated 2010. Taken from ref. [86].

5.2 Static properties: Mass-Radius configurations

Reprising the idea of R. Tolman, J. Oppenheimer and G. Volkoff, Neutron Stars macroscopic properties such as Radius and Mass can be put in correspondence with the thermodynamic - thus static - properties of the matter that composes them, i.e. strongly interacting matter, that is made of - depending on the total baryon density ρ_B - nucleons or quark and gluons degrees of freedom. Just as the Equation of State requires a microscopical description of the interaction among its constituents, to be sketched by means of some Many-Body approach, in the presented task it is Hydrodynamics, either Newtonian or Relativistic, that links the bulk properties of a nucle-

onic fluid, to hydrostatic stable configurations. The important discovery in this field is that strongly interacting matter has a strong repulsive character; what makes Neutron Stars bound is thus Gravitational Interaction.
The term static, often used throughout this thesis, recurs to indicate all those situation in which the total energy of the system and other integrals of the stated differential problems, do not depend explicitly on time. But aside from mathematics, the problem can be thought from the perspective of a δαιμονίον that stops time and interactions, aggregating particles in a "correct", "natural" way, so that the corresponding configuration, back in time, does not lose any of its property.
The method assumes that Neutron Stars are cold, non-rotational sferic, and non-magnetic objects. Their phenomenology, described in § 5.1.3, seems to contradict this picture for the second and third assumptions; rotation can be taken in account by means of a separated equations, here dropped due to non-centrality of the procedure in the scheme of the work outlined here; the last hypothesis can be relaxed observing that the strong magnetic fields have mainly effect on the external crust layers.

§ 5.2.1. Newtonian structure.— A small fluid element of volume $\mathrm{d}V = A\mathrm{d}r$, surface A and height $\mathrm{d}r$ in spherical coordinates is subjected to the gravitational attraction of the lower layers, thus experiencing a pressure that grows with decreasing distance from the centre r. The set of differential equations to be solved for the equilibrium configurations of a given fluid in classical Newtonian mechanics is:

$$\frac{\mathrm{d}p}{\mathrm{d}r} = -\frac{G\rho(r)M(r)}{r^2} = -\frac{G\epsilon(r)M(r)}{c^2 r^2} \tag{5.2}$$

$$\frac{\mathrm{d}M}{\mathrm{d}r} = 4\pi r^2 \rho(r) = \frac{4\pi r^2 \epsilon(r)}{c^2} \tag{5.3}$$

in which appears the Universal Gravitational constant $G = 6.673{\cdot}10^{-8}\,\mathrm{dine{\cdot}cm^2/g^2}$ in *cgs* units; $\rho(r)$ is the density of mass closed at distance r from the centre and $\epsilon(r) = \rho(r)c^2$ is its corresponding energy density. The function $M(r)$ represents thus the Total Gravitational Mass closed within a sphere of radius r; the total star mass is given then by:

$$M(R) = 4\pi \int_0^R \mathrm{d}r\, r^2\, \rho(r) = 4\pi \int_0^R \mathrm{d}r\, r^2\, \epsilon(r)/c^2 \tag{5.4}$$

where R represent the final star Radius. The label "Gravitational", when accosted to the mass, is used to distinguish it from the "baryonic" mass,

that is the total mass due to the nucleons, in excess of the binding energy per nucleon calculated from the theoretical approaches of Chapt. 2. The system given by eqs. 5.2,5.3 is made by two first order differential equations in $p(r)$ and $M(r)$, to be integrated in the $[0, R]$ interval with boundary conditions:

$$p(R) = 0, \qquad \text{defining } R, \text{ the star } \textit{radius} \tag{5.5}$$

$$M(0) = 0, \qquad \text{trivially.} \tag{5.6}$$

The structure equations are to be integrated parametrising $p_c = p(R)$, i.e. the central pressure reached in the star, depending on the central density ρ_c. The static configurations are calculated by trying different values for $p(R)$, on which both the total mass M and pressure p depend. Every value thus yields a different star model, whose internal characteristics are univocally determined. These equations are commonly used for stellar structure calculations; they are unsuitable for Compact Stars estimates, as in such objects the General Relativity effects become relevant and non-negligible.

§ 5.2.2. Relativistic Tolman-Oppenheimer-Volkoff equations.— Indeed, the Newtonian equations lose their validity when the star mass is high enough to "bend" the spacetime; a measure of this event conditions can be found confronting the Schwarzschild radius R^0 and the star radius R: the relativistic corrections are unavoidable when $R^0/R \approx 1$. A typical star like our sun has $R^0 \approx 10^{-6}$; for a White Dwarf it grows to 10^4 and approaches the unity in a typical Neutron Star. The first two classes of objects are then described in terms of Newtonian structure equations, while compact objects require the use of a new set of equations, to be presented here.
In the same assumptions of the previous case, for which a small fluid element experiences a hydrostatic equilibrium between the gravitational force and the layer-pressure, the Einstein Field-Equations assume the form:

$$\frac{\mathrm{d}p}{\mathrm{d}r} = -\frac{G\rho(r)M(r)}{r^2}\left[1 + \frac{p(r)}{c^2\rho(r)}\right]\left[1 + \frac{4\pi r^3 p(r)}{c^2 M(r)}\right]\left[1 - \frac{2GM(r)}{c^2 r}\right]^{-1} \tag{5.7}$$

$$\frac{\mathrm{d}M}{\mathrm{d}r} = 4\pi r^2 \rho(r) \tag{5.8}$$

generally known in literature as "Tolman Oppenheimer Volkoff equations" (TOV); eq. (5.8) conserved the same form of eq. (5.3) of the Newtonian case. In the first equation three factors appear: the first two constitute the General Relativity corrections of the order v^2/c^2; the third represent a

correction related to Schwarzschild radius. All the considerations about the boundary conditions and integrability of the Newtonian set can be applied also in this case.
A very important remark, left to be discussed in this section, is the following: the TOV equations can be soluted provided a full punctual knowledge of the relation $p(r) = p[\rho_B(r)]$ between the pressure and baryon density; in other terms, the stellar structure depends on the Equation of State for the matter that composes it. A bijective relation between NS structure and Nuclear Matter EoS arises in the problem, in which constraints on one side lead to knowledge on the other. The solutions yield a certain set of Mass-Radius static configurations that can be drawn in a diagram similar to fig. 5.2; such a curve must respect the hydrodynamic stability condition:

$$\frac{\mathrm{d}M}{\mathrm{d}\rho_c} > 0\,; \tag{5.9}$$

by means of which one can individuate its maximum: it is the so-called "Oppenheimer-Volkoff" upper limit for the Neutron Star mass, and expresses the maximum degeneracy pressure of that interacting nucleon matter can support in the competition with gravity in a particular Many-Body scheme to sketch the interactions. This can be confronted with the ones obtained by different approaches in fig. 5.1 and with the systematics of mass of fig. 5.3 to see if it fits the known constraints.

5.3 Dynamical phenomena: Oscillation Modes

The interior of Neutron Stars can also be studied from a dynamical point of view. Compact objects are made for their quasi-totality by strongly interacting matter in liquid state, and are thus subject to deformations. Their supra-nuclear density, and the average-built asteroid-size make them very massive: as seen in the previous section, they are bound by Gravity. General Relativity predicts the emission of tensorial Gravitational Waves (GW) for mass distributions of interacting matter with a non-vanishing quadrupole moment, i.e. a measure of the deviation from the spherical shape. The detection of GW emission from Neutron Stars can help to constrain the presence of a Quark-Gluon Plasma in their interior, as the properties of the oscillation are sensitive to the Equation of State and to the relevant degrees of freedom at a given phase. The phenomenon here presented is a candidate for observations at the Laser Interferometer Gravitational-Wave Observatory (LIGO),

built in 2002 in the U.S. from the joint efforts of Caltech and MIT.

§ **5.3.1. Brief Classification of Oscillation Modes.**— A very complete review of the Oscillating Modes of a Neutron Stars in comparison with Black-Hole Modes can be found in the work of K. Kokkotas and B. Schmidt [94]. The first distinction individuates toroidal and spherical modes, with respect to the direction of the displacement along the radial direction of the star: the first have perpendicular displacements, the latter parallel. Spherical modes are the most experimentally accessible and also the most interesting from the perspective of GW radiation emission; they can be further divided into radial or non-radial modes, depending on whether they preserve or not the shape of stars in the oscillations.
The study of the interior of normal stars from Helioseismology lead to the discovery of three main modes of oscillations inside our Sun, that have typical periods of a few minutes and can be found, with much shorter periods, in Neutron Stars as well. These are:

- **Pressure p-modes:** they are infinite in number and can be both radial and non-radial. They are driven by mechanical perturbations and powered by internal pressure fluctuations, depend on the local speed of sound of the stars, so they can be seen as generalised "acoustic modes".
- **Gravity g-modes:** they appear from the tendency of the gravitational interaction to destroy matter inhomogeneities on equipotential surface. They happen in the interiors of stars with a solid crust and have gravitational buoyancy as restoring force.
- **Fundamental f-modes:** they are stable g-modes that exist only for non-radial perturbations, constrained on the star surface. Their restoring force is not gravity, but the surface tension, like small perturbations on a pond surface. The frequency of such modes depends on the mean density of the star, but is not particularly sensible to the details of the interaction.

A fourth mode can exist only in Neutron Stars, and has a central role in the study of the instabilities driven by GW emission:

- **Rotational r-modes:** they appear in rotating stars where the Coriolis force acts as inertial-restoring force along the surface. They are connected with liquid matter viscosity and for orbital number $l \geq 2$ are

generically unstable to the emission of gravitational radiation. The r-modes are commonly called also "rotation dominated modes", "inertial modes" or "Rossby waves" in literature.

§ 5.3.2. Gravitational Radiation instability.— In the third work of a series about General Relativity stellar models properties, K. S. Thorne pointed out that non-radial pulsations of Neutron Stars can couple to Gravitational Wave emission [95], and that such phenomenon can carry away energy and angular momentum from the spinning systems. In non-rotating stars the emission is found to be dissipative, so that it damps the star oscillations. But S. Chandrasekhar in 1970 noted that in rotating objects the picture can be quite different, with the Gravitational Wave emission feeding certain oscillation modes, whose amplitude can grow to originate instabilities of the system [96]. This Gravitational Radiation-driven instability was first studied for the f-modes of rotating stars, and it was found that every rotating perfect fluid star is - according to General Relativity - unstable; this process can be not-detectable at all, as in real stars, the viscosity of liquid matter can easily damp any GW-induced pulsation, so that the consequent emission is suppressed.
The investigation field gained new insight from the works of N. Andersson [97], J. Friedman and S. Morsink [98], that showed that all the r-modes are driven unstable by Gravitational Radiation in all rotating perfect fluid stars. Later, phenomenological calculations by L. Lindblom et al. [99], confirmed the picture and predicted that such an instability is strong enough to overcome most of the common internal dissipation processes, due to shear and bulk viscosities of matter, even in intermediate-speed rotating stars.

§ 5.3.3. Damping timescales of r-modes.— Observed Neutron Stars are stable and resist the cooling era: this suggests that the Gravitational Radiation instability mechanism must be damped by some phenomenon inside them. The origin - according to calculations - may be attributed to the viscosity of a strongly-interacting liquid, in general dependent on the Equation of State model. The mechanism of viscous damping Neutron Stars oscillations is described by means of Newtonian fluid dynamics; here it is sketched following the treatment of L. Lindblom and C. Cutler [100].
The idea here is to calculate, by means of Newtonian Relativistic Hydrodynamics for a viscous incompressible fluid, the dissipation time-scales of the r-modes, dependent on the viscosity and temperature of the star, and

to confront them with the typical timescales of the Gravitational Radiation instability, estimated to be dependent only on the rotation frequencies of the compact objects, and generally lying in the range $10 \div 100$ s.
The Lagrangian displacement ξ is defined as the relative displacement of a fluid element in two flows starting from the same space-time point; for non-radial oscillations of matter inside a Newtonian star it is expressed as a covariant four-vector:

$$\xi_a = \frac{\epsilon R^2}{l}\, e^{i\omega t}\, \nabla_a\left[\left(\frac{r}{R}\right)^l Y_m^l\right], \tag{5.10}$$

in terms of the spherical harmonics Y_m^l, with ϵ being a small dimensionless parameter, R the total radius of the star and ω the frequency of the mode. Such displacement gives rise to a contravariant-vector velocity perturbation:

$$\delta v^a = i\omega \xi^a. \tag{5.11}$$

The kinetic energy associated to the oscillations is in Newtonian limit simply given by:

$$E_K = \frac{1}{2}\int \delta v_a^* \delta v^a \rho\, \mathrm{d}^3x \tag{5.12}$$

in which the usual Einstein convention of summation over repeated indices is implicitly used in the calculation of the δv^2 scalar product. The oscillations are supposed to be harmonic: the potential and kinetic contributions can be simply be considered of the same order of magnitude, so that the total Energy is simply $E = 2E_K$; the integral in eq. (5.12) can be quickly evaluated for a rough estimate by means of the assumption:

$$\rho = \bar{\rho} \equiv \frac{3M}{4\pi R^3} \tag{5.13}$$

of constant density for the Neutron Star; the Energy of the mode is then simply evaluated as:

$$E = l^{-1}\rho\,\omega^2\epsilon^2 R^5. \tag{5.14}$$

The total energy E in general must be evaluated by means of the full integration of eq. (5.12), provided that the Mass M, Radius R and density profile $\rho(r)$ of the Neutron Star are known. The equation that defines the timescale τ depends on such quantity:

$$\frac{\mathrm{d}E}{\mathrm{d}t} = -\frac{2E}{\tau} = -\int\left(2\eta\,\delta\sigma_{ab}^*\delta\sigma^{ab} + \zeta|\delta\theta|^2 + \frac{\kappa}{T}\nabla_a\delta T\,\nabla^a\delta T^*\right)\mathrm{d}^3x \tag{5.15}$$

where η, ζ and κ are the first, second viscosities and the thermal conductivity, so that the corresponding three terms account for their separate contributions; T is the temperature of the star; $\delta\sigma^{ab}$ and $\delta\theta$ are the shear tensor and expansion of the perturbed fluid motion. In a Newtonian scheme only the term due to shear viscosity survives, so that the theory is suitable for calculations related to this variable.
The shear tensor of perturbed fluid motion is related to the Lagrangian displacement of eq. (5.10) as:

$$\delta\sigma_{ab} = i\omega\nabla_a\xi_b; \tag{5.16}$$

again, assuming a constant shear viscosity $\eta = \bar{\eta} \equiv \eta(\bar{\rho}, T_{\rm core})$, the integral in eq. (5.15) is immediately evaluated, yielding the approximated estimate:

$$\mathrm{I}[\eta] = \int 2\eta\,\delta\sigma^*_{ab}\delta\sigma^{ab}\,\mathrm{d}^3x = 2l^{-1}(l-1)(2l+1)\,\omega^2\epsilon^2R^3\eta. \tag{5.17}$$

Under this simplification the timescale can be obtained by eq. (5.15) from the very simple relation:

$$\frac{1}{\tau_\eta} = \frac{(l-1)(2l+1)\eta}{\rho R^2}. \tag{5.18}$$

Obviously, a much better estimate can be given knowing the Shear Viscosity η for the strongly interacting liquid at every density, thus radial distance r from the centre. This will be the input for calculations and it is the expression containing effects from a phase transition to quark matter, evaluated in Chapt. 4. The corresponding τ can still be calculated from eq. (5.15), provided that the integrals in both E and $\mathrm{I}[\eta]$ are fully solved. A discussion about the change of its units can be found in [→ App. A].

189 - Er ist ein Denker: das heisst, er versteht sich darauf, die Dinge einfacher zu nehmen, als sie sind.

F. W. Nietzsche - (1882)

6 Results

The results displayed in this chapter are mainly based on the calculations of Shear Viscosity performed in year 2011 in collaboration with Prof. U. Lombardo, Dr. V. Greco, Dr. S. Plumari and A. B. Santra, in part written in an article submitted to Phys. Rev. D. They are part of a larger scheme that should continue pursuing microscopic Shear Viscosity calculations for Quark Matter, this time sketched by the Nambu-Jona Lasinio effective model of QCD.

6.1 Strongly Interacting Matter at Equilibrium

The static properties of Nuclear Matter were presented in Chapt. 2; their complete knowledge is obtained determining the correspondent Equation of State: in this work this was done with the Brueckner-Hartree-Fock method presented in Chapt. 3. Quark Matter was described as a Free Gas of Fermions in the MIT Bag Model scheme of § 3.3.1. The two approaches were combined to yield an Equation of State including a phase transition in the Glendenning scheme.

§ **6.1.1. Equations of State.**— The starting point is a system of n, p and e^- in β-equilibrium and local charge neutrality. The calculations were performed following Refs. [69, 101], that provided the Binding Energy per Nucleon for pure Neutron Matter ($I = 1$, maximum asymmetry) and of Symmetric Matter ($I = 0$) at given, parametrized ρ_B^* by means of the quasi-free gas relation:

$$\frac{B}{A}(\rho_B^*) = \frac{3}{5}\frac{k_F^2}{2m} + \frac{1}{2\rho_B^*}\,\mathrm{Re}\sum_{k,k'\leq k_F}\langle kk'|G[e(k)+e(k');\rho_B^*]|kk'\rangle_{\mathcal{A}} \qquad (6.1)$$

in terms of the Brueckner G-scattering matrix *in medio*, defined in the BBG equation (3.42) starting from the two-body potential v_{NN} in the *vacuum*.

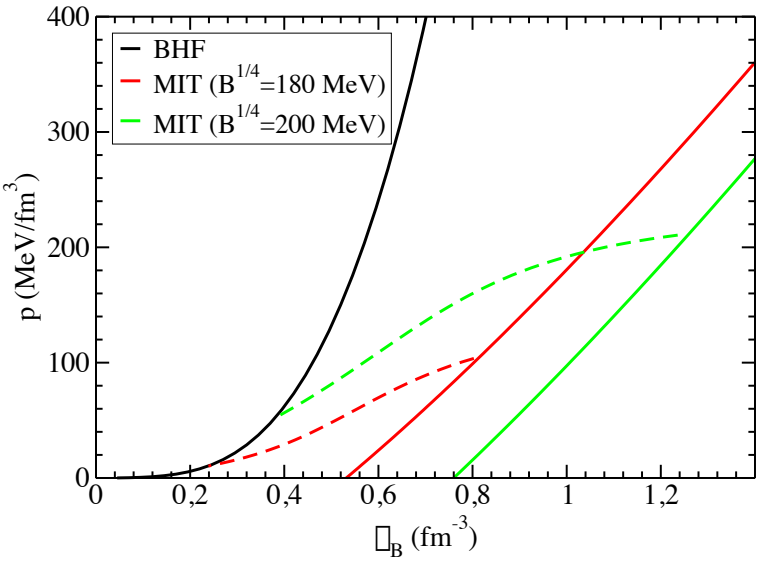

Figure 6.1: Equation of State for Hadronic and Quark Matter (for two values of the Bag Constant B). The dashed lines are obtained with the Glendenning procedure for the First Order phase transition of the second kind.

For the latter, the Bonn B realistic potential was used [102]; the cited works employed a consistent scheme for the external parameters of the Many Body theory, i.e. the bare potential and effective three-body forces parameters, yielding a particularly satisfactory result for the saturation point of Nuclear Matter and obtaining a high level of compatibility with the Relativistic Dirac-BrueckerHF calculations.

The equation of state was constructed in steps with a simple numerical code, evaluating the Symmetry Energy from the difference of the given quantities, then solving for the asymmetry parameter I the proton-fraction equation (2.14) and finally plugging them all in the expression for the total Binding Energy per Nucleon. The obtained curve is reported as $P[\rho_B]$ in fig. 6.1; it can be catalogued as a super-stiff Equation of State. The Equation of State at very low densities confrontable with $\rho_{^{50}\mathrm{Fe}}$ is devised from the works of J. Negele and D. Vautherin, to obtain a realistic description of the Neutron Star crust [9].

Quark Matter was sketched in this work as a free gas of massless u, d, s quarks in the chiral limit; the extreme choice was dictated by the later use in viscosity calculations: the Heiselberg-Pethick approach was devised in this limit. The Equation of State is straightforwardly calculated by means of a

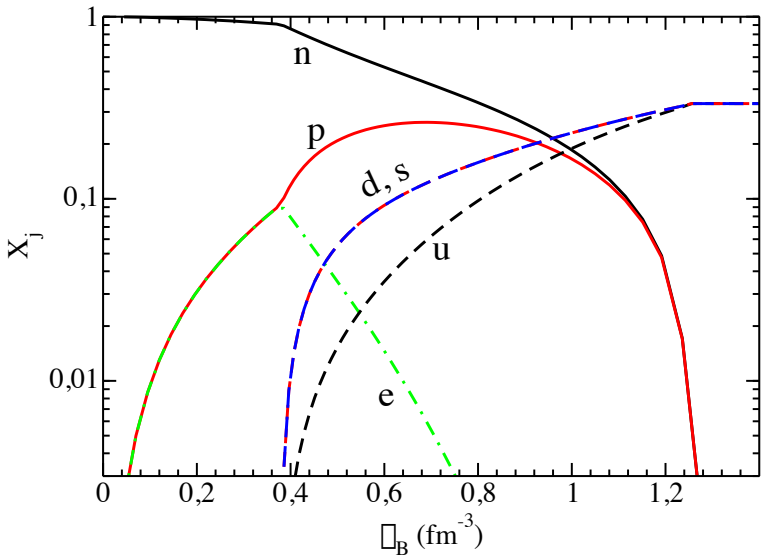

Figure 6.2: Composition of Strongly Interacting Matter with a First-Order phase transition; in the pure Quark Phase, with $B^{1/4} = 200$ MeV, the electrons are suppressed: this is due to the exact $SU_f(3)$ (chiral) symmetry employed in the calculations.

simple numeric code; two values $B^{1/4} = \{180, 200\}$ MeV of the Bag Constant were chosen; the results are reported in the coloured solid lines of fig. 6.1. The second value was kept in what follows, as the first - once put in the Glendenning scheme - yields highly unphysical results, setting a QGP phase transition immediately after the Nuclear Saturation point $\rho_0 = 0.17$ fm^{-3}.

§ 6.1.2. First Order phase transition.— The calculations for both the two phases were performed at $T = 0$: it can be proved - also operatively, by means of actual evaluations - that the equilibrium thermodynamics evaluated in this limit is valid up to temperatures of $T \sim 5$ MeV$\ll \epsilon_F \sim 100$ MeV, still very low with respect to the typical Fermi Energies of the considered systems. The phase transition among the two phases is in this work imposed in this limit, under the assumption that it is of First Order and Second Kind, as proposed by Glendenning [→ § 2.3.1]. The evaluation was done by means of a Fortran code that blends the two phases in the context of the correct Gibbs conditions with Global Charge conservation for the Mixed Phase; the results are the dashed curves of fig. 6.1. The transition sets in at $\rho_B^{c,180} \sim 0.2$ fm^{-3} and $\rho_B^{c,220} \sim 0.38$ fm^{-3} for the two Bag Constant choices: very early in the first case, that is therefore discarded from now on (the first Hybrid Star

configurations appear at 0.4 $M_\odot$!); the second case is quite standard for a realistic choice of the Bag Constant and is typical of phenomenological quark models.
It is very interesting to note the composition of the Strongly Interacting Matter at various densities for the model considered: at low densities, around saturation and before the phase transition sets in, the picture is dominated by neutrons, with an equal fraction of protons and electrons to satisfy neutrality conditions. When the transition begins strange s quarks begin to appear in the composition of matter and this changes equilibria, initially favouring the growth of proton concentration up to the 25% and the quick suppression of electrons. When the transition ends, pure quark matter is degenerate in its composition: the three chemical potentials are equal, due to the exact chiral $SU_f(3)$ limit for the quark bare masses.

6.2 Transport properties of the QCD liquid

It is important to remark that the transport properties of the two phases were calculated in a low-temperature scheme with fitting quasiparticle-approaches, while the corresponding static-input quantities - like the G-Matrix, were calculated in the $T = 0$ exact limit. Such a procedure, that might seem inconsistent, was partly already justified. To strengthen the point, however, it must be noted that the low-temperature $\eta \sim T^{-2}$ behaviour of a Normal Fermi liquid essentially descends from the action of the Pauli Blocking, so that the feeble contribution of the Equations of State can be totally neglected.

§ 6.2.1. Shear Viscosity in the two phases.— Three temperatures were chosen to evaluate the Shear Viscosity of the two phases: $T = \{10^{-5}, 10^{-4}, 1\}$ MeV, even if essentially only the two extremes were kept in actual calculations; the results are displayed in fig. 6.3. This is closely related to the study of the $r-$mode oscillations damping in Neutron Stars and is discussed in the next section. Hadronic Viscosity is always larger than the corresponding Quark-Matter calculation This is accounted for the different low-temperature behaviours: exact $\eta \sim T^{-2}$ Fermi liquid for the first, realistic screened $\eta \sim T^{-5/3}$ liquid the latter.
The calculation for quarks is worth a little more insight. Two things must be noted: (i) the goodness of the relaxation momentum approximation against the variational estimate given from the linearised equation and (ii) what choice of α_s suits best the calculations.

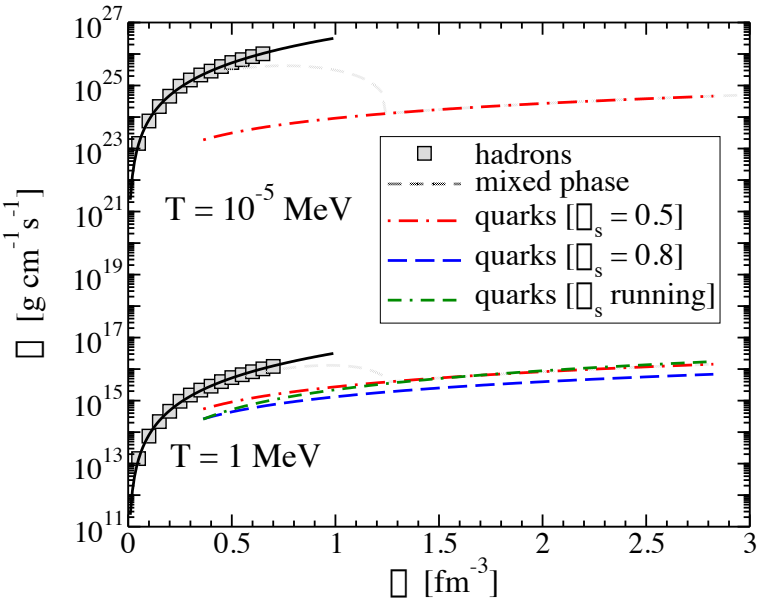

Figure 6.3: Shear Viscosity of the various phases at $T = 1$ MeV and $T = 10^{-5}$ MeV. The grey squares are the results of the calculation performed in ref. [78], on which a fit was performed (black solid line); The coloured dashed lines correspond to the calculations for quarks performed at different values of α_s. The grey short-dashed line is the result for the mixed phase.

- **Scale-Hierarchy:** the three scale parameters for the finite μ regime in the present conditions fulfil the inequality $T \ll m_D \sim \mu_q$. Thus, the calculations of Shear Viscosity can be performed by means of the much easier momentum-relaxation approximation eq. (4.47); the full integral from the variational estimate of eq. (4.59) was anyway solved by means of a complex numerical algorithm, yielding results well within the 1%.

- **Coupling constant:** the choice of the α_s value to be used in the calculation was a tricky problem to deal with. Strictly speaking, no perturbative approach has any sense at finite μ so far, due to the non-perturbative regime of QCD. Nevertheless here the chemical potential μ is the relevant energy scale: imagining to employ this assumption for the evaluation of α_s in eq. (1.22), one can conclude that with typical $\mu_q \sim 600$ MeV $\simeq 3\,\Lambda_{\rm QCD}$ non perturbative effects begin to be non-negligible and the predictions may be not reliable; but in Lattice QCD, for $T \sim 200$ MeV and $\mu \to 0$, good predictions can be made for the η/s ratio and this remains valid also naively using perturbative schemes with $\alpha_s \sim 0.6$: thus, taking a fiducial $\alpha_s = 0.5$, the predictions can be

considered accurate within a factor of 2 also in the present case. On absolute grounds this can be a risky procedure; the aim of this work is to give an estimate for Astrophysical later use, so that this degree of approximation can be considered satisfactory.

The coloured curves for $T = 1$ MeV reported in fig. 6.3, are obtained with $\alpha_s = \{0.5, 0.8\}$ (red, blue curve) and with a running approach between the two, calculated by means of:

$$\alpha_s^{-1} = \frac{7}{4\pi} \ln(4\mu_q^2/\Lambda_{\rm QCD}^2), \tag{6.2}$$

(shown as the green curve), and all the three seem to support this view, especially from the point of view of the further applications.

§ **6.2.2. Total Viscosity.**— In absence for any lead on how the onset of a Mixed-Phase in Strongly Interacting matter alters the known behaviour of the two separated phases, an ansatz was deliberately formulated to overcome the problem. The total viscosity in this work is just the χ-meshed sum of the viscosities of the two phases:

$$\eta[\eta_H(\rho_B), \eta_Q(\rho_Q)] = (1-\chi)\eta_H(\rho_B) + \chi\eta_Q(\rho_Q); \tag{6.3}$$

such an assumption has no intuitive microscopic origin and is therefore mainly a method to investigate the properties of a mixed phase without any Analytical pathology in the corresponding functions. The results are shown in the grey short-dashed curves of fig. 6.3.

6.3 Astrophysical Applications

The Equation of State is the input of the Relativistic Hydrodynamical structure equation set known as "Tolman Oppenheimer Volkoff" equations, through which static stable Neutron Star configurations can be calculated. One finds that Strongly Interacting matter is too repulsive to be self-bound above the saturation point, but when a macroscopic drop is formed, Gravity succeeds in binding it. Neutron Stars can be thus seen as giant nuclei, with $A \approx 10^{56}$, bound by the gravitational interaction. But also non equilibrium properties can be studied, by means of the Oscillation Modes discussed in Chapt. 5: some of them, like the rotational r-modes, are sensitive to the features of the Equation of State.

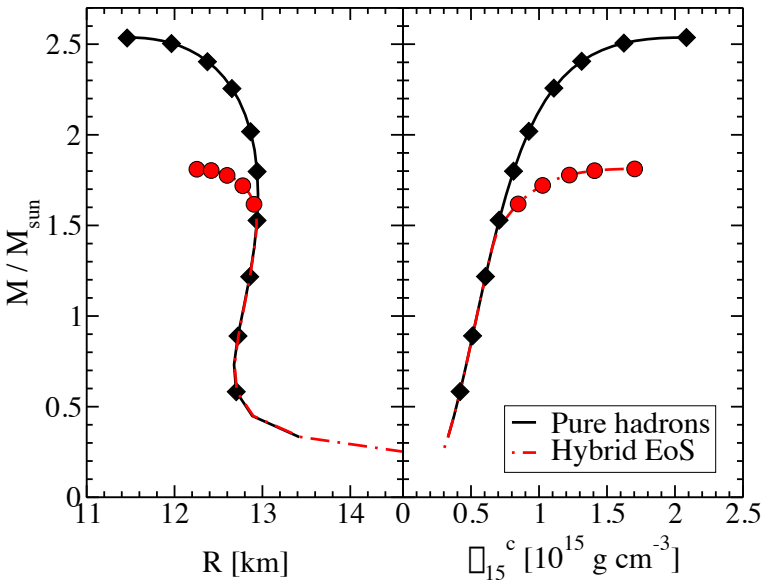

Figure 6.4: Results of the TOV Equations integration for the Hadron and Hybrid Phase Equations of State. *Left:* Mass-Radius panel of the static stable configurations. *Right:* Parametrized central densities vs Mass for the calculated Neutron/Hybrid Stars.

§ 6.3.1. Static Configurations and Oppenheimer Volkoff limit.— The TOV system integration is performed parametrizing the unknown central density ρ_c for a certain number of desired configurations, that works as input for a Runge-Kutta algorithm stopped at fourth order. The Neutron Star crust is simulated attaching smoothly a suitable realistic Equation of State to the microscopic calculations; in the present work the crust was modeled in accord with a work by J. Negele and D. Vautherin [9]. The results are then put in a Mass-Radius plot such as the left panel of fig. 6.4 and then trimming the configuration branch not satisfying the Hydrostatic condition $\mathrm{d}M/\mathrm{d}\rho$; the input central densities are shown in the right panel. A number of 10 hadronic configurations (black diamonds) and of 5 more hybrid stars (red circles) were selected for further r-mode damping calculations.

- **Upper mass-limit:** the points to the extreme left in the left panel of fig. 6.4 correspond to the Oppenheimer Volkoff limits calculated with the two theories: the purely Hadronic Equation of State can yield Neutron Stars with a maximum mass of 2.53 $\mathrm{M}_\odot$, while the corresponding upper limit for Hybrid Stars is 1.81 $\mathrm{M}_\odot$: the latter value is lower than the recent 1.97 $\mathrm{M}_\odot$ of the J1614-2230 Pulsar, so that its equation of

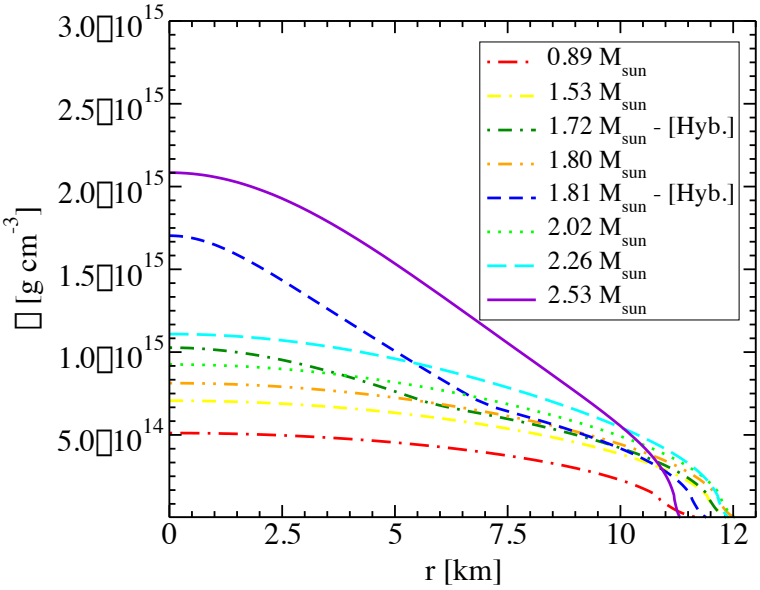

Figure 6.5: Density profiles for a selected number of purely Hadronic / Hybrid stable configurations.

state seems not to stiff enough to reproduce observed data.

- **Possible signal of QGP:** this cannot obviously be extended on general grounds, i.e. to the general question whether there can be deconfined quarks and gluons inside a Neutron Star, as the Bag Model is a very rough and phenomenological way to describe quark phase. It might - on the contrary - be seen as a supporting argument for the presence of a transition, as purely hadronic scenarios lose their meaning when the density approaches $\rho_B \sim 1$ fm^{-3}: super-stiff Equations of State such as the BHF+3BF and the DBHF (that yield similar predictions in the discussed BonnB consistent approach) give too high limits ~ 2.5 $M_\odot$, but can reach the observed configurations around 2 $M_\odot$ once a transition is imposed.

- **Role of the Phase transition:** this can be seen referring to the two ~ 1.8 $M_\odot$ configurations in the left panel of fig. 6.4: the purely Hadronic configuration has a larger radius (13 Km) with respect to the 12.5 Km of the hybrid one. This can be explained observing the corresponding central densities in the right panel of fig. 6.4 or the density profiles of fig. 6.5: the transition allows stable configurations that can reach an higher density in their cores, i.e. they can pack much more matter

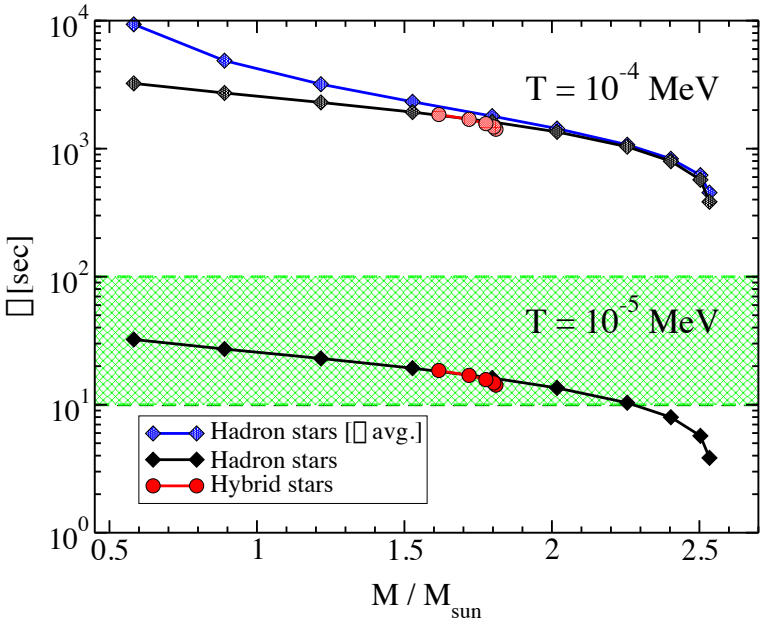

Figure 6.6: Integrated r-mode dissipation timescales at the temperatures $T = 10^{-4}$ MeV and $T = 10^{-5}$ MeV. The blue diamonds are obtained by averaging the density of the Neutron Stars, like in ref. [78]: this approximation fails for intermediate-low mass stars. The green band is the predicted range for $\tau_{\rm GW}$.

keeping stability. A precise measurement of Neutron Star *radii* for some object could help clarifying the picture, adding one or more dots in the M-R plot and therefore ruling out all those models that don't cross them.

§ 6.3.2. Damping of r-modes.— The timescale estimate of Oscillations damping in Neutron Stars is performed for the $l = m = 2$ rotational r-mode; the Energy of the mode is given by twice the integral eq. (5.12), performed with the density profiles of the stars $\rho(r)$ shown in fig. 6.5 for the 15 total configurations selected (here ρ stands for the matter density inside the star and not for the total baryon density ρ_B). The corresponding timescale is evaluated by means of the integral (5.15), dropping the contributions for the bulk viscosity ζ and the thermal conductivity κ. The input is the total Shear Viscosity of Strong Interacting matter, shown in fig. 6.3. The calculations were performed for $T = 10^{-4}$ MeV and $T = 10^{-5}$ MeV, to have a comparison with the Gravitational-Wave emission instability timescale $\tau_{\rm GW}$, estimated to for the present case $10 \div 100$ s, generally function of the revolution frequency of the star Ω and not of its temperature. The two mechanisms compete in the

dynamical evolution of a given configuration; the dominating one at a given temperature T is thus the one with the smallest timescale, as its the most rapid and effective in making the other ineffective. The resulting timescales for the 15 configurations (10 purely hadronic + 5 hybrid stars) in the two temperatures are reported in fig. 6.6, to observe the effect of temperature and of a phase transition in Nuclear Matter. General considerations can be made:

- **Goodness of the approximation:** the purely hadronic timescales in Ref. [78] were evaluated by means of an average estimate; here this calculation was performed together with the exact one (black diamonds) discussed above, and is reported in the blue diamonds of the $T = 10^{-4}$ MeV top part of the figure. The approximation is overall fairly good for the top-mass configuration, while breaks down around 1.5 $M_{\odot}$, i.e. for the mass of the most abundant Pulsars observed so-far in our Galaxy. The full calculation is performed for quarks (red circles), as a similar estimate should carefully deal with the mixed content of the configurations.

- **Dominating mechanism:** a star at $T = 10^{-4}$ MeV, so at the end-point of the cooling process, seems to be - in this picture - dominated by the Gravitational Radiation emission, as the Y_2^2-driven r-mode alone cannot overcome such instability; this picture is valid also for newborn Neutron Stars, that are candidate objects for the observations of Gravitational Waves. When corrected with other Oscillation damping modes the picture should heal, as no Gravitational Wave signal has ever been detected in the observed stars. The selected r-mode can instead dominate alone in old Neutron Stars (at least the most massive), that reach ultra-cold temperatures of $T = 10^{-5}$ MeV: this is essentially an effect of the Shear Viscosity, that for low temperatures behaves approximately as T^{-2}.

- **Effect of quarks:** the onset of a phase transition has a visible effect on the timescales. This can be checked in the lower part of fig. 6.6: the timescales get lower - this depends anyway also on the viscosity, and the model employed is not determinant in the quantitative-predictive power of this estimates - due to the higher central pressure reached inside Hybrid Stars. Such objects can damp r-modes as well as higher mass-NS of more than 2 $M_{\odot}$.

6.4 Conclusions

Recalling the title of this work, calculations can reach a satisfactory degree of accuracy, but none of them can ever be considered "Complete"; the adjective here refers to the unified scheme in which, starting from microscopic basic constituents such as nucleons and quarks, one ends up calculating macroscopic properties of Strongly Interacting matter and applications in Neutron Stars, that are in principle verifiable by means of proper observations.

§ **6.4.1. Remarks.**— Apart from the overall quantitative quality of the predictions, the scheme presented has been tested with other calculations and is generally reliable. Previous astrophysical estimates - given for example in the works of Lindblom [99, 100] - were performed by means of strong approximations and unphysical Equations of State models. Very few calculations exist for the Shear Viscosity of quark matter at finite μ: other applications often used approximate fits calculated by Heiselberg and Pethick in Ref. [82]; here the reliability of the perturbative scheme was analysed electing μ_q as the relevant energy scale and testing the goodness of the model with a confidential choice of $\alpha_S = 0.5$, in comparison with similar calculations in the high T, vanishing μ regime. Furthermore, super-stiff hadronic Equations of State like BHF+3BF and DBHF have received new attention after the measurement of the high-mass J1614-2230 PSR object [90]: they are by far the most realistic, and can account for NS mass observations once a proper softening mechanism is introduced, i.e. new degrees of freedom, such as Hyperons, π, K condensates or a transition to QGP, like in the present work.

§ **6.4.2. Future investigations.**— In the next evaluations Quark Matter should be investigated by means of a microscopic effective theory such as the Nambu-Jona Lasinio model, that incorporates a mechanism of Chiral Symmetry restoration; if one finds a way to extract a complex self-energy Σ, Viscosity can be calculated by means of the Kubo Formula, and this can be done consistently also for the Hadronic sector. New predictions should lead to more reliable r-mode damping timescales, hopefully combined with other mechanisms to solve the strict T dependence problem in the comparison with the Gravitational Radiation instability timescale. Observations from the LIGO facility could help in constraining this very open, and very challenging field of contemporary Theoretical Physics.

Part IV

Appendices

A

Units of Measurement

A.1 Natural Units

It is common in theoretical physics to suppress - or more properly to leave out - two of the constants that appear more often: $\hbar$, the reduced Planck constant, and c, the speed of light in vacuum:

$$\hbar = 6.5821 \times 10^{-25}\,\text{GeV} \cdot \text{s} \tag{A.1}$$

$$c = 2.9979 \times 10^{8}\ \text{m/s}. \tag{A.2}$$

This is sought in order to avoid annoying rewriting and iterating errors in the algebraic passages, and to generally make them more readable. It consists in a careful dimensional redefinition of all the physical observables obtained incorporating the mentioned constants; in a more concise way it is resumed by the position $\hbar = c = 1$. In this way for example the following equations become:

$$E^2 = p^2c^2 + m^2c^4 \qquad \rightarrow \qquad E^2 = p^2 + m^2$$

$$\lambda = \frac{\hbar}{mc} \qquad \rightarrow \qquad \lambda = m^{-1}$$

so that, indicating with $[X]$ the dimensions of the observable X, the previous relations imply a flattening of the units system:

$$[E] = [p] = [m] \qquad \text{with} \qquad E \sim \text{GeV}$$

$$[L] = [m]^{-1} \qquad \text{with} \qquad L \sim \text{fm};$$

all the interesting physical quantities have dimensions given by a certain product of powers of GeV and fm, and more generally the mass itself could be used as the only scale.
When dealing with thermodynamic problems, one can in addition include the

Boltzmann constant $k_B = 1.380 \times 10^{-23}$ J/K in the scheme, incorporating it into the Temperature T, that in this way gets the dimensions of a thermal energy $k_B T$.
When turning back to calculations, i.e. phenomenological estimates or numeric crunch, it is useful to revert back to the original quantities using powers of the quantity:

$$\hbar c = 0.197327 \text{ GeV} \cdot \text{fm}, \tag{A.3}$$

and then eventually convert them to S.I. units. In astrophysics it is usual to express quantities by means of the *cgs* system, but this and the related constants require a separated treatment.

A.2 Astrophysical Units: the *cgs* system

In Astrophysical applications it is customary to use the *cgs* unit system. Chapt. 5 is all formulated under this assumption and all the usual physical constants appear. The passage between the two systems can be tricky, as one must remember the $\hbar, c$ powers and pure numbers that were "left behind" in nuclear units. For example, the conversion of density is:

$$1\,\text{fm}^{-3} = 1\,\frac{[m_p]_{\text{cgs}}}{[1\,\text{fm}]^3_{\text{cgs}}} = \frac{1.67493 \times 10^{-24}\,\text{g}}{10^{-39}\,\text{cm}^3} = 1.67493\,\text{g/cm}^3 \tag{A.4}$$

that simply yields for the nuclear saturation density:

$$\rho_0 = 0.17 \text{ fm}^{-3} = 2.8 \cdot 10^{14}\,\text{g/cm}^3. \tag{A.5}$$

Viscosity is the most delicate quantity, as it is calculated in MeV^3 in nuclear units, but must be expressed in:

$$[\eta]_{\text{mks}} = \frac{\text{kg}}{\text{m} \cdot \text{s}} = \frac{\text{N} \cdot \text{s}}{\text{m}^2} = 10 \times [\eta]_{\text{cgs}} = \frac{\text{dyne} \cdot \text{s}}{\text{cm}^2}; \tag{A.6}$$

In order to perform the calculation it must be noted that:

- $c = 1 \quad \Rightarrow \quad 2.9979 \times 10^8$ m/s$= 1 \quad \Rightarrow \quad 1$ m$= \frac{1}{2.9979 \times 10^8}$ s;
- 1 MeV$= 1.6021 \times 10^{-13}$ j$= \frac{1.6021 \times 10^{-13}}{2.9979 \times 10^8}$ N·s;
- $\hbar c = 1 \quad \Rightarrow \quad 197.18$ MeV·fm $= 1 \quad \Rightarrow \quad 197.18 \times 10^{-15}$ MeV·m $= 1$;

so that finally, combining these results, the final conversion factor is evaluated as:

$$1\,\mathrm{MeV}^3 = \frac{1.6021 \times 10^{-13}}{2.9979 \times 10^8 \cdot 197.18^2 \times 10^{-30}} \frac{\mathrm{N} \cdot \mathrm{s}}{\mathrm{m}^2} = 1.3745 \times 10^5 \, \frac{\mathrm{dyne} \cdot \mathrm{s}}{\mathrm{cm}^2}. \tag{A.7}$$

To avoid writing explicitly powers of 10, a practical notation shortcut is often introduced. The values the observable O, measured by means of the X unit, whose values typically range in the power p can be specified in values of the O_p variable, in which it is implicitly meant that it is measured in units of 10^p. In this fashion the temperature of the centre of the Sun is:

$$T_\odot = 15.7 \times 10^6\,\mathrm{K} = 15.7\,T_6, \tag{A.8}$$

implicitly meaning "million kelvins". Other experimental parameters of our star are:

$$M_\odot = 1.989 \times 10^{30}\,\mathrm{kg} \tag{A.9}$$

$$R_\odot = 6.960 \times 10^5\,\mathrm{m} \tag{A.10}$$

$$L_\odot = 3.850 \times 10^{26}\,\mathrm{W} \tag{A.11}$$

Acknowledgements

I would like to thank my supervisor, Prof. Umberto Lombardo, for believing in my skills through all these years: this is the third thesis work that we co-sign, and he has been encouraging me since year 2005, feeding me with advice, insights, comments and precious critics, even in my gloomy moments. Credit goes to him also for organising the Ph.D. course, together with the ex-Director of "Scuola Superiore di Catania", Prof. E. Rizzarelli. He strongly pursued its development, constantly followed me and my colleagues dealing with our problems, and inviting many brilliant experts from allover the world to organise a full set of high-end formative courses.

A second acknowledgement goes to all the collaborators of these three years: Dr. Vincenzo Greco, that co-tutored my work, often showing my errors, dealing very honestly with me and educating me to scientific responsibility; Prof. Paolo Castorina, that introduced me to the field of Lattice QCD studies and to the Bielefeld group; together with Dr. Dario Zappalá, that later followed my work, he proposed what recently became a published work about Finite Temperature $SU(N)$ Gauge Theory. A special thanks goes finally to Dr. Salvatore Plumari, that spent many hours of his own research time working together with me, and was always deeply interested in the outcome of my work.

I would also like to thank Prof. Helmut Satz for advising my charmonium work and inviting me to in Germany, and all the Bielefeld Group for the warm welcome they gave me in the period of January-March 2010.

I cannot forget Prof. Marcello Lattuada, director of "INFN - Laboratori Nazionali del Sud", and all the Staff there, for allowing me to do research in an high-level international environment; on the same level, I thank Prof. Giacomo Pignataro, ex-Director of "Scuola Superiore di Catania", for accepting my accommodation request and for the sensitivity shown during my unfortunate accident of October 2010, together with Dr. Francesca Scollo; but a huge "thank you" goes also to all the highly competent personnel of this organisation, including the diligent Receptionists, and all the students, that made me feel at home.

Danilo Jaccarino
December 2011

Bibliography

[1] I. Langmuir, Proceedings of the National Academy of Science **14**, 627 (1928).

[2] W. Crookes, *Radiant matter: a resume of the principal lectures and papers of Prof. William Crookes, on the 'fourth state of matter'.* (James W. Queen & Co., New York, 1881).

[3] J.B. Kogut and M.A. Stephanov, *The phases of quantum chromodynamics: From confinement to extreme environments* (Cambridge University Press, United Kingdom, 2004), Vol. 21, pp. 1–364.

[4] Jean Letessier and Johann Rafelski, *Hadrons and quark - gluon plasma* (Cambridge University Press, United Kingdom, 2002), Vol. 18, pp. 1–397.

[5] K. Yagi, T. Hatsuda, and Y. Miyake, *Quark-gluon plasma: From big bang to little bang* (Cambridge University Press, United Kingdom, 2005), Vol. 23, pp. 1–446.

[6] P. Debye and E. Hückel, Physikalische Zeitschrift **24**, 185 (1923).

[7] L. D. Landau and Lifshitz E. M., *Statistical Physics* (Pergamon Press, London, 1958).

[8] J. Dobaczewski, ArXiv Nuclear Theory e-prints (2003).

[9] J.W. Negele and D. Vautherin, Nuclear Physics A **207**, 298 (1973).

[10] J. Pochodzalla, G. Raciti, and ALADIN collaboration, Phys. Rev. Lett. **75**, 1040 (1995).

[11] N. Cabibbo and G. Parisi, Physics Letters B **59**, 67 (1975).

[12] J. C. Collins and M. J. Perry, Phys. Rev. Lett. **34**, 1353 (1975).

[13] E.V. Shuryak, Physics Letters B **78**, 150 (1978).

[14] M. Plümer, S. Raha, and R. M. Weiner, Nuclear Physics A **418**, 549 (1984).

[15] T. Matsui and H. Satz, Physics Letters B **178**, 416 (1986).

[16] M. E. Peskin and D. V. Schroeder, *An Introduction To Quantum Field Theory* (Addison Wesley Program, New York, 1995).

[17] O. W. Greenberg, Physical Review Letters **13**, 598 (1964).

[18] M. Y. Han and Y. Nambu, Physical Review **139**, 1006 (1965).

[19] William A Bardeen, H Fritzch, and Murray Gell-Mann, Technical Report No. CERN-TH-1538, CERN, Geneva (unpublished).

[20] D. J. Gross and F. Wilczek, Physical Review Letters **30**, 1343 (1973).

[21] H. D. Politzer, Physical Review Letters **30**, 1346 (1973).

[22] S. Sarkar, H. Satz, and B. Sinha, *The Physics of the Quark-Gluon Plasma*, *Lecture notes in physics* (Springer, Cambridge, 2010).

[23] Olaf Kaczmarek and Felix Zantow, Phys. Rev. D **71**, 114510 (2005).

[24] F. Y. Wu, Rev. Mod. Phys. **54**, 235 (1982).

[25] Benjamin Svetitsky and Laurence G. Yaffe, Nuclear Physics B **210**, 423 (1982).

[26] Frithjof Karsch and Edwin Laermann, Phys. Rev. D **50**, 6954 (1994).

[27] Frithjof Karsch, Nucl.Phys. **A698**, 199 (2002).

[28] I. K. Yoo, Ph.D. thesis, Fachbereich Phyisk der Universität, Marburg, 2001.

[29] WA97 Collaboration, Physics Letters B **449**, 401 (1999).

[30] NA 50 Collaboration, Physics Letters B **477**, 28 (2000).

[31] J. Stachel, Nuclear Physics A **654**, 119 (1999).

[32] NA 50 Collaboration, Physics Letters B **450**, 456 (1999).

[33] NA 50 Collaboration, Nuclear Physics A **610**, 404 (1996).

[34] CERES Collaboration, Nuclear Physics A **661**, 23 (1999).

[35] WA98 Collaboration, Phys. Rev. Lett. **85**, 3595 (2000).

[36] PHOBOS, STAR, PHOENIX, BRAHMS Collaborations, Technical report, BNL 73847-2005 Formal Report (unpublished).

[37] STAR Collaboration, Phys. Rev. Lett. **103**, 251601 (2009).

[38] John W. Harris, EPIC Results from ALICE, 2011.

[39] Sebastian N. White, ATLAS Results from the first Pb-Pb Collisions, 2011.

[40] A.L. Fetter and J.D. Walecka, *Quantum theory of many-particle systems* (McGraw Hill, New York, 1971).

[41] P. Nozieres, *Theory of interacting Fermi systems* (Addison-Wesley, Reading, MA, 1997).

[42] G. Baym and C. Pethick, *Landau Fermi-liquid theory: concepts and applications*, *A Wiley-Interscience publication* (Wiley, London, 1991).

[43] L. Landau, Phys. Rev. **60**, 356 (1941).

[44] A.B. Migdal, *Theory of finite Fermi systems, and applications to atomic nuclei*, *Interscience monographs and texts in physics and astronomy* (Interscience Publishers, New York, 1967).

[45] H. Hofmann, *The physics of warm nuclei: with analogies to mesoscopic systems*, *Oxford studies in nuclear physics* (Oxford University Press, ADDRESS, 2008).

[46] Kerson Huang, *Statistical mechanics / Kerson Huang*, 2nd ed. ed. (Wiley, New York :, Chichester, 1987), pp. xiv, 493 p. :.

[47] M. Baldo, *Nuclear methods and the nuclear equation of state*, *International review of nuclear physics* (World Scientific, Singapore, 1999).

[48] I. Bombaci and U. Lombardo, Phys. Rev. C **44**, 1892 (1991).

[49] C. Fuchs and H.H. Wolter, Eur.Phys.J. **A30**, 5 (2006).

[50] V. Baran, M. Colonna, V. Greco, and M. Di Toro, Physics Reports **410**, 335 (2005).

[51] R. J. Furnstahl, LECT.NOTES PHYS. **641**, 1 (2004).

[52] Norman K. Glendenning, Phys. Rev. D **46**, 1274 (1992).

[53] Norman K. and Glendenning, Physics Reports **342**, 393 (2001).

[54] R. B. Wiringa, V. G. J. Stoks, and R. Schiavilla, Phys. Rev. C **51**, 38 (1995).

[55] S. Veerasamy and W. N. Polyzou, Phys. Rev. C **84**, 034003 (2011).

[56] R. Machleidt, Phys.Rev. **C63**, 024001 (2001).

[57] Mark I. Gorenstein and Shin Nan Yang, Phys. Rev. D **52**, 5206 (1995).

[58] P. Castorina, V. Greco, D. Jaccarino, and D. Zappalà, The European Physical Journal C - Particles and Fields **71**, 1 (2011), 10.1140/epjc/s10052-011-1826-8.

[59] K. A. Brueckner, C. A. Levinson, and H. M. Mahmoud, Phys. Rev. **95**, 217 (1954).

[60] H. A. Bethe and J. Goldstone, Proceedings of the Royal Society of London. Series A. Mathematical and Physical Sciences **238**, 551 (1957).

[61] M.R. Anastasio, L.S. Celenza, W.S. Pong, and C.M. Shakin, Physics Reports **100**, 327 (1983).

[62] R. Brockmann and R. Machleidt, Phys. Rev. C **42**, 1965 (1990).

[63] H. Müther, R. Machleidt, and R. Brockmann, Phys. Rev. C **42**, 1981 (1990).

[64] H. Q. Song, M. Baldo, G. Giansiracusa, and U. Lombardo, Phys. Rev. Lett. **81**, 1584 (1998).

[65] P. Grangé, A. Lejeune, M. Martzolff, and J.-F. Mathiot, Phys. Rev. C **40**, 1040 (1989).

[66] J. Goldstone, Proceedings of the Royal Society of London. Series A. Mathematical and Physical Sciences **239**, 267 (1957).

[67] B. D. DAY, Rev. Mod. Phys. **39**, 719 (1967).

[68] M. Baldo, A. Fiasconaro, H. Q. Song, G. Giansiracusa, and U. Lombardo, Phys. Rev. C **65**, 017303 (2001).

[69] Z. H. Li, U. Lombardo, H.-J. Schulze, and W. Zuo, Phys. Rev. C **77**, 034316 (2008).

[70] N.M. Hugenholtz and L. van Hove, Physica **24**, 363 (1958).

[71] T. Koopmans, Physica **1**, 104 (1934).

[72] M. Baldo, I. Bombaci, L.S. Ferreira, G. Giansiracusa, and U. Lombardo, Physics Letters B **209**, 135 (1988).

[73] P. Czerski, A. De Pace, and A. Molinari, Phys. Rev. C **65**, 044317 (2002).

[74] A. Chodos, R. L. Jaffe, K. Johnson, C. B. Thorn, and V. F. Weisskopf, Phys. Rev. D **9**, 3471 (1974).

[75] T. Schäfer and D. Teaney, Reports on Progress in Physics **72**, 126001 (2009).

[76] A A Abrikosov and I M Khalatnikov, Reports on Progress in Physics **22**, 329 (1959).

[77] G. A. Brooker and J. Sykes, Phys. Rev. Lett. **21**, 279 (1968).

[78] H. F. Zhang, U. Lombardo, and W. Zuo, Phys. Rev. C **82**, 015805 (2010).

[79] Gordon Baym, H. Monien, C. J. Pethick, and D. G. Ravenhall, Phys. Rev. Lett. **64**, 1867 (1990).

[80] H. Heiselberg, Phys. Rev. D **49**, 4739 (1994).

[81] H. Heiselberg, G. Baym, and C.J. Pethick, Nuclear Physics B - Proceedings Supplements **24**, 144 (1991).

[82] H. Heiselberg and C. J. Pethick, Phys. Rev. D **48**, 2916 (1993).

[83] H. Arthur Weldon, Phys. Rev. D **26**, 1394 (1982).

[84] S.L. Shapiro and S.A. Teukolsky, *Black holes, white dwarfs, and neutron stars: the physics of compact objects*, *Physics textbook* (Wiley, New York, 1983).

[85] N.K. Glendenning, *Compact stars: nuclear physics, particle physics, and general relativity*, *Astronomy and astrophysics library* (Springer, Heidelberg, 2000).

[86] J. M. Lattimer and M. Prakash, ArXiv e-prints (2010).

[87] W. Baade and F. Zwicky, Proceedings of the National Academy of Sciences **20**, 259 (1934).

[88] R. C. Tolman, Physical Review **55**, 364 (1939).

[89] A. Hewish, S. J. Bell, J. D. H. Pilkington, P. F. Scott, and R. A. Collins, Nature **217**, 709 (1968).

[90] P. B. Demorest, T. Pennucci, S. M. Ransom, M. S. E. Roberts, and J. W. T. Hessels, Nature **467**, 1081 (2010).

[91] Q.Z. Liu, J. van Paradijs, and E.P.J. van den Heuvel, Astron. Astrophys. Suppl. Ser. **147**, 25 (2000).

[92] S.E. Thorsett and Deepto Chakrabarty, Astrophys.J. **512**, 288 (1999).

[93] James M. Lattimer and Madappa Prakash, Phys. Rev. Lett. **94**, 111101 (2005).

[94] K. Kokkotas and B. Schmidt, Living Reviews in Relativity **2**, 2 (1999).

[95] K. S. Thorne, The Astrophysical Journal **158**, 1 (1969).

[96] S. Chandrasekhar, Phys. Rev. Lett. **24**, 611 (1970).

[97] Nils Andersson, The Astrophysical Journal **502**, 708 (1998).

[98] John L. Friedman and Sharon M. Morsink, The Astrophysical Journal **502**, 714 (1998).

[99] Benjamin J. Owen, Lee Lindblom, Curt Cutler, Bernard F. Schutz, Alberto Vecchio, and Nils Andersson, Phys. Rev. D **58**, 084020 (1998).

[100] C. Cutler and L. Lindblom, The Astrophysical Journal **314**, 234 (1987).

[101] W. Zuo, U. Lombardo, H.-J. Schulze, and Z. H. Li, Phys. Rev. C **74**, 014317 (2006).

[102] R. Machleidt, Phys. Rev. C **63**, 024001 (2001).